

Molded Culture: The Symbolic Content of Ceramics and Cultural Identity in Pre-Industrial Peru^{*}

Miriam Artiles[†] Gonzalo González-Melo[‡] Mateo Uribe-Castro[§]

PUC Chile

PUC Chile

Universidad de los Andes

September 29, 2025

Abstract

This paper examines the evolution of cultural differences in pre-industrial times. We use a novel dataset of approximately 30,000 ceramic objects from pre-colonial Peru, documented through both images and texts. We find significant cross-sectional and inter-temporal differences among human groups spanning two millennia of pre-Inca history, as revealed by the distinctiveness of ceramic style. Nonetheless, we find substantial heterogeneity in the explanatory power of group identity across periods and regions. We provide descriptive evidence that group identity is a stronger predictor of cultural differences during more conflictive periods and in regions with a longer history of political centralization. Examining the symbolic content of ceramics, religious themes emerge as key drivers of stylistic distinctiveness, especially during more conflictive periods. Using an IV approach, we also show that political centralization systematically reduces stylistic and thematic dispersion among objects from the same group, consistent with the idea that political centralization contributed to stronger cultural identities. We show consistent evidence for dispersion in present-day attitudes.

JEL Classification: A12, J15, N36, Z10

Keywords: cultural change, group identity, ceramics, material culture

*We thank Aureo de Paula, Klaus Desmet, Miguel Ángel Carpio, Eleonora Guarnieri, Jeanne Lafortune, Eduardo Montero, Jacob Moscona, Petra Moser, Luigi Pascali, Mauricio Romero, Ana Tur-Prats, and Hans-Joachim Voth for comments and suggestions. We thank Nicolás de Camino Pérez, Cristián Díaz Herrera, Luciano Davico Larenas, and Francisca Giner Mellado for excellent research assistance.

[†]Assistant Professor, Pontificia Universidad Católica de Chile (Instituto de Economía), e-mail: miriam.artiles@uc.cl, thanks financial support from FONDECYT Iniciación 11230265 as PI.

[‡]Economic Analyst, Quiroz & Asociados; Postgraduate student, Pontificia Universidad Católica de Chile, e-mail: gonzabgm@gmail.com.

[§]Assistant Professor, Universidad de los Andes, e-mail: m.uribecastro@uniandes.edu.co.

1 Introduction

A rich literature in economics has examined the historical origins of cultural differences and their influence on modern economic development (Guiso et al. 2006, 2009; Tabellini 2010; Nunn 2020).¹ This literature has advanced our understanding of cultural transmission and persistence, typically drawing on pre-industrial ethnographic sources (e.g., Murdock 1967; Michalopoulos and Xue 2021). More recently, the literature has turned to investigate the process of cultural change in the long run (Giuliano and Nunn 2021; Nunn 2021). Our work contributes to these recent advances.

In this paper, we systematically examine the evolution of cultural differences in pre-industrial times, before the effects of globalization and mass migrations. In some regions, culture may have remained stable across generations. In others, populations may trace their roots to groups that experienced major cultural shifts over time. Tracking and measuring culture during the pre-industrial era is challenging. If culture evolves slowly (Bisin and Verdier 2001, 2023), this task requires compiling information to infer cultural traits over long periods of time. We examine the largest electronically cataloged collection of ceramic objects from pre-colonial Peru—approximately 30,000 ceramic objects from 700 BC to the rise of the Inca Empire (around AD 1400), described through both imagery and textual data. We document significant cross-sectional and inter-temporal cultural differences, as revealed by the distinctiveness and symbolic content of ceramic style, among human groups spanning two millennia of pre-Inca history.

By focusing on ceramic style, this paper relates to the symbolic aspect of culture embedded in material forms (i.e., *material culture*). Throughout history, from Paleolithic societies to ancient civilizations (e.g., those of Egypt, Mesopotamia, the Indus Valley, Mesoamerica, and Peru), humans have often adapted tangible forms to reveal and

¹This line of research has documented the historical origins of a wide range of cultural traits, including trust (Nunn and Wantchekon 2011; Moscona et al. 2017), attitudes toward out-group members (Voigtländer and Voth 2012), civic attitudes (Guiso et al. 2016), time preferences (Galor and Özak 2016), gender norms (Alesina et al. 2013; Becker 2024), universal moral systems (Enke 2019), and attitudes toward medicine (Alsan and Wanamaker 2018; Lowes and Montero 2021), among others. For reviews of the literature, see, e.g., Spolaore and Wacziarg (2013), Nunn (2020, 2021), and Guiso et al. (2024).

preserve their ideas, shared values, and beliefs (Schortman et al. 2001; Stevenson 2011; Robinson 2015; Isbell et al. 2018; Baker et al. 2024). The conceptualization of cultures as systems of (tangible) symbols goes back to Geertz (1973)'s definition of culture as a "historically transmitted pattern of meanings embodied in symbols, a system of inherited conceptions expressed in symbolic forms by means of which men communicate, perpetuate, and develop their knowledge about and their attitudes towards life" (p. 89).² In archaeology, the study of material culture is particularly prevalent in contexts where pre-industrial societies lacked a written language, as was the case in many regions of the Americas (Isbell and Silverman 2002; more generally, Nanoglou 2009).³

We examine material culture in the context of coastal Peru. The analysis draws on a novel dataset comprising over 30,000 ceramic objects from the pre-colonial period. We use the largest electronically cataloged collection from the first 50 years of archaeological excavations. The dataset covers four periods of pre-Inca history—from the Early Horizon (700 BC–AD 1) to the Late Intermediate Period (AD 1000–1400). During this era, ceramics played a key role in symbolically imprinting and transmitting world perceptions and beliefs (Lanning 1967; Isbell and Silverman 2002, 2008). Shimada (1999) notes that "in these nonliterate cultures, depictions had to communicate effectively without written explanations; shared contextual knowledge was key to understanding" (p. 481).⁴ Numerous examples come from the many groups that once inhabited the territories later conquered by the Inca Empire. Figure 1 presents examples from Moche and Nasca (AD 1–700), who occupied the northern and southern coasts, respectively. Moche ceramics are often described as "illustrated records of oral narratives" (Shimada 1999, p. 403). They are known for fine-line painted representations of complex mythical and battle scenes. Panel A illustrates this tradition on a vessel showing the legend of *Ai Apaec*, a mythical being who traverses between worlds to maintain the balance of natural cycles.

²See Acemoglu and Robinson (2024) for a focus on *meanings*, emphasizing the aspect of culture that provides context to human interactions, rather than tangible *symbols*.

³See the Mayan hieroglyphic system for an exception (Rubio-Ramos, Isendahl and Olsson 2024).

⁴This interpretation aligns with Geertz (1976)'s view that objects "materialize a way of experiencing; bring a particular cast of mind out into the world of objects, where men can look at it" (p. 1478).

This narrative style contrasts with the polychromatic ceramics of Nasca, which combine supernatural with more naturalistic themes (Panel B; Shimada 1999; Proulx 2008).

The objects come with information on the group to which they are presumed to belong based on archaeological assessment. The collection provides extensive coverage of major coastal groups from the pre-Inca period (12 groups), with each group attributed to one of the four archaeological periods. We construct continuous, object-level measures of distinctiveness in ceramic style, by applying statistical and machine learning techniques to the objects' images, text descriptions, and ceramic traits.⁵ These measures are independent of the pre-existing group labels provided in the museum's collection. We then examine whether stylistic distinctiveness is systematically associated with group identity, comparing ceramics from different groups across space and time. Specifically, we estimate object-level regressions, using the continuous measures of stylistic distinctiveness as outcome variables, and test the joint statistical significance of group indicators—separately for each period and region.

Overall, group indicators are jointly statistically significant. On average, ceramics from different contemporaneous groups—active during the same period—tend to exhibit systematic differences in stylistic distinctiveness. We also find systematic differences between the ceramics of groups that occupied the same geographic extent at different points in time. The results from placebo tests, based on random assignments of fictitious group identities, support the interpretation that stylistic distinctiveness is systematically associated with group identity in the data. We show the results from regressions that include the year each object was electronically cataloged and archaeologist fixed effects, accounting for unobserved characteristics of the individual responsible for curating each object's information. We also control for geographic characteristics to help isolate cultural factors from purely geographic ones. Measures of stylistic distinctiveness based on standardized textual descriptions derived from objects' images, as well as measures extracted directly from the images, show consistent results.

⁵The vector of pre-defined ceramic traits is based on standardized metadata covering morphological, molding, painting, and thematic attributes (e.g., religious, fertility, death-related attributes); see Table A.1.

Nonetheless, we find substantial heterogeneity in the explanatory power of group indicators across periods and regions. First, our descriptive results suggest that group identity is a stronger predictor of cultural differences during more conflictive periods, characterized by territorial occupations and warfare. Using text- and image-based measures of stylistic distinctiveness for these periods, we find that the inclusion of group fixed effects increases the adjusted R^2 by up to 13 percent before accounting for geography and by up to 10 percent after including controls. This pattern aligns with archaeological views suggesting that material culture tends to become more differentiated during times of political instability and socioeconomic stress (Hodder 1979).

Second, the results suggest that group identity is a stronger predictor of cultural differences in regions with a longer history of political centralization. Wari, a society that emerged in the central highlands, expanded widely during the Middle Horizon (AD 700–1000), establishing a four-tiered site hierarchy. The expansion of Wari in the north extended a legacy of centralized political organization over ten centuries. Specifically, in the coastal valleys of the north, Wari expanded into areas previously controlled by Moche, which also established site-size hierarchies. In the south, it moved into territories formerly occupied by Nasca, which lacked such political centralization. This contrast is reflected in larger increases in the explanatory power of group indicators on the central-north coast (adjusted R^2 gains of up to 6–11 percent after geography controls), compared to more modest increases on the central-south coast.

Is stylistic distinctiveness related to specific cultural traits? We study the symbolic content of ceramics and find that stylistic distinctiveness, as retrieved from the estimated group fixed effects, is positively associated with religious and war-related symbology, compared to other themes (e.g., fertility). We obtain consistent results when using a matching algorithm to compare ceramics of the same form type from statistically similar environments. Within the religious domain, creation-related symbology representing cosmological origins and creation narratives emerges as the main driver. Time-varying estimates suggest that religious symbology became a more salient marker of group identity during more conflictive periods. This pattern aligns with the idea that zero-sum

views, where the gains of one group are viewed as losses for others, are linked to religious beliefs under resource stress (Foster 1965; Bergeron et al. 2024).

In the last part, we study the formation of group identity using repeated cross-sections of sites across the four periods in our sample. Each site in a given period was occupied by a single group. We measure within-site stylistic and thematic dispersion. We find that political centralization is systematically associated with reduced within-site dispersion among objects from the same group, in line with the idea that centralization contributed to stronger cultural identities. An instrumental-variables strategy—building on the idea that pre-industrial political hierarchies were more likely to emerge where geoclimatic conditions created higher expected returns to large-scale irrigation, in the spirit of Bentzen et al. (2017)—shows consistent results. We also examine dispersion in present-day attitudes toward governance. Using a time-weighted average of pre-colonial political centralization, based on the share of centuries each group occupied a given area, we find that higher historical centralization is linked to lower dispersion today. The results connect to work on the lasting effects of pre-colonial political centralization (Gennaioli and Rainer 2007; Michalopoulos and Papaioannou 2013).

Related literature and contribution. A well-established literature has documented the impact of culture on economic outcomes (Guiso et al. 2006, 2009; Fernández and Fogli 2009; Tabellini 2010; Algan and Cahuc 2013) and the role of long-run, inter-generational transmission (Bisin and Verdier 2001). Building on this literature, a rich body of research in economics has increasingly focused on studying the historical origins of cultural traits (Nunn 2020, 2021), documenting the pre-industrial roots of many shared beliefs and cultural attitudes observed around the world today. For example, Alesina, Giuliano and Nunn (2013) match modern populations to their pre-industrial ancestors and find that contemporary attitudes toward gender roles are significantly more unequal where populations descend from groups that practiced plough agriculture.

This paper contributes to a growing literature that examines the evolution of culture over the long run. Voigtländer and Voth (2012) examine anti-Semitic attitudes in

Germany over 600 years, finding lower persistence in areas with greater historical exposure to immigration and trade. [Giuliano and Nunn \(2021\)](#) find that populations descending from groups historically exposed to inter-generational climatic instability during pre-industrial times exhibit less cultural persistence today.⁶ In this paper, we turn our focus further back in time—to the cultural history of pre-industrial societies. We study the material record left by these societies to uncover cultural patterns across space and time, as revealed by the distinctiveness and symbolic content of ceramic style.

Our results show that the explanatory power of group identity is stronger during times of territorial occupations and warfare, providing empirical evidence for the archaeological view that material culture tends to differentiate under conditions of political and socioeconomic stress ([Hodder 1979; Jones 1997](#)). We find that religious symbology tends to intensify during these phases, suggesting that religion may have served to promote group identity. These findings connect to recent work linking zero-sum environments with religious beliefs ([Bergeron et al. 2024](#)), and, more broadly, to research on the role of religion throughout history ([Becker et al. 2024; Andersen and Bentzen 2025](#)).

We examine cultural differences during pre-colonial times—a period that has received increasing attention in the literature on the long-run determinants of cultural traits but for which time-varying analyses remain challenging due to data limitations. In the case of New World societies lacking writing systems, ethnographic sources often rely on colonial accounts that provide cross-sectional descriptions of pre-colonial groups (e.g., the Inca Empire in [Murdock \(1967\)](#)'s *Ethnographic Atlas*); see [Dulanto \(2008\)](#). Methodologically, tracking material culture allows us to compare societies both within and across several phases of Peruvian prehistory.

Our work relates to a growing literature in economics that increasingly relies on natural language processing (NLP) and deep neural networks (CNN) to extract quantitative information from texts and images (e.g., [Adukia et al. 2023; Ludwig and Mullainathan 2024; Dell 2025](#)). These advances have been applied to the study of cultural change

⁶See also, e.g., [Giavazzi et al. \(2019\)](#), [Desmet and Wacziarg \(2021\)](#), [Giorcelli et al. \(2022\)](#), [Bertrand and Kamenica \(2023\)](#), and [Cantoni et al. \(2024\)](#) for more recent settings.

within countries. For example, Voth and Yanagizawa-Drott (2024) examine cultural change by analyzing style choices in U.S. yearbook portraits from 1930 to 2010. Other studies have analyzed the content of traditional Chinese folktales (Xue 2024), movies (Michalopoulos and Rauh 2025), and influential scientific publications, such as *On the Origin of Species* (Giorcelli et al. 2022). There have also been applications to cultural heritage data. Cadavid-Sanchez et al. (2023) explore the performance of end-to-end entity linking methods in NLP, using a dataset of museum text descriptions covering a variety of ancient artifacts, including vessels. Gorin et al. (2025) analyze the emotions conveyed in paintings from AD 1400 onward, studying whether these emotions systematically reflect changes in socioeconomic conditions.

We exploit the fact that our dataset is labeled, which is not always granted in social science applications of ML (see Cadavid-Sánchez et al. (2023) for a discussion). Specifically, each ceramic object is labeled with the group to which it is presumed to belong based on archaeological assessment. We use ML algorithms to generate continuous, independent measures of distinctiveness in ceramic style. We then study the extent to which group identity explains variation in stylistic distinctiveness. By analyzing continuous differences among ceramics from different groups, this approach connects to an existing literature emphasizing linguistic and cultural distances between groups, rather than sharp group boundaries (Fearon 2003; Desmet et al. 2009; Guarnieri and Tur-Prats 2023). It also relates to recent studies in archaeology that rely on data-driven methods to track stylistic trends, moving beyond traditional typology-based classifications (Pawlowicz and Downum 2021).

We illustrate this approach using a dataset of ceramic objects from Peru, a country with a long-standing tradition of archaeological research and well-preserved collections of artifacts (Isbell and Silverman 2008). Archaeologists have long been interested in material expressions of culture and identity (Menzel 1976; Hodder 1982; Janusek 2005; Costin 2016). Ceramics tend to be particularly well-suited for symbolic representations because they accommodate a variety of styles and motifs, all while retaining their functionality (Lanning 1967). Furthermore, ceramic objects often survive in archaeological contexts

where other materials do not (e.g., textiles, metalworks; Shimada 1999). As such, they are among the most common and widespread artifacts found at archaeological sites. Importantly, analyses of ancient Peruvian DNA show genetic continuity across major cultural transitions (Valverde et al. 2016; Nakatsuka et al. 2020)—as in the transition from Moche and Nasca (AD 1–700) to Wari (AD 700–1000). This evidence suggests that cultural transitions were not accompanied by substantial population replacement or admixture, with internal displacements likely playing a limited role in the study region. Such evidence contrasts with the trends that have been documented in other regions of the world (Haak et al. 2015; Harney et al. 2018; Gretzinger et al. 2022).

Lastly, we study the formation of group identity in pre-colonial Peru. We find that greater political centralization contributed to lower stylistic and thematic dispersion among objects from the same group, which we interpret as evidence of a stronger cultural identity. Our results connect to studies on the effect of centralized political institutions on culture (Becker et al. 2016; Lowes et al. 2017; Heldring 2021) and, more broadly, to studies on cultural diversity (Desmet et al. 2017). While the historical origins of culture have received considerable attention (Nunn 2021), less is known about the historical roots of group identity and its formation in historical perspective (see, e.g., Dehdari and Gehring 2022; Cantoni et al. 2024). Future work with more granular, time-varying archaeological data could shed further light on these processes. Archaeological sources are not without limitations (Section 3). Nonetheless, with the growing application of machine learning techniques in both economics (Athey 2018) and archaeology (Sakai et al. 2024), the study of material culture provides a promising avenue for research on culture and identity (Akerlof and Kranton 2000; Atkin et al. 2021).

Section 2 summarizes the cultural history of coastal Peru, Section 3 describes the data, Section 4 presents the empirical results, and Section 5 concludes.

2 Background

The cultural history of coastal Peru (700 BC–AD 1400). The Peruvian coast offers a unique setting to study the evolution of cultural differences before the effects of colonization and mass migrations. In pre-colonial times, over the course of two millennia, different groups emerged, expanded, and were eventually replaced by others. Ancient DNA evidence is consistent with limited demographic disruption during these transitions (Valverde et al. 2016; Nakatsuka et al. 2020; Popović et al. 2021), providing an opportunity to study cultural differences across space and time.

Our analysis examines major coastal groups documented in the archaeological literature from the northern, central-north, and central-south coasts of Peru (12 groups). The study period extends from the initial spread of ceramics (700 BC) to the rise of the Inca Empire (around AD 1400). The most widely accepted archaeological periodization for this timeframe—first proposed by Rowe (1960, 1962)—includes the Early Horizon (700 BC–AD 1), the Early Intermediate Period (AD 1–700), the Middle Horizon (AD 700–1000), and the Late Intermediate Period (AD 1000–1400).⁷ The archaeological literature distinguishes between *Horizon* periods, marked by significant territorial expansions, and *Intermediate* periods, characterized by the absence of such large-scale expansions (Rowe 1962, 1963; Keatinge 1988).⁸

For example, during the Early Intermediate Period, Moche emerged as a dominant group in the north, with two main spheres of influence across multiple valleys: a northern sphere centered around the Motupe–Lambayeque valleys, and a central-north sphere, centered at La Libertad (from the Chicama and Moche valleys to the Nepeña valley); see Shimada (1994). Nasca, contemporaneous with Moche, was concentrated on the southern valleys. During the Middle Horizon, Wari incorporated many coastal groups into its cultural sphere, extending far beyond its original territory in the central highlands. In the north, Wari reached valleys previously dominated by Moche; in the south, it expanded into former Nasca areas. Tiahuanaco, based in the Lake Titicaca

⁷The approximate dates of each period are indicated in parentheses (Isbell and Silverman 2008).

⁸See the list of groups by period in Figure A.1.

basin, expanded in parallel, reaching the southern coast and territories in present-day Bolivia and Chile.

We systematically compare the ceramics of different groups, both within and across several periods of pre-Inca history. Rather than counting the number of coexisting groups in a given period, we examine cultural differentiation by analyzing the extent to which group identity explains variation in the distinctiveness of ceramic style. We then turn to the symbolic content of ceramics, examining which themes are more closely linked to stylistic distinctiveness.

Archaeological research in Peru. Archaeological research in Peru has a long tradition ([Isbell and Silverman 2008](#)). The beginnings of Peruvian archaeology can be traced back to around 1900, with excavations near Lima (central coast) and at the Moche ruins (north coast); see [Rowe \(1954\)](#). The [Peruvian National Museum of Archaeology \(MNAAHP\)](#) and the [Larco Museum](#) preserve extensive collections from the initial period of excavations. Particularly, the [Larco Museum](#), founded in 1926 by the scholar R. Larco Hoyle, contains the largest electronically cataloged and systematically organized collection of ceramics from the first 50 years of archaeological excavations ([Schaedel and Shimada 1982](#); [Castillo Butters 2013](#); [Daggett 2013](#); [Tantaleán and González 2013](#)).

Efforts during this period of excavations were largely concentrated along the coast ([Daggett 2013](#)). This focus aligns with archaeological evidence on the early adoption of ceramic production in Peru. Specifically, archaeological research suggests that ceramic production first appeared on the northern coast of Peru during the Initial Period (2000–700 BC), with the earliest evidence found in the Viru Valley ([Strong and Evans 1952](#); [Willey 1953](#); [Collier 1955](#); [Pozorski and Pozorski 2008](#)). It was not until the Early Horizon (700 BC–AD 1), and especially the Early Intermediate Period (AD 1–700), that ceramic production became more geographically widespread ([Lanning 1967](#)).

R. Larco Hoyle was one of the pioneers of this first period of excavations. He is widely recognized for his efforts to catalog large acquisitions of ceramic objects ([Castillo Butters 2013](#)). As noted in [Moore \(2014\)](#), “not only did Larco Hoyle dramatically increase

the collections ...but he also engaged in survey, site recording, and excavations” (p. 316), setting early standards for cataloging and documentation. The [Larco Museum](#) started electronically cataloging the entire collection of R. Larco Hoyle in 2001. By 2006, nearly all objects had been electronically cataloged, with 98 percent of objects cataloged between 2002 and 2006, and the remaining two percent cataloged after 2007.

3 Data

We examine cultural differences across space and time using a novel dataset of 30,212 ceramic objects from the pre-Inca period. Our primary data source is the [Larco Museum](#)’s ceramics collection.⁹ The dataset includes object-level information from the four pre-Inca periods, comprising 1,299 objects from the Early Horizon (700 BC–AD 1), 17,464 from the Early Intermediate Period (AD 1–700), 6,192 from the Middle Horizon (AD 700–1000), and 5,257 from the Late Intermediate Period (AD 1000–1400).¹⁰ Were most ceramic objects simple, plain vessels, or did they have distinctive traits that can be compared across space and time?

Ceramic traits. The collection is electronically cataloged and provides photographs and a textual description of each object. It also provides information on weight, dimensions (width, length, height), and detailed morphological, molding, painting, and thematic attributes. The information was curated by a team of 11 archaeologists, with an average of seven archaeologists contributing to each period. As a first step in describing the data, we use the objects’ text descriptions and attributes to construct a repertoire of 109 ceramic traits, listed in [Table A.1](#). The remainder of the section describes the data using this trait-based classification. We then complement this approach by applying machine-learning algorithms to the objects’ images and text descriptions—allowing for

⁹The collection was accessed in June 2023.

¹⁰Throughout the paper, we use this standard periodization, which allows us to match data from various archaeological sources. For recent economic studies incorporating archaeological periodizations in the empirical analysis, see, e.g., [Allen et al. \(2023\)](#).

a data-driven analysis that does not rely on pre-defined ceramic traits (Section 4.1.2).

Approximately 20 percent of the objects are open forms (e.g., plates, bowls), while 80 percent are closed forms (e.g., bottles, jars) and molded sculptures. Among the sculptures, themes are diverse: 45.5 percent represent animal species (e.g., felines, camelids, sea animals), 9.4 percent represent plant species, 7.2 percent are human portraits, and 45.8 percent illustrate ceremonial scenes and anthropomorphic beings, along with molded representations of fertility, death, war, and other themes.¹¹ Figure A.2 shows examples of ceramic sculptures representing various themes; see, e.g., the representation of a ceremonial dance with individuals standing in a circle.

Around 94 percent of the objects have painted designs on their exterior. As we do for sculptures, we categorized these designs by theme. Out of all objects with painted designs, 81 percent share themes with molded sculptures (i.e., animals, plants, anthropomorphic beings, war scenes, among other themes), while 24 percent have geometric motifs (non-mutually exclusive). Figure A.3 shows examples of the painted representations of different themes, including an anthropomorphic supernatural being and two warriors engaged in combat. Painted designs are further classified by color pigment (11 different colors), whether the design is polychromatic (defined as containing four or more colors), and according to the combination of colors used (with a total of 269 unique combinations).

Archaeological groups. Each object comes with information on the group to which its production can presumably be attributed based on archaeological markers of ceramic style (Willey 1945; Schreiber 1992; Shimada 1999). Figure A.6 shows examples from different groups. The center image of Panel A shows the sculpted head of an elderly Cupisnique woman, who was believed to play a ceremonial role during the Early Horizon (Larco Hoyle 1941). The most notable Salinar sculptures from the same period include feline depictions (left image of Panel B) and burial scenes (see, e.g., the representation of

¹¹The same sculpture can fall into multiple themes (i.e., these classifications are not mutually exclusive).

body preparation before burial in the center image of Panel B; Larco Hoyle 1944; Shimada 1999). Panel C shows representations of Sican-Lambayeque deities from the Middle Horizon. Sican deities had distinctive wing-shaped eyes and circular ear ornaments. They were often depicted using a “white-black-red” tricolor style (Lumbreñas 1999; Vogel 2018). Panel D shows examples of Chimu ceramics from the Late Intermediate Period. One notable example is a masculine human figure carrying a deer on his shoulders as a symbol of power (illustrated in the left image of Panel D), possibly related with the lord of the “deer hunters” (Moseley and Cordy-Collins 1990; Cagnato et al. 2021).

We focus on groups with at least 150 objects—the 5th percentile—resulting in a total of 30,212 objects distributed across 12 groups. These include three groups from the Early Horizon (700 BC–AD 1), four from the Early Intermediate Period (AD 1–700), three from the Middle Horizon (AD 700–1000), and two from the Late Intermediate Period (AD 1000–1400); see Figure A.1. Most well-documented groups from the coastal regions of Peru are represented in the data (see, e.g., Isbell and Silverman 2008). A notable exception is Paracas, an Early Horizon group from the southern coast, which falls below the 150-object threshold. Chavín, which originated in the central highlands and expanded during the Early Horizon, also falls below this threshold. The number of objects varies by group, with an average of 2,518 objects per group and a median of 682 objects. On average, six archaeologists contributed to curating the information of each group. We discuss spatial coverage and sample biases in the next subsection.

Spatial coverage and sample biases. Figure 2 displays the spatial distribution of the archaeological sites from which ceramic objects were recovered, with the gray area representing the approximate territorial extent of the Inca Empire between AD 1400 and 1525. We assign site coordinates to objects based on the information provided in the collection. Each object is assigned the coordinates of its corresponding site. When the site is not available, we use information on the valley’s hydrographic basin where the object was recovered and the identity of the archaeological group reported in the object’s record. Specifically, we infer site coordinates based on known archaeological

sites occupied by the group within the specified basin and period. [Figure A.4](#) shows the spatial distribution of the hydrographic basins. The list of archaeological sites located in each basin-period was compiled from [Isbell and Silverman \(2002, 2008\)](#), which provide a comprehensive survey of Andean archaeological research conducted by leading scholars.

As with most archaeological datasets, ours is subject to several sources of sample bias. For example, sample selection may result from factors related to object preservation and survival. When examining the number of objects across sites, we find an uneven distribution—with an average of 49 and a maximum of 762 objects per site. We plot the density of objects across space in [Figure A.5](#). The figure splits the sample of objects into binned percentiles of latitude-longitude, with the negative slope mirroring the Peruvian coastline. Bin size represents the density of objects, while the color gradient indicates the period of the earliest object within each bin. Reassuringly, the observed geographic pattern aligns with archaeological research on the historical diffusion of ceramic production, which initially reached the central-south coast before spreading more broadly during the Early Intermediate Period ([Lanning 1967; Patterson and Edward Moseley 1968; Pozorski and Pozorski 2008](#)).

Since the objects come from the first wave of excavations in the country (Section 2), inter-temporal differences in excavation methodologies are unlikely to have significantly influenced spatial coverage. However, the sample may reflect the acquisition priorities of the museum’s founder, as well as broader research priorities in the field of archaeology, potentially introducing an additional source of selection bias. The founder is best known for his research on the north coast (e.g., [Larco Hoyle 1938, 1941, 1944](#)). Although major coastal groups are represented in the data, the regional distribution of objects reflects this focus: 22 percent of the objects are from the north coast, 61 percent from the central-north coast, 16 percent from the central-south coast, and the remaining 1 percent from other regions.

It is worth noting that objects from the same group tend to be spatially concentrated within the group’s homeland, with objects from different groups forming distinct clusters across space. [Figure A.7](#) illustrates this pattern, mapping the spatial distribution

of sites with objects from the Early Intermediate Period by group. This evidence is consistent with the view that ceramics may not have been well suited for long-distance transportation (Morris 1995). It also aligns with evidence of limited population admixture during the pre-Inca period (Valverde et al. 2016; Nakatsuka et al. 2020).

Finally, although the Larco collection was closed and electronically cataloged, it is possible that the information recorded for each object reflects curatorial preferences. To account for this, all regressions include the year in which the object was electronically cataloged and archaeologist fixed effects, capturing any unobserved variation related to the individual responsible for curating the object’s information. We also present results based on standardized textual descriptions generated from the objects’ images, as well as results directly derived from the images.

4 Empirical Analysis

4.1 Culture and Identity in Pre-Colonial Peru

4.1.1 Baseline Regression Framework

Research on cultural identity has often relied on discrete classifications, creating markers of “belonging” and sharp distinctions between groups (Barth 1969; Huntington 1996). In this section, we systematically examine cross-sectional and inter-temporal cultural differences among human groups spanning two millennia of pre-Inca history, as revealed by the distinctiveness of ceramic style. We apply statistical and machine learning techniques to the objects’ images, text descriptions, and ceramic traits to generate continuous measures of distinctiveness (Section 4.1.2). These measures are independent of the pre-existing group classifications provided in the collection (G_i^j). Using the continuous measures of stylistic distinctiveness as outcome variables (y_i), we estimate

the following equation, separately for each period and region:

$$y_i = \alpha + \sum_{j=1}^J \delta_j G_i^j + X_i' \gamma + \epsilon_i \quad (1)$$

where i indexes an object, G_i^j is a dummy variable taking value one if object i is attributed to group j in the museum's collection (for $j = 1, \dots, J$), X_i is a vector of object-level control variables, and ϵ_i represents an error term.

We start by examining cross-sectional differences in stylistic distinctiveness. Specifically, we estimate Equation (1) separately for each of the four archaeological periods in our sample and test the joint statistical significance of the group indicators, in a spirit similar to [Desmet et al. \(2017\)](#). This allows us to examine whether ceramics from different groups, active during the same period, exhibit systematic differences in stylistic distinctiveness, on average. The equation is estimated by OLS, clustering standard errors at the site level to account for potential unobserved similarities among objects from the same site. We also report the results from using Conley standard errors to account for spatial autocorrelation ([Conley 1999](#)).

All regressions include a vector of object-level control variables (X_i), which incorporates the year each object was electronically cataloged and archaeologist fixed effects. A natural question is whether ceramic style merely reflects local geographic conditions. To help isolate cultural factors from purely geographic ones, we report the results from augmenting Equation (1) with a vector of geographic characteristics measured at the site level (W_s). This vector includes the site's absolute latitude, mean elevation, standard deviation of elevation, mean caloric suitability prior to AD 1500 ([Galor and Özak 2016](#)), log distance to the nearest river, and log distance to the coastline. Elevation and caloric suitability are measured within a 10km buffer around each site.

We then turn to inter-temporal differences in the distinctiveness of ceramic style. We estimate the same equation separately for one region at a time. Within a given region, we test the joint statistical significance of the group indicators to examine whether, on average, ceramics from groups that occupied the same geographical extent at different

points in time tend to exhibit systematic differences in stylistic distinctiveness. We present the results for the three regions: the north coast, the central-north coast, and the central-south coast, each of which is well documented in the archaeological literature (Willey 1971) and substantially represented in our data.

Importantly, we do not interpret the joint statistical significance of the group indicators as causal. In this part of the empirical analysis, given the nature of our data, we examine whether there is any statistically significant evidence that stylistic distinctiveness is systematically associated with group identity across space and time. We then quantify the degree of cultural differentiation within each period and region by examining the explanatory power of group indicators. Specifically, we measure how much additional variation in stylistic distinctiveness is explained when group indicators are included in the regression, as captured by the change in the adjusted R^2 relative to otherwise identical specifications without these indicators.

4.1.2 Measuring Stylistic Distinctiveness

We construct object-level measures of stylistic distinctiveness from three sources—the objects’ text descriptions, images, and ceramic traits. The objects’ text descriptions and images allow us to measure stylistic distinctiveness using a data-driven approach. We rely on text and image embeddings, which are becoming increasingly used in applied economics (e.g., Giorcelli et al. 2022; Adukia et al. 2023; Voth and Yanagizawa-Drott 2024). Nonetheless, some stylistic attributes related to modeling and decoration may not be fully captured. As a complementary approach, we draw on the repertoire of pre-defined ceramic traits (Table A.1) described in Section 3. This repertoire is based on the information curated by the museum’s team of archaeologists and covers a wide range of attributes, including morphological, molding, painting, and thematic attributes.

Text-based measures. We first measure stylistic distinctiveness at the object level using text descriptions. Specifically, we measure the distinctiveness of an object by comparing its description to those of benchmark objects—using a common, plain vessel

as a reference point provides an interpretable basis for comparison. We rely on sentence-based embeddings—a family of Natural Language Processing (NLP) techniques that transform text descriptions into numerical representations. These embeddings map each description into a high-dimensional vector such that semantically similar sentences are geometrically close in the resulting vector space. Cosine similarity is then used to summarize the degree of semantic similarity between objects’ descriptions, quantifying how close two embeddings are in the vector space.

To implement this approach, we proceed in three steps. First, we construct a set of benchmark ceramic objects that serve as a baseline for comparison—an *origin* point in the multi-dimensional space. These are plain vessels—without painted designs or molded adornments—randomly selected from the open-access online collection of ancient ceramics available on the [Metropolitan Museum of Art’s website](#). We use GPT-4o ([OpenAI et al. 2023](#)) to generate an objective English-language description of each benchmark object, providing the object’s image as input to the model.¹² [Figure A.8](#) displays the images and corresponding descriptions of the benchmark objects.

Second, we compute the cosine similarity score between each object in our pre-Inca database and each of the benchmark objects, based on their vector embeddings. We generate embeddings using three different models, separately: Sentence-BERT ([Reimers and Gurevych 2019](#)), RoBERTa ([Liu et al. 2019](#)), and OpenAI’s embedding model.¹³ Because the original Spanish-language descriptions provided by the [Larco Museum](#) may reflect archaeologists’ perceptions—and therefore correlate with the pre-existing group classifications (G_i^j)—we generate objective English-language descriptions for each object, as we did for the benchmark objects.¹⁴ These generated descriptions are then used to compute the embeddings. [Figure A.9](#) displays examples from the Moche and Nasca

¹²Descriptions are generated using a prompt that instructs the model to describe the object in an objective, matter-of-fact style, avoiding interpretations. We encode each image as a `base64` string. Although GPT-4o is not fully deterministic ([Atil et al. 2024](#)), we set the temperature parameter to zero in order to minimize the randomness of the output ([Renze 2024](#)).

¹³We use OpenAI’s `text-embedding-3-large` model.

¹⁴We follow the same procedure used for the benchmark objects, but adjust the prompt to instruct GPT-4o to adopt the voice of an academic archaeologist specializing in pre-Columbian Peru.

groups. As a robustness check, we additionally report the results from using the original Spanish descriptions. For these, embeddings are generated using a RoBERTa model pre-trained in Spanish; see [Figure A.10](#) for examples. Specifically, we use [Fandiño et al. \(2022\)](#)’s RoBERTa model, which has been pre-trained on 135 billion words from the Spanish Web Archive of the National Library of Spain.¹⁵

As a final step, we compute the average stylistic distinctiveness for each object in our pre-Inca database. We average across the benchmark set, as in [Ren Tan and Wang \(2024\)](#) and [Xue \(2024\)](#). Specifically, we calculate the object’s average cosine similarity with the three benchmark objects, for each embedding model separately. The lower the average similarity score, the more the object diverges from the plain benchmark forms, which is interpreted as higher distinctiveness.

Image-based measures. We complement our text-based analysis of stylistic distinctiveness with an image-based approach, which may capture stylistic features not fully represented in textual descriptions. To measure stylistic distinctiveness from images, we use a similar methodology: we (*i*) compare each object in our pre-Inca database to a benchmark object by computing the cosine similarity between their image embeddings, and then (*ii*) compute the average similarity score across benchmark objects.

To generate image embeddings, we use deep convolutional neural networks, specifically the VGG16 model ([Simonyan and Zisserman 2015](#)). VGG16 is a widely used architecture in computer vision, consisting of 16 weight layers—13 convolutional and 3 fully connected layers. Notably, it has been applied to a variety of image recognition tasks beyond its original training dataset ([Khan et al. 2020](#)). The model was originally trained on [ImageNet](#), a large-scale dataset of over two million labeled images spanning 1,000 classes ([Deng et al. 2009](#)). These include, for instance, more than 100 distinct classes of dogs and cats. We apply the VGG16 architecture to our collection of pre-Inca images, which come in a highly standardized format—all show the front view of the object, against a

¹⁵This model is part of the MarIA project, developed by the Barcelona Supercomputing Center and funded by the Spanish Secretariat for Digitalization and Artificial Intelligence (SEDIA).

similar background, and are approximately 380×285 pixels in size.

To meet the input requirements of the model, each image is resized to 224×224 pixels. The resized image is then passed through the VGG16 network. Finally, the output of the final layer prior to classification is extracted in order to save the object’s image embeddings.¹⁶ These embeddings provide a high-dimensional numerical representation of each object’s visual content. We use cosine similarity to measure the distance between each pre-Inca object and the benchmark objects in the embedding space (see [Figure A.11](#) for examples from Moche and Nasca). As before, we compute an average similarity score for each object by averaging its cosine similarity with the three objects in the benchmark set. Lower similarity indicates greater visual divergence from the plain benchmark forms and is interpreted as higher stylistic distinctiveness.

[Figure A.12](#) shows the densities of the four measures of stylistic distinctiveness, based on text and image embeddings, separately by period and region.

Trait-based measures. Our third approach relies on the repertoire of ceramic traits ([Table A.1](#)). We apply multiple correspondence analysis (MCA) to this repertoire in order to construct a composite measure of stylistic distinctiveness at the object level. MCA is a dimensionality reduction technique for categorical variables—a generalization of principal component analysis (PCA), applied to the relative frequencies of all possible combinations of categories in the data ([Greenacre and Blasius 2006; Nenadic and Greenacre 2007](#)). Since MCA operates on the cross-tabulation of all possible combinations of categories across variables, it is particularly well suited for datasets like ours, in which all variables (i.e., ceramic traits) are categorical; see [Kamdar and Ray \(2023\)](#) for a recent application in economics. We follow [Dolbunova et al. \(2023\)](#), who apply MCA to a dataset documenting the absence or presence of ceramic traits among European hunter-gatherers. In our case, we apply MCA to the vector of ceramic traits recorded for each object in the pre-Inca dataset. We then extract the scores from the first MCA dimension—which captures the

¹⁶Image processing and embedding are implemented using Keras, a Python-based deep learning library.

largest share of dispersion in the data—and interpret them as a continuous, composite measure of stylistic distinctiveness.

4.1.3 Baseline Results

Graphical analysis. We start by visually exploring differences in trait-based stylistic distinctiveness, based on MCA conducted on the full repertoire of ceramic traits. Figures 3 and 4 summarize cross-sectional and inter-temporal patterns, respectively. Each graph plots object-level scores on the first (x-axis) and second (y-axis) MCA dimensions, separately for different periods (Figure 3) and regions (Figure 4).

Objects belonging to the same group are displayed in the same color. For example, Graph B of Figure 3, corresponding to the Early Intermediate Period (AD 1–700), shows that Moche and Cajamarca objects are relatively separated in the MCA space. This evidence is consistent with archaeological interpretations suggesting that these groups had “few commonalities …, there is nothing that suggests the spread and sharing of a total corpus of beliefs” (Shimada 1999, p. 384). A similar pattern appears when comparing Recuay with Cajamarca, suggesting that “they participated in very distinct cultural traditions” (Lau 2006, p. 162). Graphs C and D show marked stylistic differences between Wari and Tiahuanaco during the Middle Horizon (AD 700–1000), and between Chimu and Chançay during the Late Intermediate Period (AD 1000–1400), respectively.

In Figure 4, each graph shows the data for a long-term sequence of cultural transitions within a given region, comparing objects from groups that occupied the same territorial extent at different points in time, successively. We focus on transitions involving the groups most extensively documented in the data—covering 26,843 objects and seven groups distributed across the three coastal regions.¹⁷ The sequences allow us to examine Wari’s expansion, highlighting regional contrasts that suggest greater cultural differentiation on the central-north coast, where Wari succeeded Moche (Graph B), than

¹⁷In the upper-north coast (Graph A) and the central-north coast (Graph B), the sequences span the four archaeological periods covered in the data. The sequence for the central-south coast covers the last three periods only (Graph C). While other groups can also be geographically assigned to these regions, it is less clear that they occupied overlapping territories over time.

on the central-south coast, where it succeeded Nasca (Graph C).

Despite these broad patterns, all graphs reveal some degree of stylistic overlap between groups. This overlap suggests that analyzing continuous differences in stylistic distinctiveness, rather than discrete differences, can help us better understand the variation in the data across space and time. In what follows, we formally test whether differences in stylistic distinctiveness between ceramics from different groups are statistically significant, using the set of continuous measures described in Section 4.1.2. We then examine the extent to which these differences may be driven by systematic variation in the geographic environment or by geographic distance alone. We also conduct placebo tests based on random assignments of fictitious group identities.

Regression analysis: stylistic distinctiveness across space and time. Tables 1 and 2 present the results from estimating Equation (1) by OLS at the object level, separately for each period (top panels) and region (bottom panels). Standard errors are clustered at the site level. In Table 1, the outcome variable is the trait-based measure of stylistic distinctiveness (i.e., the score of the first dimension after applying MCA to the full repertoire of ceramic traits). In Table 2, the outcome variables are our measures of stylistic distinctiveness based on text and image embeddings. All regressions include the year each object was electronically catalogued and archaeologist fixed effects (X_i), with standard errors clustered at the site level.

We first examine cross-sectional differences in stylistic distinctiveness, analyzing the results for different periods of pre-Inca history. On average, ceramics from different groups, active during the same period, tend to exhibit systematic differences. Columns 1 and 2 of Table 1 report the F-statistic and the p-value for the joint statistical significance of group fixed effects, respectively, using the measure of stylistic distinctiveness based on ceramic traits. Differences in trait-based stylistic distinctiveness between ceramics from different groups are statistically significant at the 1 percent level in all periods.

Since the groups in our sample generally occupied distinct territories (Section 3), differences in the geographic environment may help explain cultural differences (Galor

and Özak 2016; Buggle and Durante 2021). On average, local geographic factors such as absolute latitude, terrain elevation, and proximity to water are individually associated with stylistic distinctiveness (Figure A.13), suggesting that environmental conditions contributed to shaping symbolic contents. Nonetheless, controlling for geography in Equation (1) does not affect the statistical significance of group fixed effects in any period. In columns 5 and 6 of Table 1 (top panel), we report F-test results after controlling for the vector of site-level geographic characteristics (W_s)—cross-sectional differences in stylistic distinctiveness persist after accounting for geography.

Group fixed effects account for a considerable share of the cross-sectional variation in stylistic distinctiveness, though their explanatory power varies across periods. First, the adjusted R^2 of regressions with cataloging year, archaeologist fixed effects, and group fixed effects averages 51 percent across periods, ranging from 25 to 68 percent (column 4). Including group fixed effects leads to an average increase in the adjusted R^2 of 18 percent (columns 3 and 4). After controlling for geography, group fixed effects continue to explain additional variation in stylistic distinctiveness, with increases in the adjusted R^2 ranging from 1 to 7 percent (columns 7 and 8). Once group affiliation is controlled for, geography explains only a small share of the remaining variation in stylistic distinctiveness (0.8 percent, on average; columns 4 and 8 and Figure A.14).

Second, across regressions with outcomes based on text and image embeddings (top panels of Table 2), the explanatory power of group fixed effects is consistently notable for the Early Horizon (700 BC–AD 1) and the Middle Horizon (AD 700–1000). All regressions include geography controls, cataloging year, and archaeologist fixed effects. In line with trait-based results, group fixed effects are jointly statistically significant in all periods. For the Early and Middle Horizons, the inclusion of group fixed effects increases the adjusted R^2 by 3 to 10 percent (columns 3 and 6). This is particularly noteworthy given the relatively lower variance of embedding-based outcomes, compared to trait-based ones (see Figure A.15), as well as the fact that these regressions include the full set of control variables.

These results align with archaeological interpretations suggesting that political

instability and socioeconomic stress may lead to greater differentiation in material culture (Hodder 1979; Jones 1997). During the Early Horizon, coastal valleys experienced episodes of escalated inter-community conflict, as evidenced by cranial trauma and the presence of defensive settlements, which together have been interpreted as signs of warfare (Arkush and Tung 2013). The Middle Horizon was marked by the expansions of Wari and Tiahuanaco, which extended far beyond their respective heartlands in the central highlands and Lake Titicaca, incorporating coastal groups. Evidence of cranial trauma is more prevalent for Wari—particularly in southern Peru—suggesting that violence may have played a more relevant role in their territorial expansion (Arkush and Tung 2013).¹⁸ Archaeological evidence suggests that both Wari and Tiahuanaco used religious activities to promote group identity (Nash and Williams 2004, 2016; Isbell 2008). One advantage of our approach is that it allows us to examine cultural differentiation by measuring the extent to which group identity explains variation in stylistic distinctiveness, rather than focusing solely on the number of groups.

The bottom panels of Tables 1 and 2 show the F-test results from inter-temporal regressions. We consider a long-term series of group transitions in a given region (as in Figure 4) and test the joint statistical significance of group fixed effects. Inter-temporal differences in stylistic distinctiveness are statistically significant at the 1 percent level, both before and after geography controls. Ceramics from different groups—active in the same region but in different periods of pre-Inca history—tend to exhibit systematic differences in stylistic distinctiveness, on average. When examining trait-based results, we find that including group fixed effects increases the adjusted R^2 by an average of 27 percent across regions, relative to regressions that include only cataloging year and archaeologist fixed effects (columns 3 and 4 of Table 1). Even after accounting for any remaining geographic variation within regions, the inclusion of group fixed effects leads to a substantial increase in the adjusted R^2 (14 percent, on average; see columns 7 and 8 of Table 1). Consistent with the graphical evidence, the increase in explanatory power

¹⁸Conflict during the Late Intermediate Period seems to have escalated primarily in the Andean highlands (Isbell and Silverman 2008; Arkush and Tung 2013).

is larger for the north coast (11–24 percent) than for the central-south coast (6 percent). Embedding-based results show a similar regional contrast, particularly when comparing the central-north and central-south coasts ([Table 2](#)).

The results from inter-temporal regressions suggest that group identity is a stronger predictor of cultural differences in regions with a longer history of political centralization. Wari was an expansionist society during the Middle Horizon (AD 700–100), characterized by a four-tiered site hierarchy, administrative centers, and palaces ([Isbell and Schreiber 1978](#))—consistent with state-level organization in [Murdock \(1967\)](#)'s *Ethnographic Atlas*. In the north, Wari expanded into valleys previously controlled by Moche; in the south, it expanded into areas occupied by Nasca. During the Early Intermediate Period (AD 1–700), Moche expanded across multiple northern valleys, constructing monumental pyramids (e.g., *Huaca del Sol* and *Huaca de la Luna*) and establishing site hierarchies as well ([Stanish 2001](#))—there is no such archaeological evidence for Nasca on the southern coast.¹⁹ The northern expansion of Wari prolonged a history of centralized political rule in the region that spanned ten centuries; a history later continued by the Chimor Kingdom in former Moche territory during the Late Intermediate Period (AD 1000–1400). These results connect to research highlighting the role of state experience throughout history ([Bockstette et al. 2002](#); [Borcan et al. 2018](#)).

In [Table A.2](#), we show the results from regressions that pool all groups and objects in the dataset, after including the full set of control variables and region fixed effects. The increase in the adjusted R^2 associated with the inclusion of group fixed effects closely mirrors the average increase observed in region-by-region regressions (14 percent), alleviating concerns that regional differences in sample size may be influencing the results. Group fixed effects are jointly statistically significant across all outcomes. A similar exercise cannot be conducted for period-by-period regressions (i.e., estimating a pooled regression with both group and period fixed effects), as each group is present in only one period. We return to this point in sections [4.1.4](#) and [4.2](#).

Overall, our results show that stylistic distinctiveness is systematically associated

¹⁹The evidence of political centralization prior to Moche is limited ([Stanish 2001](#); [Tantaleán 2021](#)).

with group identity in the data. At the same time, the explanatory power of group fixed effects reveals interesting heterogeneity across both periods and regions. The next paragraphs describe supplementary analyses and robustness exercises. Our results may also reflect meaningful variation in stylistic distinctiveness across objects from the same group—a point we explore in Section 4.2.

Fictitious group identities. To examine whether our baseline results could have arisen by chance, we conduct a series of placebo tests by randomly assigning fictitious group identities to the objects. These placebo tests are especially important given the relatively small number of groups involved in the previous regressions. We randomly assign a group identity to each ceramic object while preserving the original group sizes (i.e., maintaining the number of ceramic objects per group as in the original data). We repeat the random assignment of fictitious group identities 1,000 times, separately for each period and region. In each iteration, we estimate the full specification (i.e., with geography controls, cataloging year, and archaeologist fixed effects) and test whether the fixed effects for the fictitious group identities are jointly significant at the 1 percent level. Table A.3 summarizes the results for the five outcomes of stylistic distinctiveness. Fictitious group fixed effects are jointly significant only in a small fraction of cases (2.2 percent, on average, across all regressions). Figures A.16 to A.20 show the distributions of the placebo F-statistics across the 1,000 iterations, by period and region, for each outcome. The relatively small size of these placebo F-statistics—compared to those obtained from regressions using the original group identities—supports the interpretation that the association between stylistic distinctiveness and group identity observed in the original data is unlikely to have arisen by chance.

Spatial autocorrelation and robustness checks. Geographic proximity may systematically contribute to cultural similarity. Groups that were geographically close (e.g., Moche and Recuay, who were neighbours in the north) may have shared symbolic repertoires or trade connections that probably influenced their ceramic styles. This is likely to

affect our cross-sectional regressions more significantly. In Tables A.4-A.7, we formally examine whether the joint statistical significance of group fixed effects is affected by spatial autocorrelation. Specifically, we report F-test results from using standard errors adjusted for spatial autocorrelation (Conley 1999), based on the geographic coordinates of the sites. Groups fixed effects remain statistically significant across all outcomes, at both 50km and 100km distance cutoffs.

In Table A.8, we use frequency-based embeddings (TF-IDF), constructed from the objects' English-language descriptions, to measure stylistic distinctiveness. In Table A.9, we use sentence-based embeddings, generated with the RoBERTa model pre-trained in Spanish (Fandiño et al. 2022), based on the original Spanish-language descriptions instead. The results support the joint statistical significance of group fixed effects.

Beyond material form. Although morphology may also convey symbolic meaning (e.g., Costin 2016), in Table 3 we focus on the variation in stylistic distinctiveness that is not explained by differences in material form. We present the results from two empirical exercises. First, we directly analyze whether differences in stylistic distinctiveness persist after accounting for object form (Panel A). Specifically, we extend Equation (1) by including dummy variables for morphological types (i.e., open forms, closed containers, and molded sculptures). Second, we save the residuals from regressions of stylistic distinctiveness on morphological type fixed effects, and use these residuals as outcome variables in Panel B. This exercise allows us to isolate the variation in stylistic distinctiveness that is not explained by differences in material form. The results are reported for the image-based measure of stylistic distinctiveness in Table 3. Table A.10 reports consistent results for the other measures of stylistic distinctiveness.

The results are consistent with our previous findings, showing statistically significant group fixed effects, and reinforcing that group identity tends to be a stronger predictor of cultural differences during more conflictive periods (i.e., horizon periods) and in regions with a longer history of political centralization (i.e., northern regions). If anything, the explanatory power of group identity is amplified, particularly during the Early

Horizon. Overall, these results suggest that differences in stylistic distinctiveness cannot be explained solely by variation in morphology, or in the geographic environment of objects, motivating a closer examination of whether the differences linked to group identity are connected to specific cultural traits, symbolically embedded in material form (Section 4.1.4).

4.1.4 The Symbolic Content of Ceramics

Is stylistic distinctiveness related to specific cultural traits? Having established that group identity is systematically associated with stylistic distinctiveness, we now examine whether the differences between groups are related to symbolic cultural meanings. Our approach proceeds in two steps. First, we run a full-sample OLS regression of image-based stylistic distinctiveness on group fixed effects and baseline controls (geography, cataloging year, and archaeologist fixed effects) at the object level, clustering standard errors at the site level. We then save the estimated coefficients on the group fixed effects. These coefficients provide a continuous, group-level measure of the differences in stylistic distinctiveness captured by group identity. We refer to this measure as group-retrieved stylistic distinctiveness.

Second, we test whether the differences in stylistic distinctiveness are systematically associated with thematic content. Using the repertoire of ceramic traits (Table A.1), we construct a dummy variable equal to one if a theme is present—either in sculpted or in painted form—and zero otherwise. For example, if an object has fertility symbology in sculpted (*trait 42*) and/or painted (*trait 73*) form, the fertility dummy equals one. Considering the full sample (30,212 objects), we then regress each thematic dummy on the group-retrieved measure of stylistic distinctiveness. Since this measure is estimated in the first stage, it is subject to measurement error. Following Bertrand and Schoar (2003), we address this by weighting observations by the inverse of the standard errors from the first-stage estimates of the group fixed effects.

OLS estimates. Table 4 reports the results for the religious, fertility, death, agriculture, fishing, and war-related thematic traits. In Panel A, the regressions include baseline controls (i.e., geography, cataloging year, and archaeologist fixed effects). In Panel B, the regressions additionally include dummy variables for morphological types (i.e., open forms, closed containers, and molded sculptures). Panel C reports the results from more saturated specifications that include period and region fixed effects. In this case, period fixed effects can be included in the specification because the group-retrieved measure of stylistic distinctiveness is a continuous measure, though the specification becomes more saturated. In Table 4, we report the results with standard errors clustered at the Group×Region level (25 clusters).²⁰ Table A.11 shows the results with standard errors clustered at the group level (12 clusters) and with standard errors adjusted for spatial autocorrelation (Conley 1999).

The group-retrieved measure of stylistic distinctiveness is normalized between 0 and 1, with 1 corresponding to the group with the highest value—Wari—and 0 to the group with the lowest value—Cupisnique. Thus, a one-unit increase reflects the full difference between Cupisnique and Wari. A 0.9-point increase corresponds roughly to the difference between Wari and Tiahuanaco, for example, while a half-point increase is equivalent to the difference between Wari and Moche. Stylistic distinctiveness, as captured by group identity, is positively associated with religious (column 1) and war-related (column 6) representations. On average, holding other factors constant, a one-unit increase in stylistic distinctiveness is associated with an 8 percent increase in the probability of religious symbology and with a 2 percent increase in the probability of war-related symbology, relative to sample means of 13 percent and 3 percent, respectively.²¹

Coarsened exact matching. Table 5 shows consistent results from a matching analysis. We create a subsample of objects that differ in their level of group-retrieved stylistic distinctiveness but are statistically comparable along key covariates. Specifically,

²⁰83 percent of the objects are from groups that extend over more than one region.

²¹The correlation between religious and war-related thematic traits among objects is 6 percent.

we apply the Coarsened Exact Matching (CEM) algorithm of Iacus et al. (2012), stratifying the sample at the median level of group-retrieved stylistic distinctiveness. The algorithm produces a matched subsample of 5,697 objects (about 20 percent of the sample). Each stratum contains objects above and below median stylistic distinctiveness that are (*i*) statistically similar in terms of geography and cataloging year, and (*ii*) exactly matched on form type and archaeologist identity. Panel A shows the results with geography and cataloging year as control variables. In Panel B, we compare the thematic content of objects within each stratum by including stratum fixed effects.²² Panel C shows the results from more saturated specifications that include period and region fixed effects. [Table A.12](#) shows alternative standard errors.

Religious domains. The previous results suggest that the religious symbology positively associated with stylistic distinctiveness is not primarily connected to fertility or death-related domains (columns 2–3 of tables [4](#) and [5](#)). Fertility and death-related contents tend to be broadly shared across groups, conditional on baseline covariates. In our data, the religious category includes two dimensions: (*i*) ancestor-related ceremonial symbology, which includes ceremonial representations related to ancestors and *hanan pacha* (the upper world), and (*ii*) creation-related symbology, which involves representations of anthropomorphic and mythological beings related to cosmological origins and creation narratives.²³ In [Table A.13](#), we examine these two dimensions, separately. The results suggest that creation-related symbology is the main driver of the positive association between stylistic distinctiveness, as captured by group identity, and religious imagery (columns 1–2). Consistently, columns 3–4 show that animal motifs related to supernatural-religious beliefs (e.g., snake- and feline-related deities; Shimada 1999) are positively associated with group-retrieved stylistic distinctiveness; see [Table A.14](#) for alternative standard errors. These findings align with archaeological interpretations of religious beliefs in the study setting, where “creation deities, especially, had the power

²²Note that form type and archaeologist identity are absorbed by the stratum fixed effects.

²³The correlation between the indicator for ancestor-related religious representations and the indicator for death-related representations is 13 percent among objects.

to visit abundance or scarcity of irrigation waters on the desert coast of Peru” (Nash and Williams 2016).

Time-varying estimates: religious symbology and zero-sum environments. Zero-sum perceptions, where the gains of one group are believed to imply losses for others, have been closely linked to religious beliefs in contexts of resource stress (Foster 1965; Bergeron et al. 2024). In the study setting, such dynamics may have been especially pronounced during horizon periods, characterized by territorial occupations and warfare. We test whether the association between religious symbology and group-retrieved stylistic distinctiveness strengthened during these periods. Specifically, we estimate regressions that interact period fixed effects with the group-retrieved measure of stylistic distinctiveness.

Figure 5 plots the estimated coefficients on these interactions relative to sample means, using the Late Intermediate Period as the omitted category. The results show that stylistic distinctiveness, as captured by group identity, is positively and significantly associated with religious symbology during horizon periods. War- and death-related themes also tend to intensify, particularly death-related contents.²⁴ This pattern suggests that religious beliefs became a salient marker of group identity during expansionist, zero-sum phases of pre-Inca history. It also aligns with archaeological evidence suggesting that religious activities played a role in promoting group identity during the Middle Horizon (see Section 4.1.3).

4.2 Identity Formation: The Role of Political Centralization

4.2.1 Cultural Dispersion and Political Centralization

In the first part of the paper, we document that group identity helps explain the stylistic and thematic content of ceramics, particularly in regions with a longer history of political centralization (Section 4.1.3). In this second part, we investigate the formation of group

²⁴The correlation between the war and death-related indicators among objects is 8.5 percent.

identity. Specifically, we explore whether greater political centralization contributed to a stronger cultural identity, reflected in lower stylistic and thematic dispersion among objects from the same group. This analysis connects to recent work showing that historical political centralization can shape culture (Becker et al. 2016; Lowes et al. 2017; Heldring 2021). For the study region, Shimada (1999, p. 388) notes that “not surprisingly, we see a notable population increase ... hand in hand with increasing sociopolitical complexity and concern for and sophistication in material expression of their identity, including their cosmological visions and political dogma.”

We estimate regressions of the following form, using repeated cross-sections of sites from the four periods in the sample (422 sites):

$$CulturalDispersion_{sjt} = \beta_0 + \beta_1 PoliticalCentr_{jt} + X'_{sjt}\theta + X'_{jt}\phi + \varepsilon_{sjt} \quad (2)$$

where $CulturalDispersion_{sjt}$ denotes the degree of within-site stylistic or thematic variation for site s of group j in period t ; $PoliticalCentr_{jt}$ denotes the group’s level of political centralization; X_{sjt} is a vector of site-level controls, and X_{jt} is a vector of group-level controls. Each site in a given period was occupied by a single group. The main coefficient of interest in Equation (2), β_1 , captures the association between within-site cultural dispersion and the corresponding group’s level of political centralization, pooling all sites in the sample. Lower within-site stylistic and thematic dispersion—among objects from the same group—is interpreted as evidence of a stronger cultural identity, in the same spirit as in Hodder (1982). We also report the results from more saturated specifications that include period and region fixed effects.²⁵

In what follows, we describe the data, present OLS estimates, and then report the results from a 2SLS strategy to mitigate concerns about omitted variable bias and reverse causality. We present the results with standard errors clustered at the Group \times Region level.²⁶ In the Appendix, we report standard errors clustered at the group level and

²⁵Half of the period \times region combinations include sites from two or three groups, while the other half include sites from only one group.

²⁶325 out of 422 sites are from groups that extend over more than one region.

adjusted for spatial autocorrelation. We also report the results from using wild cluster bootstrap inference (Cameron et al. 2008).

Measuring cultural dispersion. We construct proxies for within-site cultural dispersion using two approaches. First, we compute the standard deviation of stylistic distinctiveness across all objects from a site, using our measures based on text and image embeddings. Second, we compute an index of thematic fractionalization at the site level, based on the share of objects classified by theme (Table A.1).²⁷ We exclude sites with fewer than four objects (the 25th percentile), resulting in a sample of 422 sites. The mean level of thematic fractionalization across sites is 0.52, with a median of 0.66.

Measuring political centralization. We construct a group-level index of political centralization. Following Stanish (2001), we focus on evidence of political complexity, such as (*i*) administrative centers and (*ii*) monumental structures including temples, palaces, and public platforms (see also Mayshar et al. 2022; Artiles 2025). For each group, we aggregate in-text references to political complexity from comprehensive archaeological sources (Lanning 1967; Silva Sifuentes 2000; Isbell and Silverman 2002, 2008) and normalize the index between 0 and 1—Wari ranks highest, followed by Moche. The resulting index aligns with archaeological evidence of site hierarchies (e.g., Stanish 2001; Tantaleán 2021), which have been interpreted as indicative of more centralized political power (Flannery 1998).

OLS estimates. Table 6 reports OLS estimates for the coefficient on political centralization ($\hat{\beta}_1$). In column 1, the outcome variable is the index of thematic fractionalization, constructed from the share of objects classified by theme. Columns 2 and 3 use the standard deviation of stylistic distinctiveness across objects within a site as the outcome, based on SBERT text embeddings (column 2) and VGG16 image embeddings (column 3), respectively. Column 4 reports the Average Effect Size (AES, Clingingsmith et al.

²⁷Because objects can be linked to more than one theme, we assign each object to the theme with the highest score based on its textual description.

2009) across all proxies of cultural dispersion, including thematic fractionalization and embedding-based measures of stylistic dispersion (for SBERT, RoBERTa, and OpenAI text embeddings, as well as VGG16 image embeddings). All variables are standardized to have a mean of zero and a standard deviation equal to one.

Panel A shows the results with a vector of baseline controls. This vector includes a set of site-level controls (X_{sjt}) and a dummy variable equal to one if the number of mentions found for the group in the corresponding period is above the median (i.e., to account for the fact that political centralization is constructed from references to political complexity). The set of site-level controls includes the share of open-form objects, the share of close-form objects, the log of the number of objects, and time-invariant geography controls (absolute latitude, mean elevation, standard deviation of elevation, mean caloric suitability prior to AD 1500, log distance to the nearest river, and log distance to the coastline). The estimated average effect size in column 4 indicates that a one standard deviation increase in political centralization is associated with a 0.29 standard deviation decrease in within-site cultural dispersion, on average. [Figure 6](#) presents binscatters for the estimated relationship.

Panel B of [Table 6](#) shows consistent results when adding group-level controls (X_{jt}) to account for historical group size. Specifically, we control for the log of land area and the log of the number of sites.²⁸ These controls refer to the group's historical homeland, considering all 10×10 km grid cells with sites attributed to the group in the corresponding period (i.e., occupied cells). Panel C presents results from more saturated specifications that also include period and region fixed effects. The standardized average effect size remains stable across the three panels. [Table A.15](#) reports standard errors clustered at the group level and adjusted for spatial autocorrelation (columns 1-3). Columns 4-6 of [Table A.15](#) report the results from wild cluster bootstrap ([Cameron et al. 2008](#)).

As [Shimada \(1999\)](#) points out, sociopolitical complexity, standards of living, and identity seem to have evolved together, preventing us from interpreting our estimates

²⁸Unfortunately, population data are not available to compute population density for all groups as a proxy for pre-industrial development ([Ashraf and Galor 2011](#)).

causally. To move closer to a causal interpretation, one approach would be to compare within-site cultural dispersion across geographically close sites, focusing on sites from pairs of groups with contrasting levels of political centralization in the same period. In practice, only a small number of such pairs are available in the Early Intermediate Period and the Middle Horizon, which prevents this strategy from being applied systematically across all periods. In what follows, we complement the analysis with a 2SLS approach.

2SLS estimates. The Peruvian coast is among the driest regions of the world (Ochoa et al. 2025). The first stage of our 2SLS approach builds on the idea that pre-industrial political hierarchies were more likely to emerge where geoclimatic conditions created high expected returns to large-scale irrigation—a hypothesis classically advanced for arid regions such as ancient Egypt (Wittfogel 1957). Bentzen et al. (2017) show that societies historically more dependent on irrigation are more likely to be governed by authoritarian regimes today. Exploiting river shifts in ancient Mesopotamia, Allen et al. (2023) show that the demand for coordinating irrigation after rivers changed course led to the formation of early states. In our setting, reliance on irrigation agriculture expanded from the Early Horizon and intensified during the Early Intermediate Period (e.g., Moore 2014). Archaeological studies of the coastal valleys suggest that controlling irrigation systems contributed to the consolidation of leaders' authority and the centralization of political power (Steward 1949, 1971; Billman 2002). We explore whether political power was more centralized where adopting large-scale irrigation systems for cultivation under arid conditions had relatively higher expected returns.

To mitigate endogeneity concerns, we avoid using archaeological evidence of actual irrigation (e.g., canals) as an instrument for political centralization. We first consider measures of irrigation potential, as in Bentzen et al. (2017). The FAO's Global Agro-Ecological Zones (GAEZ) project provides data on potential irrigation impact based on modern soils (i.e., maximum attainable yield under irrigation *versus* rainfed conditions). However, this source detects little variation along the Peruvian coast, especially in the north (Table A.16). Furthermore, archaeological evidence suggests that larger areas

were irrigated in the past than today in the coastal valleys (Clement and Moseley 1991), and whether this difference reflects varying soil conditions is unclear. As an alternative, we consider exposure to perennial water. Perennial rivers originating in the highland Andes and flowing into coastal valleys were an important water source for irrigation systems (Caramanica 2024). We examine whether greater exposure to perennial rivers is associated with the adoption of large-scale irrigation, as less costly access to water may have increased the expected returns, and political centralization. Since it cannot be ensured that exposure to perennial rivers strongly correlates with political centralization while not directly affecting within-site cultural dispersion, we assess the exclusion restriction using the plausibly exogenous framework of Conley et al. (2012), complemented with placebo exercises.

As a proxy for exposure to perennial water, we compute the log of total perennial river length within each group’s historical homeland (i.e., the set of $10 \times 10\text{km}$ grid cells occupied by the group in the corresponding period). To compute this measure, we use the river basemap from the Seamless Digital Chart of the World (SDCW).²⁹ Figure A.21 shows the density of log perennial river length at the group level. In Figure A.22, we examine its relationship with evidence of canals. We construct a normalized index of canal infrastructure at the group level, based on in-text references to canals during the corresponding period. The top graph of Figure A.22 suggests a positive correlation between exposure to perennial rivers and the canal index across groups, although this should be interpreted cautiously given the small sample size. The raw data also suggest a positive correlation between political centralization and the canal index (bottom graph).

Figure 7 shows that exposure to perennial rivers is also positively associated with political centralization across groups (Panel A). To compare groups exposed to similar climatic conditions, potentially influencing the possibility of crop cultivation in arid settings, we control for mean temperature and temperature stability. Specifically, for each group’s historical homeland, we compute mean temperature and mean temperature stability (i.e., isothermality), averaging across centuries within the corresponding period.

²⁹Note that this measure does not capture water volume or floodwaters (Caramanica et al. 2020).

We use the high-resolution paleo-climate reconstructions from the CHELSA-TraCE21k project (Karger et al. 2023; see Flückiger et al. 2024 for a recent application). Panel B shows this positive association in the sample of sites, after controlling for site-level geography controls. In Table 7, we examine whether political centralization affects within-site cultural dispersion, instrumenting political centralization with the group’s log perennial river length, and report first stage F-statistics for the sample of sites.

Columns 1 to 3 of Table 7 show the results for the site’s level of thematic fractionalization, columns 4 to 6 for text-based stylistic dispersion (SBERT), and columns 7 to 9 for image-based stylistic dispersion (VGG16). In each case, the first column includes baseline controls, along with the group’s log mean temperature and mean temperature stability. The second column additionally controls for log land area and log number of sites at the group level. The third column adds period and region fixed effects. The first stage F-statistic is strong, and Anderson-Rubin tests suggest no power asymmetry concerns (Keane and Neal 2024). Overall, the estimated negative coefficient on political centralization aligns with the hypothesis that greater political centralization contributed to lower cultural dispersion.

Table A.17 shows reduced-form estimates for the specification with group-level controls (i.e., columns 2, 5 and 8 of Table 7). Consistent with our previous results, log river length is negatively associated with cultural dispersion, particularly for our measures of thematic fractionalization and text-based stylistic dispersion. This negative association remains significant when controlling for mean caloric suitability (Galor and Özak 2016) and maize’s caloric suitability (Mayshar et al. 2022). We use Conley et al. (2012)’s plausibly exogenous framework to examine the extent to which the direct effect of log river length should be sizable enough for the coefficient on political centralization to become insignificant. Figure A.23 displays 95-percent confidence intervals for the estimated coefficient on political centralization, using the union of confidence intervals (UCI) approach. The coefficient on political centralization remains statistically significant under varying assumptions about the potential support of the direct effect.

Placebo evidence and robustness checks. In columns 1-3 of [Table 8](#), we show consistent results when using the log of perennial river length, computed only for the portion of the group’s homeland with evidence of political complexity (i.e., 10×10 km grid cells with evidence of administrative centers and monumental structures only). The estimates correspond to the specification with group-level controls. As a placebo, we compute the log of perennial river length using random portions of each group’s homeland without evidence of political complexity. Columns 4-6 present results for a 20 percent random sample of grid cells, while columns 7-9 present results for a 60 percent random sample. We find no significant results when perennial river length is based on these random portions of the groups’ homelands. [Table A.18](#) reports results for the total length of perennial rivers, without logarithmic transformation.

[Table A.19](#) reports 2SLS results with standard errors clustered at the group level and adjusted for spatial autocorrelation. [Table A.20](#) reports consistent results when instrumenting political centralization with the log of river density, defined as the total length of perennial rivers divided by the group’s historical area. In this case, we do not include the log of the group’s area as a control variable.

4.2.2 Evidence on Contemporary Attitudes

As a final step, we explore whether historical political centralization helps explain lower dispersion in contemporary attitudes. For this analysis, we use individual-level survey data from the Peruvian ENAHO household survey for 2007–2017. The survey includes a module on attitudes toward political institutions. We focus on a set of 40 categorical questions consistently asked across survey years, covering governance-related attitudes, perceptions of democracy, transparency, and confidence in institutions.³⁰

We construct an individual-level measure of average cultural distance. First, for each question, we compute the average distance between an individual’s answer and those of other respondents in the same district (the third administrative level in Peru). Specifically, since the set of possible responses to a question q is an ordered set (e.g.,

³⁰Unfortunately, the survey does not cover attitudes on other topics such as gender or religion.

“nothing”, “a little”, “enough”, “quite a lot”), we measure the relative distance between individual i and respondent n as $|r_i^q - r_n^q|/(D(q)) \in [0, 1]$, where r_i^q and r_n^q denote their responses to question q and $D(q)$ is the maximum possible distance for that question. Second, we then average across respondents in the same district-year to obtain an individual-level measure of average distance for each question. We use the average distance across questions, in a spirit similar to Desmet et al. (2017), as the dependent variable in individual-level regressions.

We measure historical political centralization at the district level. Specifically, we construct two measures of average centralization, based on the groups that occupied a district’s territory in pre-colonial times. The first is a simple average of political centralization across all groups present during the four pre-Inca periods. The second is a time-weighted average, where each group’s political centralization is weighted by the share of centuries that the group occupied the district’s territory.³¹ We examine the estimated coefficient on the average level of pre-colonial political centralization, clustering standard errors at the district level. The ENAHO survey covers individuals from 57 districts in our study region (i.e., 172 districts with pre-colonial objects).

Table 9 reports the results. All regressions include individual-level controls (gender dummy, age, age squared, and education dummies), to compare individuals with similar socioeconomic characteristics, as well as district-level controls (mean elevation, standard deviation of elevation, mean caloric suitability, log area, longitude, and latitude), year fixed effects, and province fixed effects. All variables except dummies are standardized to have zero mean and standard deviation equal to one.

Columns 1 and 2 present OLS estimates. The estimated coefficient on historical political centralization is negative, consistent with previous findings (Table 6), and becomes statistically significant when using time weights to measure average centralization (column 2). A one standard deviation increase in pre-colonial political centralization

³¹The Inca Empire extended across the entire region during AD 1400–1525. Our measures refer to the four pre-Inca periods and do not consider the Inca’s level of centralization (corresponding to a large state), which would enter equally into the computation for all districts, since political centralization is assigned at the group level.

is associated with a 0.13 standard deviation decrease in average cultural distance, on average (column 2). Columns 3 and 4 report consistent 2SLS estimates, instrumenting pre-colonial political centralization with the log of perennial river length within pre-colonial homelands, using either the simple average (column 3) or the time-weighted average (column 4) at the district level. The results are similar when standard errors are adjusted for spatial autocorrelation (at 50km and 100km thresholds), based on the geographic coordinates provided by ENAHO.

5 Conclusion

This paper examines the evolution of cultural differences in pre-industrial Peru. We use a novel dataset of approximately 30,000 ceramic objects spanning two millennia before the rise of the Inca Empire, analyzed through statistical and machine-learning techniques. We document that stylistic distinctiveness in ceramics is systematically associated with group identity. We also provide descriptive evidence that the explanatory power of group identity is stronger during more conflictive periods and in regions with a longer history of political centralization. An analysis of the symbolic content of ceramics shows that religious themes are key drivers of stylistic distinctiveness, especially during more conflictive periods. Finally, using an instrumental-variables identification strategy, we show that political centralization systematically reduces cultural dispersion, as reflected in stylistic and thematic variation among objects from the same group. We find consistent evidence when examining dispersion in present-day attitudes.

While our results highlight systematic evidence on the evolution of culture and identity, they should be interpreted cautiously given the limitations of archaeological sources. Nonetheless, integrating more granular archaeological data with economic analysis offers a promising avenue to advance our understanding of cultural evolution and the processes through which group identity takes shape in the long run.

References

- Acemoglu, Daron and James A Robinson**, “Culture, Institutions and Social Equilibria: A Framework,” *Journal of Economic Literature*, 2024. forthcoming.
- Adukia, Anjali, Alex Eble, Emileigh Harrison, Hakizumwami Birali Runesha, and Teodora Szasz**, “What We Teach About Race and Gender: Representation in Images and Text of Children’s Books*,” *The Quarterly Journal of Economics*, 2023, 138 (4), 2225–2285.
- Akerlof, George A and Rachel E Kranton**, “Economics and Identity,” *The Quarterly Journal of Economics*, 2000, 115 (3), 715–753.
- Alesina, Alberto, Paola Giuliano, and Nathan Nunn**, “On the Origins of Gender Roles: Women and the Plough,” *The Quarterly Journal of Economics*, 2013, 128 (2), 469–530.
- Algan, Yann and Pierre Cahuc**, “Trust and Growth,” *Annual Review of Economics*, 2013, 5 (1), 521–549.
- Allen, Robert C, Mattia C Bertazzini, and Leander Heldring**, “The Economic Origins of Government,” *American Economic Review*, 2023, 113 (10), 2507–2545.
- Alsan, Marcella and Marianne Wanamaker**, “Tuskegee and the Health of Black Men,” *The Quarterly Journal of Economics*, 2018, 133 (1), 407–455.
- Andersen, Lars Harhoff and Jeanet Bentzen**, “In the Name of God! Religiosity and the Production of Science,” 2025. Working Paper.
- Arkush, Elizabeth and Tiffiny A Tung**, “Patterns of War in the Andes from the Archaic to the Late Horizon: Insights from Settlement Patterns and Cranial Trauma,” *Journal of Archaeological Research*, 2013, 21, 307–369.
- Artiles, Miriam**, “Ethnic Diversity, Historical Economic Exchange, and Development: Evidence from Andean Peru,” *American Economic Journal: Applied Economics*, 2025. Forthcoming.
- Ashraf, Quamrul and Oded Galor**, “Dynamics and Stagnation in the Malthusian Epoch,” *American Economic Review*, 2011, 101 (5), 2003–41.
- Athey, Susan**, “The Impact of Machine Learning on Economics,” in “The Economics of Artificial Intelligence: An Agenda,” University of Chicago Press, 2018, pp. 507–547.
- Atil, Berk, Alexa Chittams, Liseng Fu, Ferhan Ture, Lixinyu Xu, and Breck Baldwin**, “LLM Stability: A Detailed Analysis with Some Surprises,” *arXiv preprint arXiv:2408.04667*, 2024.

Atkin, David, Eve Colson-Sihra, and Moses Shayo, “How Do We Choose Our Identity? A Revealed Preference Approach using Food Consumption,” *Journal of Political Economy*, 2021, 129 (4), 1193–1251.

Baker, Jack, Solange Rigaud, Daniel Pereira, Lloyd A Courtenay, and Francesco d’Errico, “Evidence from Personal Ornaments Suggest Nine Distinct Cultural Groups between 34,000 and 24,000 Years Ago in Europe,” *Nature Human Behaviour*, 2024, 8 (3), 431–444.

Barth, Fredrik, *Ethnic Groups and Boundaries: The Social Organization of Culture Difference*, Universitetsforlaget, 1969.

Becker, Anke, “On the Economic Origins of Concerns Over Women’s Chastity,” *Review of Economic Studies*, 2024, p. rdae084.

Becker, Sascha O, Jared Rubin, and Ludger Woessmann, “Religion and Growth,” *Journal of Economic Literature*, 2024, 62 (3), 1094–1142.

—, **Katrin Boeckh, Christa Hainz, and Ludger Woessmann**, “The Empire is Dead, Long Live the Empire! Long-Run Persistence of Trust and Corruption in the Bureaucracy,” *The Economic Journal*, 2016, 126 (590), 40–74.

Bentzen, Jeanet Sinding, Nicolai Kaarsen, and Asger Moll Wingender, “Irrigation and Autocracy,” *Journal of the European Economic Association*, 2017, 15 (1), 1–53.

Bergeron, Augustin, Jean-Paul Carvalho, Joe Henrich, Nathan Nunn, and Jonathan Weigel, “Zero-Sum Environments, the Evolution of Effort-Suppressing Beliefs, and Economic Development,” 2024.

Bertrand, Marianne and Antoinette Schoar, “Managing with Style: The Effect of Managers on Firm Policies,” *The Quarterly Journal of Economics*, 2003, 118 (4), 1169–1208.

— and **Emir Kamenica**, “Coming Apart? Cultural Distances in the United States over Time,” *American Economic Journal: Applied Economics*, October 2023, 15 (4), 100–141.

Billman, Brian R, “Irrigation and the Origins of the Southern Moche State on the North Coast of Peru,” *Latin American Antiquity*, 2002, 13 (4), 371–400.

Bisin, Alberto and Thierry Verdier, “The Economics of Cultural Transmission and the Dynamics of Preferences,” *Journal of Economic Theory*, 2001, 97 (2), 298–319.

— and —, “Advances in the Economic Theory of Cultural Transmission,” *Annual Review of Economics*, 2023, 15 (1), 63–89.

Bockstette, Valerie, Areendam Chanda, and Louis Putterman, “States and Markets: The Advantage of an Early Start,” *Journal of Economic growth*, 2002, 7 (4), 347–369.

Borcan, Oana, Ola Olsson, and Louis Putterman, “State History and Economic Development: Evidence from Six Millennia,” *Journal of Economic Growth*, 2018, 23 (1), 1–40.

Buggle, Johannes C and Ruben Durante, “Climate Risk, Cooperation and the Co-Evolution of Culture and Institutions,” *The Economic Journal*, 2021, 131 (637), 1947–1987.

Butters, Luis Jaime Castillo, “110 Años de Arqueología Mochica: Cambios Paradigmáticos y Nuevas Perspectivas,” in “Historia de la Arqueología en el Perú del Siglo XX,” Instituto Francés de Estudios Andinos, 2013, pp. 157–205.

Cadavid-Sanchez, Sebastian, Khalil Kacem, Rafael Aparecido Martins Frade, Johannes Boehm, Thomas Chaney, Danial Lashkari, and Daniel Simig, “Evaluating End-to-End Entity Linking on Domain-Specific Knowledge Bases: Learning about Ancient Technologies from Museum Collections,” *arXiv preprint arXiv:2305.14588*, 2023.

Cagnato, Clarissa, Nicolas Goepfert, Michelle Elliott, Gabriel Prieto, John Verano, and Elise Dufour, “Eat and Die: The Last Meal of Sacrificed Chimú Camelids at Huanchaquito-Las Llamas, Peru, as Revealed by Starch Grain Analysis,” *Latin American Antiquity*, 2021, 32 (3), 595–611.

Cameron, A Colin, Jonah B Gelbach, and Douglas L Miller, “Bootstrap-Based Improvements for Inference with Clustered Errors,” *The Review of Economics and Statistics*, 2008, 90 (3), 414–427.

Cantoni, Davide, Cathrin Mohr, and Matthias Weigand, “Individualism, Identity, and Institutional Change. Evidence from First Names in Germany, 1700–1850,” 2024. Working Paper.

Caramanica, Ari, “Prehispanic Arid Zone Farming: Hybrid Flood and Irrigation Systems along the North Coast of Peru,” *Agronomy*, 2024, 14 (3), 407.

—, **Luis Huaman Mesia, Claudia R Morales, Gary Huckleberry, Luis Jaime Castillo B, and Jeffrey Quilter**, “El Niño Resilience Farming on the North Coast of Peru,” *Proceedings of the National Academy of Sciences*, 2020, 117 (39), 24127–24137.

Clement, Christopher Ohm and Michael E Moseley, “The Spring-Fed Irrigation System of Carrizal, Peru: A Case Study of the Hypothesis of Agrarian Collapse,” *Journal of Field Archaeology*, 1991, 18 (4), 425–443.

- Clingingsmith, David, Asim Ijaz Khwaja, and Michael Kremer**, “Estimating the Impact of the Hajj: Religion and Tolerance in Islam’s Global Gathering,” *The Quarterly Journal of Economics*, 2009, 124 (3), 1133–1170.
- Collier, Donald**, “Cultural Chronology and Change: As Reflected in the Ceramics of the Virú Valley, Peru,” *Fieldiana. Anthropology*, 1955, 43, 1–226.
- Conley, Timothy G**, “GMM Estimation with Cross Sectional Dependence,” *Journal of econometrics*, 1999, 92 (1), 1–45.
- , **Christian B Hansen, and Peter E Rossi**, “Plausibly Exogenous,” *Review of Economics and Statistics*, 2012, 94 (1), 260–272.
- Costin, Cathy L**, “Crafting Identities Deep and Broad: Hybrid Ceramics on the Late Prehispanic North Coast of Peru,” in “Making Value, Making Meaning: Techné in the Precolumbian World,” Dumbarton Oaks, 2016, pp. 319–360.
- Daggett, Richard E.**, “Un Panorama de la Arqueología Peruana: 1896-1930,” in “Historia de la Arqueología en el Perú del Siglo XX,” Instituto Francés de Estudios Andinos, 2013, pp. 31–41.
- Dehdari, Sirus H and Kai Gehring**, “The Origins of Common Identity: Evidence from Alsace-Lorraine,” *American Economic Journal: Applied Economics*, 2022, 14 (1), 261–292.
- Dell, Melissa**, “Deep learning for economists,” *Journal of Economic Literature*, 2025, 63 (1), 5–58.
- Deng, Jia, Wei Dong, Richard Socher, Li-Jia Li, Kai Li, and Li Fei-Fei**, “Imagenet: A Large-Scale Hierarchical Image Database,” in “2009 IEEE Conference on Computer Vision and Pattern Recognition” IEEE 2009, pp. 248–255.
- Desmet, Klaus and Romain Wacziarg**, “The Cultural Divide,” *The Economic Journal*, 2021, 131 (637), 2058–2088.
- , **Ignacio Ortúñoz-Ortín, and Romain Wacziarg**, “Culture, Ethnicity, and Diversity,” *American Economic Review*, 2017, 107 (9), 2479–2513.
- , **Shlomo Weber, and Ignacio Ortúñoz-Ortín**, “Linguistic Diversity and Redistribution,” *Journal of the European Economic Association*, 2009, 7 (6), 1291–1318.
- Dolbunova, Ekaterina, Alexandre Lucquin, T Rowan McLaughlin, Manon Bondetti, Blandine Courel, Ester Oras, Henny Piezonka, Harry K Robson, Helen Talbot, Kamil Adamczak et al.**, “The Transmission of Pottery Technology Among Prehistoric European Hunter-Gatherers,” *Nature Human Behaviour*, 2023, 7 (2), 171–183.

Dulanto, Jálh, “Between Horizons: Diverse Configurations of Society and Power in the Late pre-Hispanic Central Andes,” in “The Handbook of South American Archaeology,” Springer, 2008, pp. 761–782.

Enke, Benjamin, “Kinship, Cooperation, and the Evolution of Moral Systems,” *The Quarterly Journal of Economics*, 2019, 134 (2), 953–1019.

Fandiño, Asier Gutiérrez, Jordi Armengol Estapé, Marc Pàmies, Joan Llop Palao, Joaquin Silveira Ocampo, Casimiro Pio Carrino, Carme Armentano Oller, Carlos Rodriguez Penagos, Aitor Gonzalez Agirre, and Marta Villegas, “MarIA: Spanish Language Models,” *Procesamiento del Lenguaje Natural*, 2022, 68.

Fearon, James D, “Ethnic and Cultural Diversity by Country,” *Journal of Economic Growth*, 2003, 8, 195–222.

Fernández, Raquel and Alessandra Fogli, “Culture: An Empirical Investigation of Beliefs, Work, and Fertility,” *American economic journal: Macroeconomics*, 2009, 1 (1), 146–177.

Flannery, Kent V, “The Ground Plans of Archaic States,” in “Archaic States,” School of American Research Press, 1998, pp. 15–57.

Flückiger, Matthias, Mario Larch, Markus Ludwig, and Luigi Pascali, “The Dawn of Civilization: Metal Trade and the Rise of Hierarchy,” 2024. CEPR Discussion Paper No. 18767.

Foster, George M, “Peasant Society and the Image of Limited Good,” *American Anthropologist*, 1965, 67 (2), 293–315.

Galor, Oded and Ömer Özak, “The Agricultural Origins of Time Preference,” *American Economic Review*, 2016, 106 (10), 3064–3103.

Geertz, Clifford, *The Interpretation of Cultures*, Vol. 5043, New York: Basic Books, 1973.

— , “Art as a Cultural System,” *MLN (Modern Language Notes)*, 1976, 91 (6), 1473–1499.

Gennaioli, Nicola and Ilia Rainer, “The Modern Impact of Precolonial Centralization in Africa,” *Journal of Economic Growth*, 2007, 12 (3), 185–234.

Giavazzi, Francesco, Ivan Petkov, and Fabio Schiantarelli, “Culture: Persistence and Evolution,” *Journal of Economic Growth*, 2019, 24, 117–154.

Giorcelli, Michela, Nicola Lacetera, and Astrid Marinoni, “How Does Scientific Progress Affect Cultural Changes? A Digital Text Analysis,” *Journal of Economic Growth*, 2022, 27 (3), 415–452.

- Giuliano, Paola and Nathan Nunn**, “Understanding Cultural Persistence and Change,” *The Review of Economic Studies*, 2021, 88 (4), 1541–1581.
- Gorin, Clément, Stephan Hebllich, and Yanos Zylberberg**, “State of the Art: Economic Development Through the Lens of Paintings,” 2025. Working Paper.
- Greenacre, Michael and Jorg Blasius**, *Multiple Correspondence Analysis and Related Methods*, New York: Chapman and Hall/CRC, 2006.
- Gretzinger, Joscha, Duncan Sayer, Pierre Justeau, Eveline Altena, Maria Pala, Katharina Dulias, Ceiridwen J Edwards, Susanne Jodoin, Laura Lacher, Susanna Sabin et al.**, “The Anglo-Saxon Migration and the Formation of the Early English Gene Pool,” *Nature*, 2022, 610 (7930), 112–119.
- Guarnieri, Eleonora and Ana Tur-Prats**, “Cultural Distance and Conflict-Related Sexual Violence*,” *The Quarterly Journal of Economics*, 2023, 138 (3), 1817–1861.
- Guiso, Luigi, Paola Sapienza, and Luigi Zingales**, “Does Culture Affect Economic Outcomes?,” *Journal of Economic Perspectives*, 2006, 20 (2), 23–48.
- , — , and — , “Cultural Biases in Economic Exchange?,” *The Quarterly Journal of Economics*, 2009, 124 (3), 1095–1131.
- , — , and — , “Long-Term Persistence,” *Journal of the European Economic Association*, 2016, 14 (6), 1401–1436.
- , — , and — , “Embedded Culture as a Source of Comparative Advantage,” Technical Report, NBER Working Paper, No. 33268 2024.
- Haak, Wolfgang, Iosif Lazaridis, Nick Patterson, Nadin Rohland, Swapan Mallick, Bastien Llamas, Guido Brandt, Susanne Nordenfelt, Eadaoin Harney, Kristin Stewardson et al.**, “Massive Migration from the Steppe Was a Source for Indo-European Languages in Europe,” *Nature*, 2015, 522 (7555), 207–211.
- Harney, Éadaoin, Hila May, Dina Shalem, Nadin Rohland, Swapan Mallick, Iosif Lazaridis, Rachel Sarig, Kristin Stewardson, Susanne Nordenfelt, Nick Patterson et al.**, “Ancient DNA from Chalcolithic Israel Reveals the Role of Population Mixture in Cultural Transformation,” *Nature Communications*, 2018, 9 (1), 3336.
- Heldring, Leander**, “The Origins of Violence in Rwanda,” *The Review of Economic Studies*, 2021, 88 (2), 730–763.
- Hodder, Ian**, “Economic and Social Stress and Material Culture Patterning,” *American Antiquity*, 1979, 44 (3), 446–454.
- , *Symbols in Action: Ethnoarchaeological Studies of Material Culture*, Cambridge University Press, 1982.

Hoyle, Rafael Larco, “Los Mochicas, Tomo I,” 1938. Casa Editora La Crónica y Variedades.

— , “Los Cupisniques,” 1941. Trabajo Presentado al Congreso Internacional de Americanistas de Lima, XXVII Sesión.

— , “La Cultura Salinar,” 1944. Síntesis Monográfica.

Huntington, Samuel P, *The Clash of Civilizations and the Remaking of World Order*, New York: Simon & Schuster Paperbacks, 1996.

Iacus, Stefano M, Gary King, and Giuseppe Porro, “Causal Inference Without Balance Checking: Coarsened Exact Matching,” *Political Analysis*, 2012, 20 (1), 1–24.

Isbell, William H, “Wari and Tiwanaku: International Identities in the Central Andean Middle Horizon,” in “The Handbook of South American Archaeology,” Springer, 2008, pp. 731–759.

— and **Helaine Silverman**, *Andean Archaeology I: Variations in Sociopolitical Organization*, Springer, 2002.

— and — , *The Handbook of South American Archaeology*, Springer, 2008.

— and **Katharina J Schreiber**, “Was Huari a State?,” *American Antiquity*, 1978, 43 (3), 372–389.

Isbell, William Harris, Mauricio Uribe, Anne Tiballi, and Edward P Zegarra, *Images in Action: The Southern Andean Iconographic Series*, UCLA Cotsen Institute of Archaeology Press, 2018.

Janusek, John Wayne, “Of Pots and People: Ceramic Style and Social Identity in the Tiwanaku State,” in “Us and Them: Archaeology and Ethnicity in the Andes,” The Cotsen Institute of Archaeology, UCLA, 2005, pp. 34–53.

Jones, Siân, *The Archaeology of Ethnicity: Constructing Identities in the Past and Present*, London: Routledge, 1997.

Kamdar, Rupal and Walker Ray, “Polarized Expectations, Polarized Consumption,” 2023. SSRN Working Paper: <http://dx.doi.org/10.2139/ssrn.4251955>.

Karger, Dirk Nikolaus, Michael P Nobis, Signe Normand, Catherine H Graham, and Niklaus E Zimmermann, “CHELSA-TraCE21k—High-Resolution (1 km) Downscaled Transient Temperature and Precipitation Data Since the Last Glacial Maximum,” *Climate of the Past*, 2023, 19 (2), 439–456.

Keane, Michael P and Timothy Neal, “A Practical Guide to Weak Instruments,” *Annual Review of Economics*, 2024, 16.

Keatinge, Richard W, “Peruvian Prehistory: An Overview of Pre-Inca and Inca Society,” 1988.

Khan, Asifullah, Anabia Sohail, Umme Zahoor, and Aqsa Saeed Qureshi, “A Survey of the Recent Architectures of Deep Convolutional Neural Networks,” *Artificial Intelligence Review*, 2020, 53, 5455–5516.

Kling, Jeffrey R, Jeffrey B Liebman, Lawrence F Katz, and Lisa Sanbonmatsu, “Moving to Opportunity and Tranquility: Neighborhood Effects on Adult Economic Self-Sufficiency and Health from a Randomized Housing Voucher Experiment,” 2004. KSG Working Paper No. RWP04-035.

Lanning, Edward P, *Peru before the Incas*, New Jersey: Prentice Hall Inc., 1967.

Lau, George F., “Northern Exposures: Recuay-Cajamarca Boundaries and Interaction,” in “in,” Springer, 2006, pp. 143–170.

Liu, Yinhan, Myle Ott, Naman Goyal, Jingfei Du, Mandar Joshi, Danqi Chen, Omer Levy, Mike Lewis, Luke Zettlemoyer, and Veselin Stoyanov, “Roberta: A Robustly Optimized Bert Pretraining Approach,” *arXiv preprint arXiv:1907.11692*, 2019.

Lowes, Sara and Eduardo Montero, “The Legacy of Colonial Medicine in Central Africa,” *American Economic Review*, 2021, 111 (4), 1284–1314.

— , **Nathan Nunn, James A Robinson, and Jonathan L Weigel**, “The Evolution of Culture and Institutions: Evidence from the Kuba Kingdom,” *Econometrica*, 2017, 85 (4), 1065–1091.

Ludwig, Jens and Sendhil Mullainathan, “Machine Learning as a Tool for Hypothesis Generation,” *The Quarterly Journal of Economics*, 2024, 139 (2), 751–827.

Lumbreras, Luis, “Andean Urbanism and Statecraft (CE 550–1450),” in “The Cambridge History of the Native Peoples of the Americas,” Vol. 3, Cambridge University Press, 1999, pp. 518–576.

Mayshar, Joram, Omer Moav, and Luigi Pascali, “The Origin of the State: Land Productivity or Appropriability?,” *Journal of Political Economy*, 2022, 130 (4), 1091–1144.

Menzel, Dorothy, *Pottery Style and Society in Ancient Peru: Art as a Mirror of History in the Ica Valley, 1350-1570*, Berkeley: University of California Press, 1976.

Michalopoulos, Stelios and Christopher Rauh, “Myths, Morals, and Movies,” 2025. Working Paper.

— and **Elias Papaioannou**, “Pre-Colonial Ethnic Institutions and Contemporary African Development,” *Econometrica*, 2013, 81 (1), 113–152.

- and Melanie Meng Xue, “Folklore,” *The Quarterly Journal of Economics*, 2021, 136 (4), 1993–2046.
- Moore, Jerry D.**, *A Prehistory of South America: Ancient Cultural Diversity on the Least Known Continent*, University Press of Colorado, 2014.
- Morris, Craig**, “Symbols to Power: Styles and Media in the Inka State,” in “Style, Society, and Person: Archaeological and Ethnological Perspectives,” Springer, 1995, pp. 419–433.
- Moscona, Jacob, Nathan Nunn, and James A Robinson**, “Keeping It in the Family: Lineage Organization and the Scope of Trust in Sub-Saharan Africa,” *American Economic Review: Papers & Proceedings*, 2017, 107 (5), 565–571.
- Moseley, Michael E. and Alana Cordy-Collins**, *The Northern Dynasties: Kinship and Statecraft in Chimor*, Washington, DC: Dumbarton Oaks Research Library and Collection, 1990. A Symposium at Dumbarton Oaks, 12th and 13th October 1985.
- Murdock, George P.**, *Ethnographic Atlas*, University of Pittsburgh Press, 1967.
- Nakatsuka, Nathan, Iosif Lazaridis, Chiara Barbieri, Pontus Skoglund, Nadin Rohland, Swapan Mallick, Cosimo Posth, Kelly Harkins-Kinkaid, Matthew Ferry, Éadaoin Harney et al.**, “A Paleogenomic Reconstruction of the Deep Population History of the Andes,” *Cell*, 2020, 181 (5), 1131–1145.
- Nanoglou, Stratos**, “The Materiality of Representation: A Preface,” *Journal of Archaeological Method and Theory*, 2009, 16, 157–161.
- Nash, Donna J and Patrick Ryan Williams**, “Architecture and Power on the Wari–Tiwanku Frontier,” *Archeological Papers of the American Anthropological Association*, 2004, 14 (1), 151–174.
- and —, “Religious Ritual and Wari State Expansion,” in “Ritual and Archaic States,” University Press of Florida, 2016, pp. 131–156.
- Nenadic, Oleg and Michael Greenacre**, “Correspondence Analysis in R, with Two- and Three-Dimensional Graphics: The ca Package,” *Journal of Statistical Software*, 2007, 20, 1–13.
- Nunn, Nathan**, “The Historical Roots of Economic Development,” *Science*, 2020, 367 (6485), eaaz9986.
- , “History as Evolution,” in “The Handbook of Historical Economics,” Elsevier, 2021, pp. 41–91.
- and Leonard Wantchekon, “The Slave Trade and the Origins of Mistrust in Africa,” *American Economic Review*, 2011, 101 (7), 3221–52.

Ochoa, Diana, Matthieu Carré, Juan-Felipe Montenegro, Thomas J DeVries, Dayenari Caballero-Rodríguez, Oris Rodríguez-Reyes, Angel Barbosa-Espitia, Jorge Cardich, Edgar Cruz-Acevedo, Danilo Cruz et al., “Late Miocene Greening of the Peruvian Desert,” *Nature Communications Earth & Environment*, 2025, 6 (1), 391.

OpenAI, Josh Achiam, Steven Adler, Sandhini Agarwal, Lama Ahmad, Ilge Akkaya, Florencia Leoni Aleman, Diogo Almeida, Janko Altenschmidt, Sam Altman, Shyamal Anadkat et al., “Gpt-4 Technical Report,” *arXiv preprint arXiv:2303.08774*, 2023.

Patterson, Thomas C and M Edward Moseley, “Late Preceramic and Early Ceramic Cultures of the Central Coast of Peru,” *Ñawpa Pacha*, 1968, 6 (1), 115–133.

Pawlówicz, Leszek M. and Christian E. Downum, “Applications of Deep Learning to Decorated Ceramic Typology and Classification: A case study using Tusayan White Ware from Northeast Arizona,” *Journal of Archaeological Science*, 2021, 130, 105375.

Popović, Danijela, Martyna Molak, Mariusz Ziółkowski, Alexei Vranich, Maciej Sobczyk, Delfor Ulloa Vidaurre, Guido Agresti, Magdalena Skrzypczak, Krzysztof Ginalska, Thisseas Christos Lamnidis et al., “Ancient Genomes Reveal Long-Range Influence of the Pre-Columbian Culture and Site of Tiwanaku,” *Science Advances*, 2021, 7 (39), eabg7261.

Pozorski, Shelia and Thomas Pozorski, “Early Cultural Complexity on the Coast of Peru,” in “The Handbook of South American Archaeology,” Springer, 2008, pp. 607–631.

Proulx, Donald, “Paracas and Nasca: Regional Cultures on the South Coast of Peru,” in “The Handbook of South American Archaeology,” Springer, 2008, pp. 563–585.

Reimers, Nils and Iryna Gurevych, “Sentence-Bert: Sentence Embeddings Using Siamese Bert-Networks,” *arXiv preprint arXiv:1908.10084*, 2019.

Renze, Matthew, “The Effect of Sampling Temperature on Problem Solving in Large Language Models,” in “Findings of the Association for Computational Linguistics: EMNLP 2024” 2024, pp. 7346–7356.

Robinson, Andrew, “Ancient Civilization: Cracking the Indus Script,” *Nature*, 2015, 526 (7574), 499–501.

Rowe, John, “Urban Settlements in Ancient Peru,” *Ñawpa Pacha*, 1963, 1 (1), 1–27.

Rowe, John H, “Cultural Unity and Diversification in Peruvian Archaeology,” in “Men and Cultures: Selected Papers of the Fifth International Congress of Anthropological and Ethnological Sciences,” University of Pennsylvania Press, 1960, pp. 627–631.

— , “Stages and Periods in Archaeological Interpretation,” *Southwestern Journal of Anthropology*, 1962, 18 (1), 40–54.

Rowe, John Howland, “Max Uhle, 1856–1944: A Memoir of the Father of Peruvian Archaeology,” *University of California Publications in American Archaeology and Ethnology*, 1954, 46 (1), 1–134.

Rubio-Ramos, Melissa, Christian Isendahl, and Ola Olsson, “The Political Economy of Bread and Circuses: Weather Shocks and Classic Maya Monument Construction,” 2024. Working Paper.

Sakai, Masato, Akihisa Sakurai, Siyuan Lu, Jorge Olano, Conrad M Albrecht, Hendrik F Hamann, and Marcus Freitag, “AI-Accelerated Nazca Survey Nearly Doubles the Number of Known Figurative Geoglyphs and Sheds Light on Their Purpose,” *Proceedings of the National Academy of Sciences*, 2024, 121 (40), e2407652121.

Schaedel, Richard P and Izumi Shimada, “Peruvian Archaeology, 1946–80: An Analytic Overview,” *World Archaeology*, 1982, 13 (3), 359–371.

Schortman, Edward M, Patricia A Urban, and Marne Ausec, “Politics with Style: Identity Formation in Prehispanic Southeastern Mesoamerica,” *American Anthropologist*, 2001, 103 (2), 312–330.

Schreiber, Katharina J, *Wari Imperialism in Middle Horizon Peru*, Vol. 87, University of Michigan Museum of Anthropological Archaeology, 1992.

Shimada, Izumi, *Pampa Grande and the Mochica Culture*, University of Texas Press, 1994.

— , “The Evolution of Andean Diversity: Regional Formations (500 BCE–CE 600),” in “The Cambridge History of the Native Peoples of the Americas,” Vol. 3, Cambridge University Press, 1999, p. 350–517.

Sifuentes, Jorge Silva, “Origen de las Civilizaciones Andinas,” in “Historia del Perú,” Barcelona: Lexus Editores, 2000.

Simonyan, Karen and Andrew Zisserman, “Very Deep Convolutional Networks for Large-Scale Image Recognition,” in “3rd International Conference on Learning Representations (ICLR 2015)” 2015.

Spolaore, Enrico and Romain Wacziarg, “How Deep Are the Roots of Economic Development?,” *Journal of Economic Literature*, 2013, 51 (2), 325–369.

Stanish, Charles, “The Origin of State Societies in South America,” *Annual Review of Anthropology*, 2001, 30 (1), 41–64.

- Stevenson, Alice**, “Material Culture of the Predynastic period,” in “Before the Pyramids: The Origins of Egyptian Civilization,” The Oriental Institute of the University of Chicago, 2011, pp. 65–74.
- Steward, Julian H.**, “Cultural Causality and Law: A Trial Formulation of the Development of Early Civilizations,” *American Anthropologist*, 1949, 51 (1), 1–27.
- , “Some Implications of the Symposium,” in “Pre-historic Agriculture,” Garden City, New York: The Natural History Press, 1971, pp. 614–648.
- Strong, William Duncan and Clifford Evans**, *Cultural Stratigraphy in the Virú Valley Northern Peru: The Formative and Florescent Epochs*, New York: Columbia University Press, 1952.
- Tabellini, Guido**, “Culture and Institutions: Economic Development in the Regions of Europe,” *Journal of the European Economic association*, 2010, 8 (4), 677–716.
- Tan, Hui Ren and Tianyi Wang**, “McCarthyism, Media, and Political Repression: Evidence from Hollywood,” 2024. NBER Working Paper: <http://www.nber.org/papers/w32682>.
- Tantaleán, Henry**, *Los Antiguos Estados Andinos: Una Arqueología de las Formaciones Políticas del Perú Prehispánico*, Lima: Instituto de Estudios Peruanos, 2021.
- and **César W Astuhuamán González**, *História de la Arqueología en el Perú del Siglo XX*, Instituto Francés de Estudios Andinos, 2013.
- Valverde, Guido, María Inés Barreto Romero, Isabel Flores Espinoza, Alan Cooper, Lars Fehren-Schmitz, Bastien Llamas, and Wolfgang Haak**, “Ancient DNA Analysis Suggests Negligible Impact of the Wari Empire Expansion in Peru’s Central Coast During the Middle Horizon,” *PLoS One*, 2016, 11 (6), e0155508.
- Vogel, Melissa A.**, “New Research on the Late Prehistoric Coastal Polities of Northern Peru,” *Journal of Archaeological Research*, 2018, 26, 165–195.
- Voigtländer, Nico and Hans-Joachim Voth**, “Persecution Perpetuated: The Medieval Origins of Anti-Semitic Violence in Nazi Germany,” *The Quarterly Journal of Economics*, 2012, 127 (3), 1339–1392.
- Voth, Hans-Joachim and David Yanagizawa-Drott**, “Image(s),” 2024. CEPR Discussion Papers, No. 19219.
- Willey, Gordon R.**, “Horizon Styles and Pottery Traditions in Peruvian Archaeology,” *American Antiquity*, 1945, 11 (1), 49–56.
- , *Prehistoric Settlement Patterns in the Virú Valley, Peru*, Bulletin 155, Bureau of American Ethnology, Smithsonian Institution, 1953.

— , *An Introduction to American Archaeology. Volume 2. South America*, Englewood Cliffs: Prentice-Hall, 1971.

Wittfogel, Karl A., *Oriental Despotism: A Comparative Study of Total Power*, New Haven: Yale University Press, 1957.

Xue, Melanie Meng, “Values of China: Toward a Cultural Map,” 2024. SSRN Working Paper: <http://dx.doi.org/10.2139/ssrn.5078516>.

FIGURE 1: Ceramic Objects from Moche and Nasca



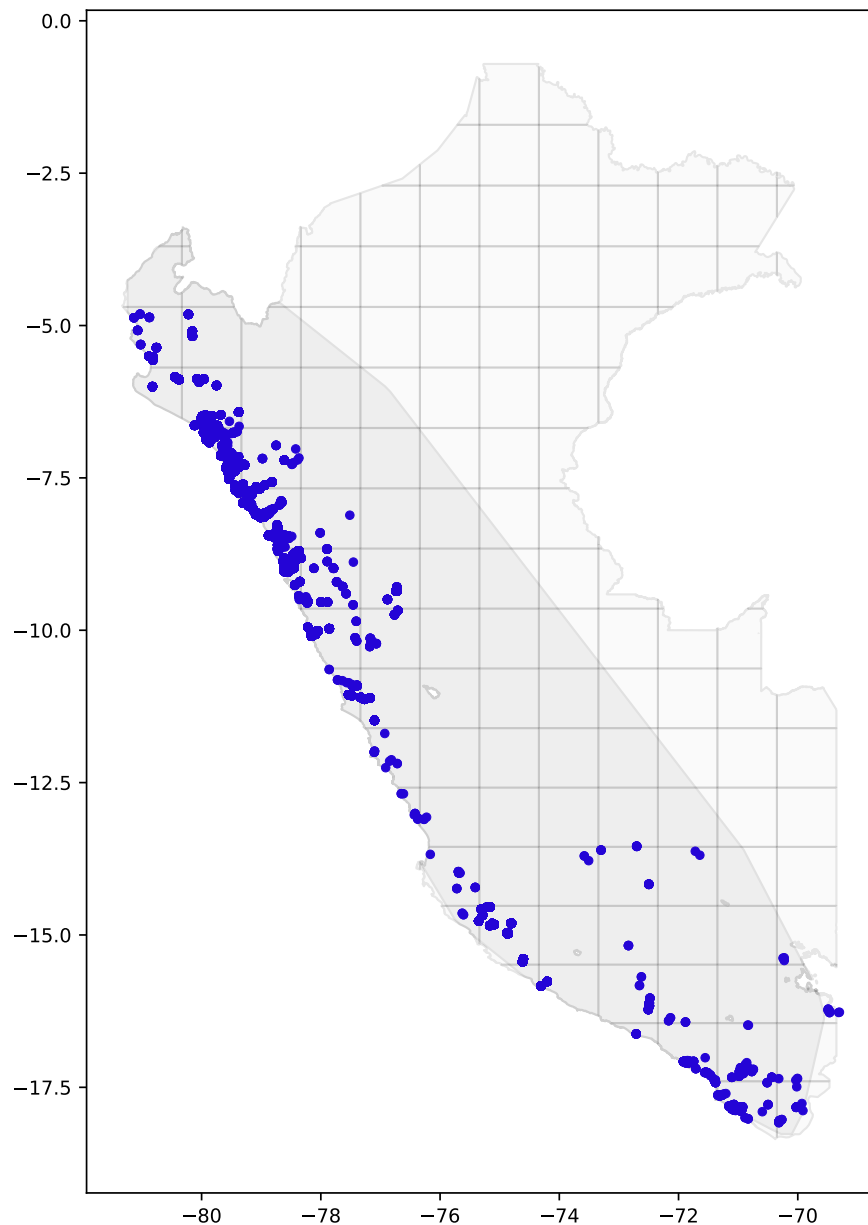
(A) Moche



(B) Nasca

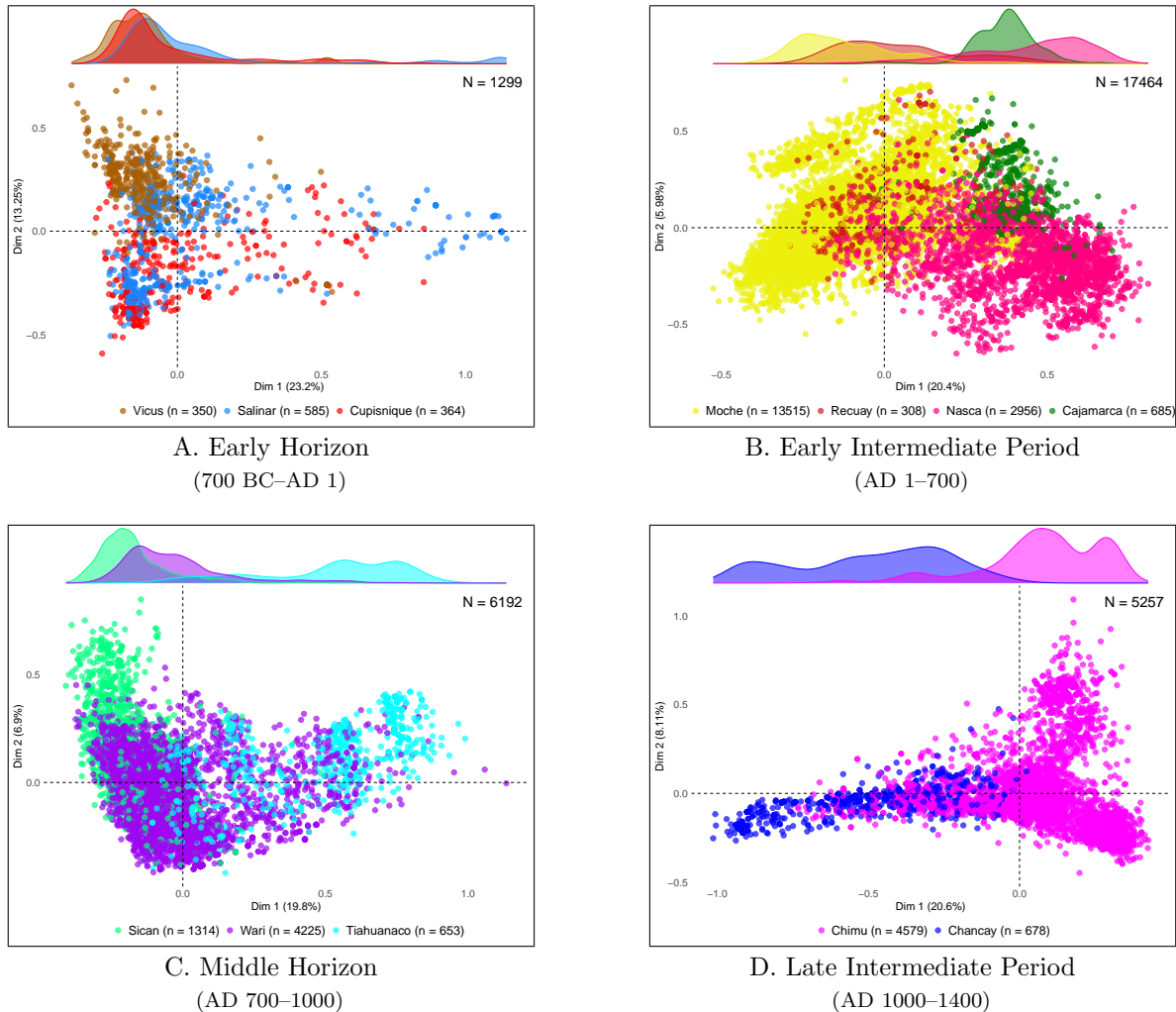
Notes. Examples of Moche and Nasca ceramics during the Early Intermediate Period (AD 1 - 700). Own elaboration with images from the [Larco Museum](#) (Lima, Perú).

FIGURE 2: Spatial Distribution of Archaeological Sites



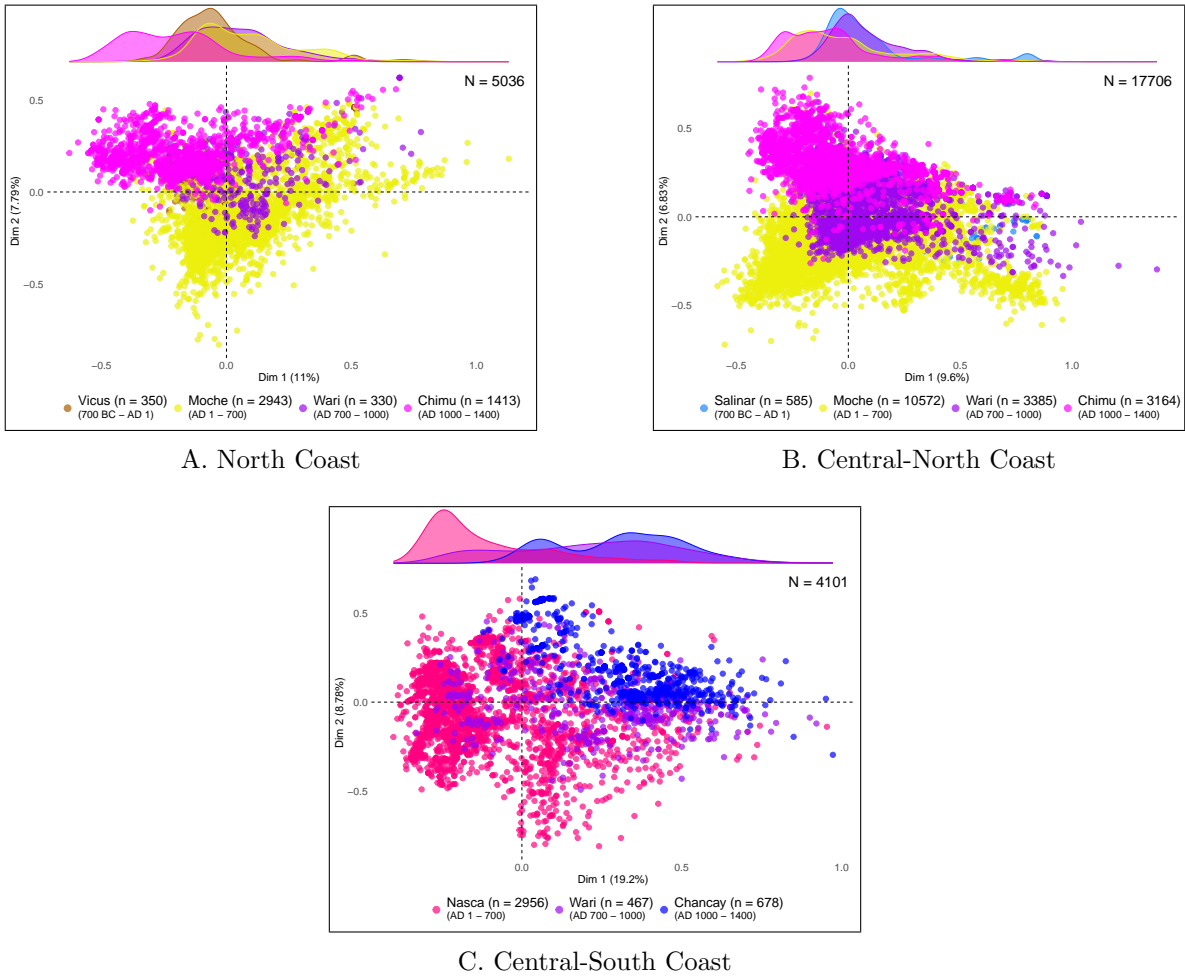
Notes. Spatial distribution of archaeological sites. Each point represents a site where ceramic objects were recovered, mapped using the World Geodetic System projection (WGS 1984). The gray area represents the approximate territorial extent of the Inca between AD 1400 and 1525. Grid cells of approximately 1 degree by 1 degree at the equator in the background.

FIGURE 3: Cross-Sectional Differences in Stylistic Distinctiveness



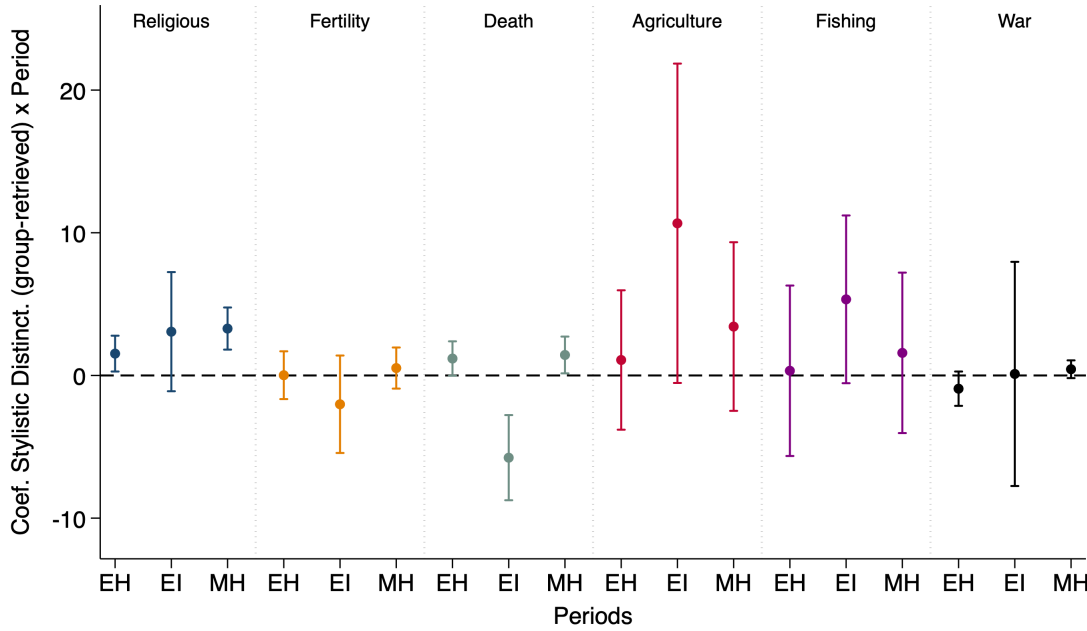
Notes. The unit of observation is a ceramic object. The graphs summarize the results of the multiple correspondence analysis (MCA, Greenacre and Blasius 2006; Nenadic and Greenacre 2007) for the full repertoire of ceramic traits (Table A.1). The axes represent the MCA scores of the first two dimensions. The contribution of each dimension to total dispersion (i.e., the percentage of *inertia*) is displayed in parentheses. The results are displayed separately for each archaeological period, with each color representing a different group. The densities at the top of each graph summarize the score of the first MCA dimension by group.

FIGURE 4: Inter-Temporal Differences in Stylistic Distinctiveness



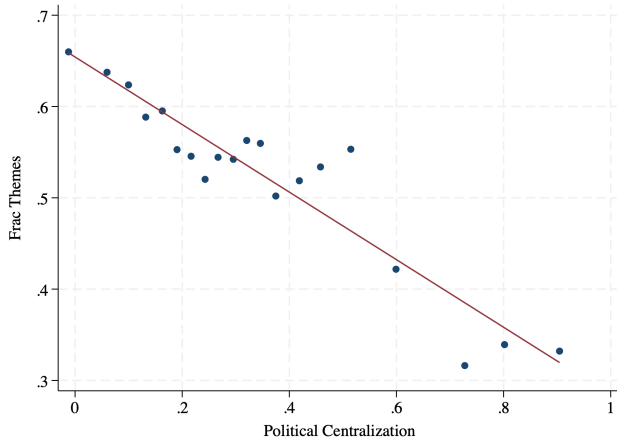
Notes. The unit of observation is a ceramic object. The graphs summarize the results of the multiple correspondence analysis (MCA, Greenacre and Blasius 2006; Nenadic and Greenacre 2007) for the full repertoire of ceramic traits (Table A.1). The axes represent the MCA scores of the first two dimensions. The contribution of each dimension to total dispersion (i.e., the percentage of *inertia*) is displayed in parentheses. The results are displayed separately for each region, with each color representing a different group. The densities at the top of each graph summarize the score of the first MCA dimension by group.

FIGURE 5: The Symbolic Content of Ceramics - Time-Varying Estimates

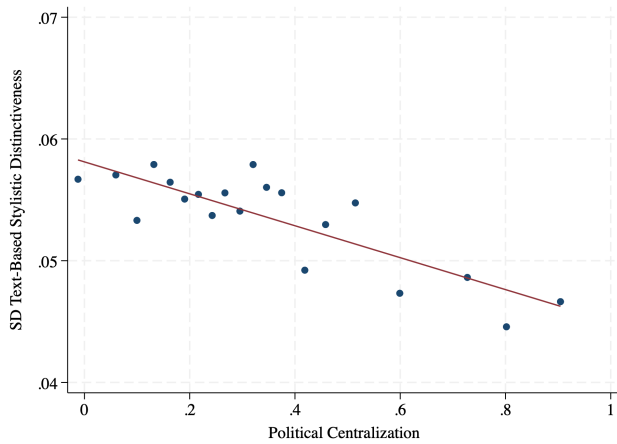


Notes. Estimates from full-sample OLS regressions at the object level. The figure reports time-varying estimates of group-retrieved stylistic distinctiveness and 95 percent confidence intervals by theme, relative to sample means. Standard errors are clustered at the Group \times Region level. EH refers to the Early Horizon (700 BC–AD 1), EIP to the Early Intermediate Period (AD 1–700), and MH to the Middle Horizon (AD 700–1000). We interact the group-retrieved measure of stylistic distinctiveness with period fixed effects, using the Late Intermediate Period (AD 1000–1400) as the omitted category. The group-retrieved measure of stylistic distinctiveness corresponds to the estimated group fixed effects from a regression of image-based stylistic distinctiveness (based on VGG16 image embeddings) on group fixed effects and baseline controls (geography, cataloguing year, and archaeologist fixed effects). All regressions include baseline controls (cataloguing year, archaeologist fixed effects, and the vector of site-level geographic controls, including absolute latitude, mean elevation, standard deviation of elevation, mean caloric suitability prior to AD 1500, log distance to the nearest river, and log distance to the coastline). Observations are weighted by the inverse of the standard errors from the first-stage estimates of the group fixed effects. Each outcome variable indicates whether a theme is present in sculpted and/or painted form.

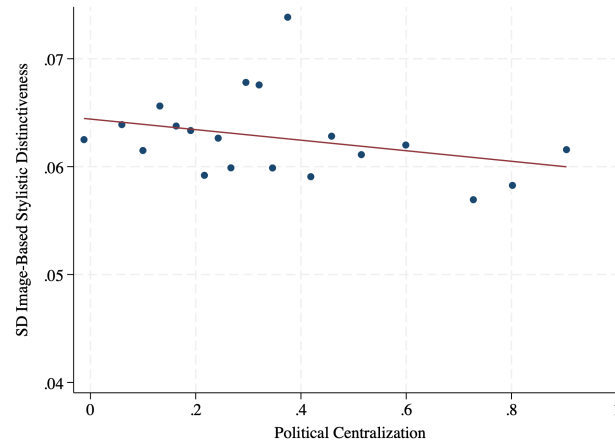
FIGURE 6: Binscatters - Cultural Dispersion and Political Centralization



A. Frac Themes



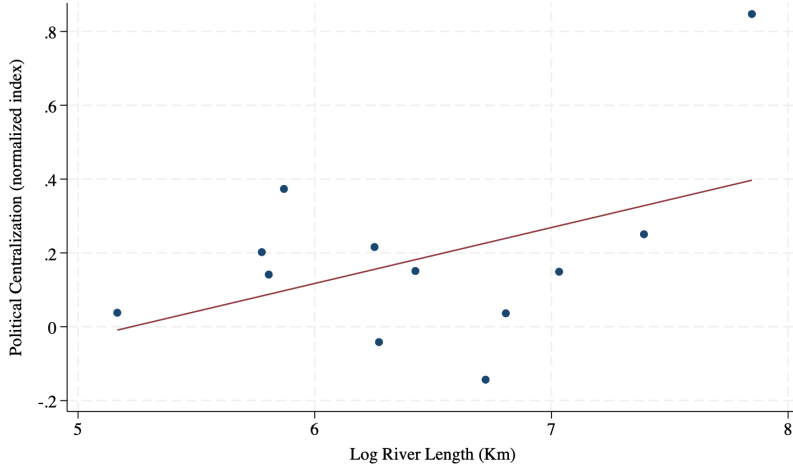
B. SD Text-Based Stylistic Distinctiveness



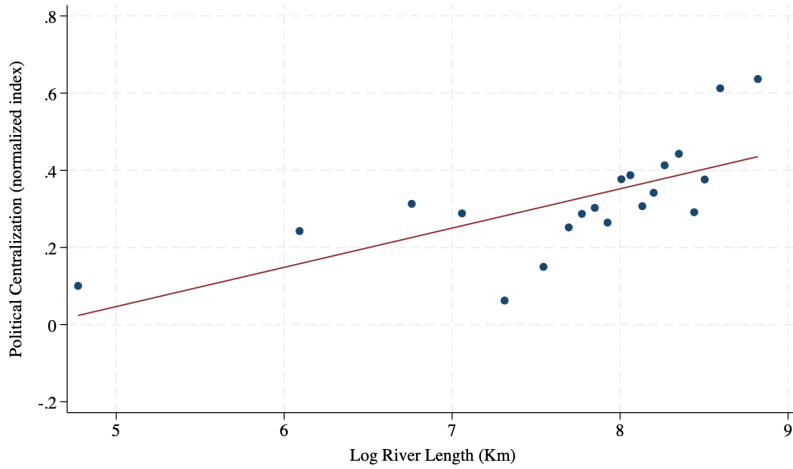
C. SD Image-Based Stylistic Distinctiveness

Notes. Binscatters of cultural dispersion against the group's level of political centralization across sites. Panel A uses an index of thematic fractionalization, based on the share of objects classified by theme, to proxy for cultural dispersion. In Panel B and Panel C, we use the standard deviation of stylistic distinctiveness across objects within a site, based on SBERT text embeddings (Panel B) and VGG16 image embeddings (Panel C). All binscatters include baseline controls: the share of open-form objects, the share of close-form objects, the log number of objects, a dummy variable equal to one if the number of mentions found for the group is above the median, and site-level geographic controls (absolute latitude, mean elevation, standard deviation of elevation, mean caloric suitability prior to AD 1500, log distance to the nearest river, and log distance to the coastline).

FIGURE 7: Political Centralization and Log Perennial River Length



A. Sample of Groups



B. Sample of Sites

Notes. Relationship between the group's level of political centralization and log perennial river length. In Panel A, each dot represents a group (binscatter at the group level after controlling for the group's log mean temperature, temperature stability (isothermality), and a dummy variable equal to one if the number of mentions found for the group is above the median). The graph in Panel B shows the binscatter of the group's level of political centralization against log perennial river length across sites, after controlling for site-level geography controls (absolute latitude, mean elevation, standard deviation of elevation, mean caloric suitability prior to AD 1500, log distance to the nearest river, and log distance to the coastline).

TABLE 1: Stylistic Distinctiveness (Trait-Based) and Joint Significance of Group Fixed Effects

Period	N. Groups	N. Objects	Panel A				Panel B			
			(1)	(2)	(3)	(4)	(5)	(6)	(7)	(8)
Region	N. Groups	N. Objects	F-stat	P-value	Adj. R2 without Group FE	Adj. R2 with Group FE	F-stat	P-value	Adj. R2 without Group FE	Adj. R2 with Group FE
Early Horizon	3	1299	39.4	< 0.001	.077	.252	7.4	.003	.236	.255
Early Intermediate Period	4	17464	1302.6	< 0.001	.557	.683	723.4	< 0.001	.617	.684
Middle Horizon	3	6192	1001.8	< 0.001	.196	.527	57.9	< 0.001	.539	.559
Late Intermediate Period	2	5257	314.6	< 0.001	.447	.558	102.1	< 0.001	.549	.558
Catalog Year			Yes	Yes	Yes	Yes	Yes	Yes	Yes	Yes
Archaeologist FE			Yes	Yes	Yes	Yes	Yes	Yes	Yes	Yes
Geographic Controls			No	No	No	No	Yes	Yes	Yes	Yes

Notes. The table reports F-test results for the joint significance of group fixed effects. The outcome variable is the measure of stylistic distinctiveness based on the score of the first MCA dimension, derived from the full repertoire of ceramic traits. The top panel presents one regression per period; the bottom panel presents one regression per region. Each regression is estimated by OLS at the object level and includes group fixed effects. In Panel A, all regressions include the year the object was electronically cataloged and archaeologist fixed effects. In Panel B, the vector of site-level geographic controls includes the site's absolute latitude, mean elevation, standard deviation of elevation, mean caloric suitability prior to AD 1500, log distance to the nearest river, and log distance to the coastline. Standard errors are clustered at the site level.

TABLE 2: Stylistic Distinctiveness (Text- and Image-Based)
and Joint Significance of Group Fixed Effects

			Panel A: Text-Based (SBERT)			Panel B: Text-Based (RoBERTa)		
			(1)	(2)	(3)	(4)	(5)	(6)
Period	N. Groups	N. Objects	F-stat	P-val	Δ Adj. R2	F-stat	P-val	Δ Adj. R2
Early Horizon	3	1299	57.7	< 0.001	6.1	39.3	< 0.001	2.7
Early Intermediate Period	4	17464	11.4	< 0.001	0.1	48.5	< 0.001	0.5
Middle Horizon	3	6192	51.5	< 0.001	2.6	87.1	< 0.001	3.3
Late Intermediate Period	2	5257	4.0	0.045	0.1	12.3	0.001	0.3
Region	N. Groups	N. Objects	F-stat	P-val	Δ Adj. R2	F-stat	P-val	Δ Adj. R2
North Coast	4	5036	127.1	< 0.001	2.3	18.8	< 0.001	0.9
Central-North Coast	4	17706	162.3	< 0.001	2.8	89.5	< 0.001	2.1
Central-South Coast	3	4101	25.2	< 0.001	2.2	49.5	< 0.001	2.4
			Panel C: Text-Based (OpenAI)			Panel D: Image-Based (VGG16)		
			(7)	(8)	(9)	(10)	(11)	(12)
Period	N. Groups	N. Objects	F-stat	P-val	Δ Adj. R2	F-stat	P-val	Δ Adj. R2
Early Horizon	3	1299	166.2	< 0.001	9.9	149.5	< 0.001	8.8
Early Intermediate Period	4	17464	19.4	< 0.001	0.4	5.3	0.002	0.1
Middle Horizon	3	6192	148.8	< 0.001	6.9	121.7	< 0.001	4.3
Late Intermediate Period	2	5257	19.5	< 0.001	0.5	10.3	0.002	0.2
Region	N. Groups	N. Objects	F-stat	P-val	Δ Adj. R2	F-stat	P-val	Δ Adj. R2
North Coast	4	5036	93.1	< 0.001	2.9	195.0	< 0.001	4.8
Central-North Coast	4	17706	233.3	< 0.001	5.7	229.3	< 0.001	6.1
Central-South Coast	3	4101	16.6	< 0.001	1.2	35.5	< 0.001	1.3
Catalog Year			Yes	Yes	Yes	Yes	Yes	Yes
Archaeologist FE			Yes	Yes	Yes	Yes	Yes	Yes
Geographic Controls			Yes	Yes	Yes	Yes	Yes	Yes

Notes. The table reports F-test results for the joint significance of group fixed effects. The outcome variable is a measure of average stylistic distinctiveness based on text embeddings (SBERT in Panel A, RoBERTa in Panel B, OpenAI's embedding model in Panel C) or image embeddings (VGG16, Panel D). In each panel, the top sub-panel presents one regression per period, while the bottom sub-panel presents one regression per region. All regressions are estimated by OLS at the object level and include group fixed effects, the year the object was electronically cataloged, archaeologist fixed effects, and a vector of site-level geographic controls (absolute latitude, mean elevation, standard deviation of elevation, mean caloric suitability prior to AD 1500, log distance to the nearest river, and log distance to the coastline). Standard errors are clustered at the site level. The change in adjusted R^2 , relative to the specification without group fixed effects (Δ Adj. R^2), is reported in percentage terms.

TABLE 3: Beyond Object Form —
Stylistic Distinctiveness and Joint Significance of Group Fixed Effects

			Panel A: Image-Based (VGG16)			Panel B: Image-Based (Residuals)		
	(1)	(2)	(3)		(4)	(5)	(6)	
Period	N. Groups	N. Objects	F-stat	P-value	Δ Adj. R2	F-stat	P-value	Δ Adj. R2
Early Horizon	3	1299	291	< 0.001	9.3	175.9	< 0.001	10
Early Intermediate Period	4	17464	10.2	< 0.001	.2	10.6	< 0.001	.2
Middle Horizon	3	6192	117.2	< 0.001	3	120.3	< 0.001	4
Late Intermediate Period	2	5257	3.1	.078	.1	3.4	.065	0
Region	N. Groups	N. Objects	F-stat	P-value	Δ Adj. R2	F-stat	P-value	Δ Adj. R2
North Coast	4	5036	239.3	< 0.001	5.2	222.9	< 0.001	5.7
Central-North Coast	4	17706	271.7	< 0.001	5.8	265.9	< 0.001	6.3
Central-South Coast	3	4101	11.4	< 0.001	.4	10.4	< 0.001	.4
Catalog Year			Yes	Yes	Yes	Yes	Yes	Yes
Archaeologist FE			Yes	Yes	Yes	Yes	Yes	Yes
Geographic Controls			Yes	Yes	Yes	Yes	Yes	Yes
Type of Form FE			Yes	Yes	Yes	No	No	No

Notes. The table reports F-test results for the joint significance of group fixed effects. The top panel presents one regression per period; the bottom panel presents one regression per region. Each regression is estimated by OLS at the object level and includes group fixed effects, the year the object was electronically cataloged, archaeologist fixed effects, and geographic controls. The vector of site-level geographic controls includes the site's absolute latitude, mean elevation, standard deviation of elevation, mean caloric suitability prior to AD 1500, log distance to the nearest river, and log distance to the coastline. In Panel A, the regressions also include fixed effects for type of form (open forms, closed forms, and molded sculptures), using the measure of stylistic distinctiveness based on VGG16 image embeddings as outcome variable. In Panel B, the outcome variables are the residuals from regressions of image-based stylistic distinctiveness against form fixed effects. Standard errors are clustered at the site level. The change in adjusted R^2 , relative to the specification without group fixed effects (Δ Adj. R^2), is expressed in percentage terms.

TABLE 4: The Symbolic Content of Ceramics

	Religious (1)	Fertility (2)	Death (3)	Agriculture (4)	Fishing (5)	War (6)
Panel A: Baseline Controls						
Stylistic Distinct. (group-retrieved)	0.089*** (0.021)	-0.005*** (0.001)	-0.005*** (0.001)	0.001 (0.001)	0.002 (0.002)	0.015** (0.005)
Panel B: Type of Form FE						
Stylistic Distinct. (group-retrieved)	0.087*** (0.020)	-0.004*** (0.001)	-0.005*** (0.001)	0.001 (0.001)	0.002 (0.001)	0.015** (0.006)
Panel C: Period and Region FE						
Stylistic Distinct. (group-retrieved)	0.115** (0.048)	-0.005*** (0.001)	-0.002 (0.002)	0.004** (0.002)	0.002 (0.002)	0.017* (0.010)
Mean Dep. Var.	0.129	0.005	0.009	0.001	0.003	0.031
N	30212	30212	30212	30212	30212	30212

Notes. All regressions are estimated by OLS at the object level. Each column presents the results for a different outcome variable—a dummy variable indicating whether a trait is present in sculpted and/or painted form. The table reports the estimated coefficient on the measure of stylistic distinctiveness retrieved from the group fixed effects. This measure corresponds to the estimated group fixed effects from a regression of image-based stylistic distinctiveness (based on VGG16 image embeddings) on group fixed effects and baseline controls (geography, cataloging year, and archaeologist fixed effects). The measure is normalized between 0 and 1, with 1 corresponding to the group with the highest value. All regressions include baseline controls (the year the object was electronically catalogued, archaeologist fixed effects, and a vector of site-level geographic controls, including absolute latitude, mean elevation, standard deviation of elevation, mean caloric suitability prior to AD 1500, log distance to the nearest river, and log distance to the coastline). In Panel B, the regressions also include fixed effects for type of form (open forms, closed forms, and molded sculptures). In Panel C, the regressions additionally include period and region fixed effects. Standard errors are clustered at the Group×Region level (25 clusters). We weight observations by the inverse of the standard errors from the first-stage estimates of the group fixed effects. *** p<0.01, ** p<0.05, * p<0.1.

TABLE 5: The Symbolic Content of Ceramics — Coarsened Exact Matching (CEM)

	Religious (1)	Fertility (2)	Death (3)	Agriculture (4)	Fishing (5)	War (6)
Panel A: Baseline Controls						
Stylistic Distinct. (group-retrieved)	0.103*** (0.026)	-0.012*** (0.004)	-0.007*** (0.002)	0.000 (0.000)	0.007* (0.003)	0.018** (0.007)
Panel B: Stratum FE						
Stylistic Distinct. (group-retrieved)	0.089*** (0.005)	-0.010** (0.004)	-0.008*** (0.002)	0.000* (0.000)	0.002* (0.001)	0.017*** (0.003)
Panel C: Period and Region FE						
Stylistic Distinct. (group-retrieved)	0.122** (0.048)	-0.008 (0.032)	-0.020** (0.007)	-0.000 (0.001)	-0.009*** (0.002)	0.019* (0.010)
Mean Dep. Var.	0.150	0.005	0.010	0.001	0.005	0.034
N	5697	5697	5697	5697	5697	5697

G

Notes. All regressions are estimated by OLS at the object level for the matched sample. We use Coarsened Exact Matching (CEM, Iacus et al. 2012) to create this matched sample of objects, which are (*i*) statistically similar in terms of geography and cataloging year, and (*ii*) identical in terms of form type and archaeologist identity. Each column presents the results for a different outcome variable—a dummy variable indicating whether a trait is present in sculpted and/or painted form. The table reports the estimated coefficient on the measure of stylistic distinctiveness retrieved from the group fixed effects. This measure corresponds to the estimated group fixed effects from a regression of image-based stylistic distinctiveness (based on VGG16 image embeddings) on group fixed effects and baseline controls (geography, cataloging year, and archaeologist fixed effects). The measure is normalized between 0 and 1, with 1 corresponding to the group with the highest value. All regressions include baseline controls (the year the object was electronically cataloged and a vector of site-level geographic controls, including absolute latitude, mean elevation, standard deviation of elevation, mean caloric suitability prior to AD 1500, log distance to the nearest river, and log distance to the coastline). In Panel B, the regressions also include stratum fixed effects. In Panel C, the regressions additionally include period and region fixed effects. Standard errors clustered at the Group \times Region level (11 clusters) in parentheses. We weight observations by the inverse of the standard errors from the first-stage estimates of the group fixed effects. *** p<0.01, ** p<0.05, * p<0.1.

TABLE 6: Cultural Dispersion and Political Centralization — OLS Results

	Frac Themes	SD Text-Based Stylistic Distinct. (SBERT)	SD Image-Based Stylistic Distinct. (VGG16)	Average Effect Size (AES)
	(1)	(2)	(3)	(4)
Panel A: Baseline Controls				
Political Centr.	-0.410*** (0.099)	-0.306*** (0.083)	-0.090 (0.065)	-0.286
Adj R^2	0.797	0.414	0.387	
Panel B: Group-Level Controls				
Related Contr.	-0.480*** (0.095)	-0.269** (0.109)	0.038 (0.070)	-0.250
Adj R^2	0.843	0.428	0.412	
Panel C: Period and Region FE				
Political Centr.	-0.546*** (0.123)	-0.339*** (0.084)	-0.029 (0.128)	-0.251
Adj R^2	0.868	0.482	0.458	
N	422	422	422	

Notes. All regressions are estimated by OLS at the site level. In column (1), the dependent variable is the index of thematic fractionalization, based on the share of objects classified by theme. In columns (2)-(3), the dependent variables correspond to the standard deviation of stylistic distinctiveness, based on SBERT text embeddings (column 2) or VGG16 image embeddings (column 3), across all objects from a site. Column (4) reports the Average Effect Size (AES, [Clingingsmith et al. 2009](#)) across all measures of cultural dispersion, including thematic fractionalization and embedding-based dispersion measures (i.e., the standard deviation of stylistic distinctiveness, based on SBERT text embeddings, RoBERTa text embeddings, OpenAI text embeddings, and VGG16 image embeddings). The table reports the estimated coefficient on the group-level index of political centralization. In Panel A, the set of baseline controls includes the share of open-form objects, the share of close-form objects, the log number of objects, a dummy variable equal to one if the number of mentions found for the group is above the median, and a vector of site-level geographic controls (absolute latitude, mean elevation, standard deviation of elevation, mean caloric suitability prior to AD 1500, log distance to the nearest river, and log distance to the coastline). In Panel B, the regressions additionally include the log of the group's area and the log of the group's number of sites. In Panel C, the regressions additionally include period and region fixed effects. Standard errors clustered at the Group×Region level (22 clusters) in parentheses. All variables are standardized to have zero mean and standard deviation equal to one. *** p<0.01, ** p<0.05, * p<0.1.

TABLE 7: Cultural Dispersion and Political Centralization — 2SLS Results

	Frac Themes			SD Text-Based (SBERT)			SD Image-Based (VGG16)		
	(1)	(2)	(3)	(4)	(5)	(6)	(7)	(8)	(9)
Political Centr.	-0.157 (0.122)	-0.375*** (0.080)	-0.579*** (0.059)	-0.388*** (0.117)	-0.419*** (0.079)	-0.463*** (0.099)	-0.295* (0.163)	-0.001 (0.158)	0.135 (0.154)
N	422	422	422	422	422	422	422	422	422
F-Stat (excluded instrument)	33.99	44.64	146.03	33.99	44.64	146.03	33.99	44.64	146.03
F-Stat (AR)	1.33	11.26	148.60	15.85	36.07	31.49	3.67	0.00	0.86
P-value (AR)	0.262	0.003	0.000	0.001	0.000	0.000	0.069	0.994	0.365
Baseline Controls	Yes	Yes	Yes	Yes	Yes	Yes	Yes	Yes	Yes
Group-Level Controls	No	Yes	Yes	No	Yes	Yes	No	Yes	Yes
Period and Region FE	No	No	Yes	No	No	Yes	No	No	Yes

Notes. 2SLS results at the site level. In column (1)-(3), the dependent variable is the index of thematic fractionalization, based on the share of objects classified by theme. In columns (4)-(6) and (7)-(9), the dependent variables correspond to the standard deviation of stylistic distinctiveness, based on SBERT text embeddings (column 2) or VGG16 image embeddings (column 3), across all objects from a site. The table reports the estimated coefficient on the group-level index of political centralization, instrumented with the log of the total length of perennial rivers within each group's historical homeland. The set of baseline controls includes the share of open-form objects, the share of close-form objects, the log number of objects, a dummy variable equal to one if the number of mentions found for the group is above the median, the group's log mean temperature and temperature stability (isothermality), and a vector of site-level geographic controls (absolute latitude, mean elevation, standard deviation of elevation, mean caloric suitability prior to AD 1500, log distance to the nearest river, and log distance to the coastline). Columns (2), (5), and (8) additionally include the log of the group's area and the log of the group's number of sites. In columns (3), (6), and (9), the regressions additionally include period and region fixed effects. Standard errors clustered at the Group×Region level (22 clusters) in parentheses. All variables are standardized to have zero mean and standard deviation equal to one. F-Stat (excluded instrument) reports the F-statistic on the excluded instrument from the first stage regression. F-Stat (AR) and p-value (AR) refer to the Anderson-Rubin Wald test. *** p<0.01, ** p<0.05, * p<0.1.

TABLE 8: Politically Complex *versus* Placebo Random Areas — 2SLS Results

	Homeland: Political Sites Only			Homeland: 20% Random			Homeland: 60% Random		
	Frac Themes	SD Text	SD Image	Frac Themes	SD Text	SD Image	Frac Themes	SD Text	SD Image
	(1)	(2)	(3)	(4)	(5)	(6)	(7)	(8)	(9)
Political Centr.	-0.413*** (0.067)	-0.359*** (0.064)	0.090 (0.112)	-0.242 (0.448)	-0.968 (1.132)	0.906 (1.316)	-0.198 (0.256)	-0.874 (0.542)	0.445 (0.604)
N	422	422	422	422	422	422	422	422	422
F-Stat (excluded instrument)	60.76	60.76	60.76	0.37	0.37	0.37	0.90	0.90	0.90
Baseline Controls	Yes	Yes	Yes	Yes	Yes	Yes	Yes	Yes	Yes
Group-Level Controls	Yes	Yes	Yes	Yes	Yes	Yes	Yes	Yes	Yes

Notes. 2SLS results at the site level. In columns (1), (4), and (7) the dependent variable is the index of thematic fractionalization, based on the share of objects classified by theme. In the remaining columns, the dependent variables correspond to the standard deviation of stylistic distinctiveness, based on SBERT text embeddings (columns 2, 5, and 8) or VGG16 image embeddings (columns 3, 6, and 9), across all objects from a site. The table reports the estimated coefficient on the group-level index of political centralization, instrumented with log perennial river length. Columns (1)–(3) use river length within politically complex areas of the group’s pre-colonial homeland. Columns (4)–(6) use a 20 percent random portion of the homeland without evidence of political complexity, and columns (7)–(9) use a 60 percent random portion. The set of baseline controls includes the share of open-form objects, the share of close-form objects, the log number of objects, a dummy variable equal to one if the number of mentions found for the group is above the median, the group’s log mean temperature and temperature stability (isothermality), and a vector of site-level geographic controls (absolute latitude, mean elevation, standard deviation of elevation, mean caloric suitability prior to AD 1500, log distance to the nearest river, and log distance to the coastline). The set of group-level controls refers to the log of the group’s area and the log of the group’s number of sites. Standard errors clustered at the Group \times Region level (22 clusters) in parentheses. All variables are standardized to have zero mean and standard deviation equal to one. F-Stat (excluded instrument) reports the F-statistic on the excluded instrument from the first stage regression. *** p<0.01, ** p<0.05, * p<0.1.

TABLE 9: Dispersion in Contemporary Attitudes
and Pre-Colonial Political Centralization

	OLS		2SLS	
	(1)	(2)	(3)	(4)
Political Centr. (simple average)	-0.107 (0.069) [0.065] [[0.070]]		-0.058 (0.042) [0.040] [[0.040]]	
Political Centr. (time-weighted average)		-0.130 (0.049)*** [0.046]*** [[0.048]]***		-0.192 (0.080)** [0.057]*** [[0.055]]***
N	31,849	31,849	31,849	31,849
F-Stat (excluded instrument)			35.58	12.35
F-Stat (AR)			1.59	4.02
p-value (AR)			0.213	0.050
Individual Controls	Yes	Yes	Yes	Yes
District Controls	Yes	Yes	Yes	Yes
Province FE	Yes	Yes	Yes	Yes
Year FE	Yes	Yes	Yes	Yes

Notes. The unit of observation is an individual (yearly data from the ENAHO survey, 2004–2017). The dependent variable is average cultural distance across 40 possible questions, depending on data availability by district-year. Political centralization is measured at the district level as (*i*) the simple average across groups that occupied a district during the four pre-Inca periods, or (*ii*) a time-weighted average based on the share of centuries each group occupied the district. Columns (1)-(2) report OLS estimates; columns (3)-(4) report 2SLS estimates, instrumenting political centralization with the district-level average of log perennial river length within pre-colonial homelands (simple average in col. 3; time-weighted average in col. 4). Columns (3)-(4) also control for pre-colonial log mean temperature and temperature stability (isothermality). All regressions include individual controls (gender, age, age squared, and education dummies), district controls (mean elevation, standard deviation of elevation, mean caloric suitability, log area, longitude, and latitude), year fixed effects, and province fixed effects. Standard errors in (·) are clustered at the district level (57 clusters); in [·] and [[·]], standard errors are adjusted for spatial correlation with a distance cutoff of approximately 50km and 10km at the equator (Conley 1999), respectively. All variables except dummies are standardized to have zero mean and standard deviation equal to one. F-Stat (excluded instrument) reports the F-statistic on the excluded instrument from the first stage regression. F-Stat (AR) and p-value (AR) refer to the Anderson-Rubin Wald test.

Online Appendix

A Appendix - Figures and Tables

FIGURE A.1: Archaeological Groups

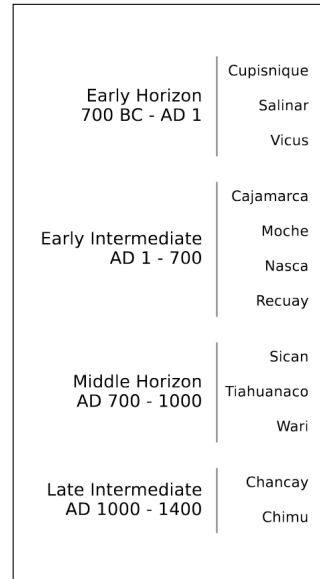
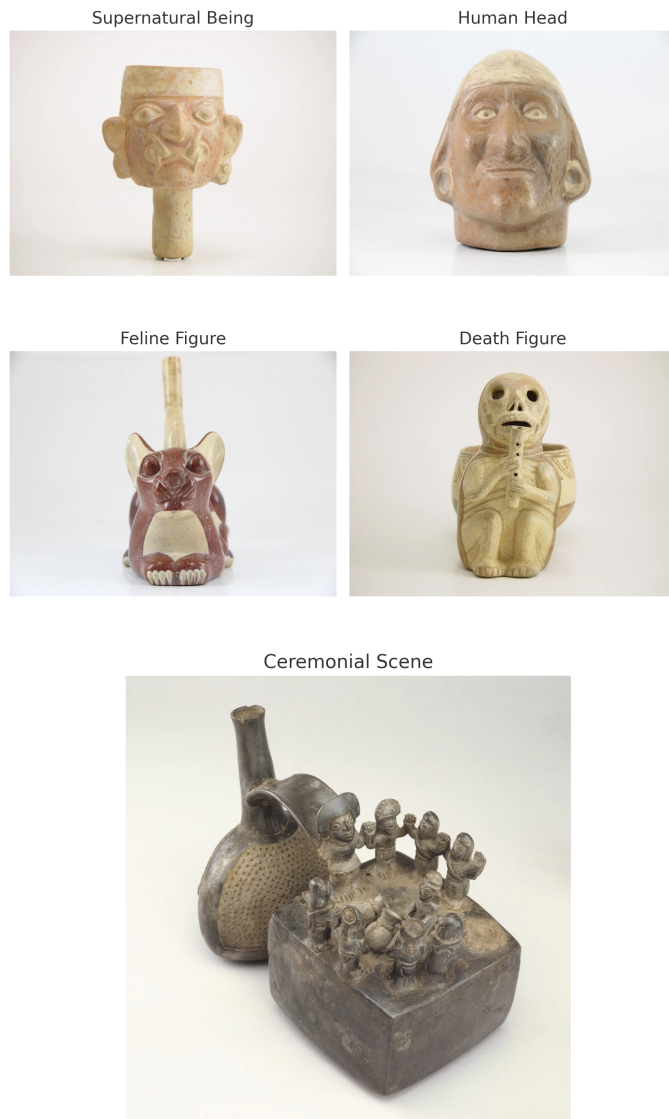
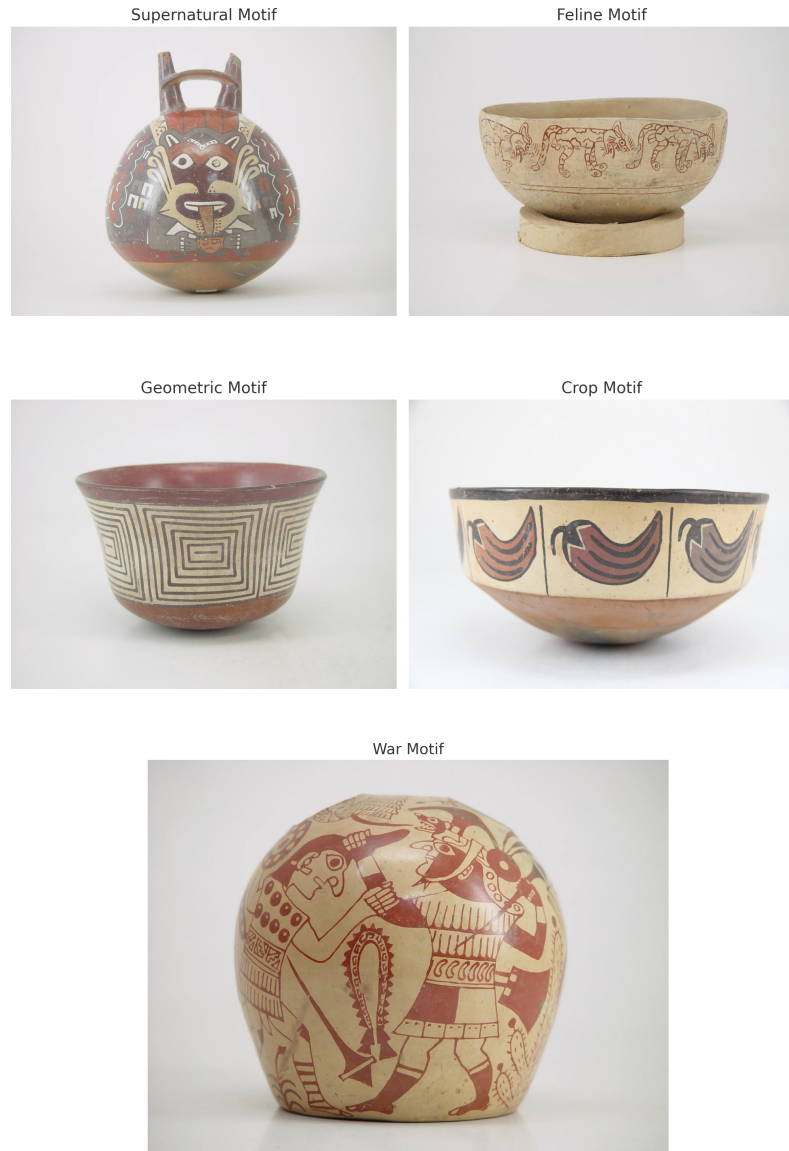


FIGURE A.2: Examples of Molded Representations



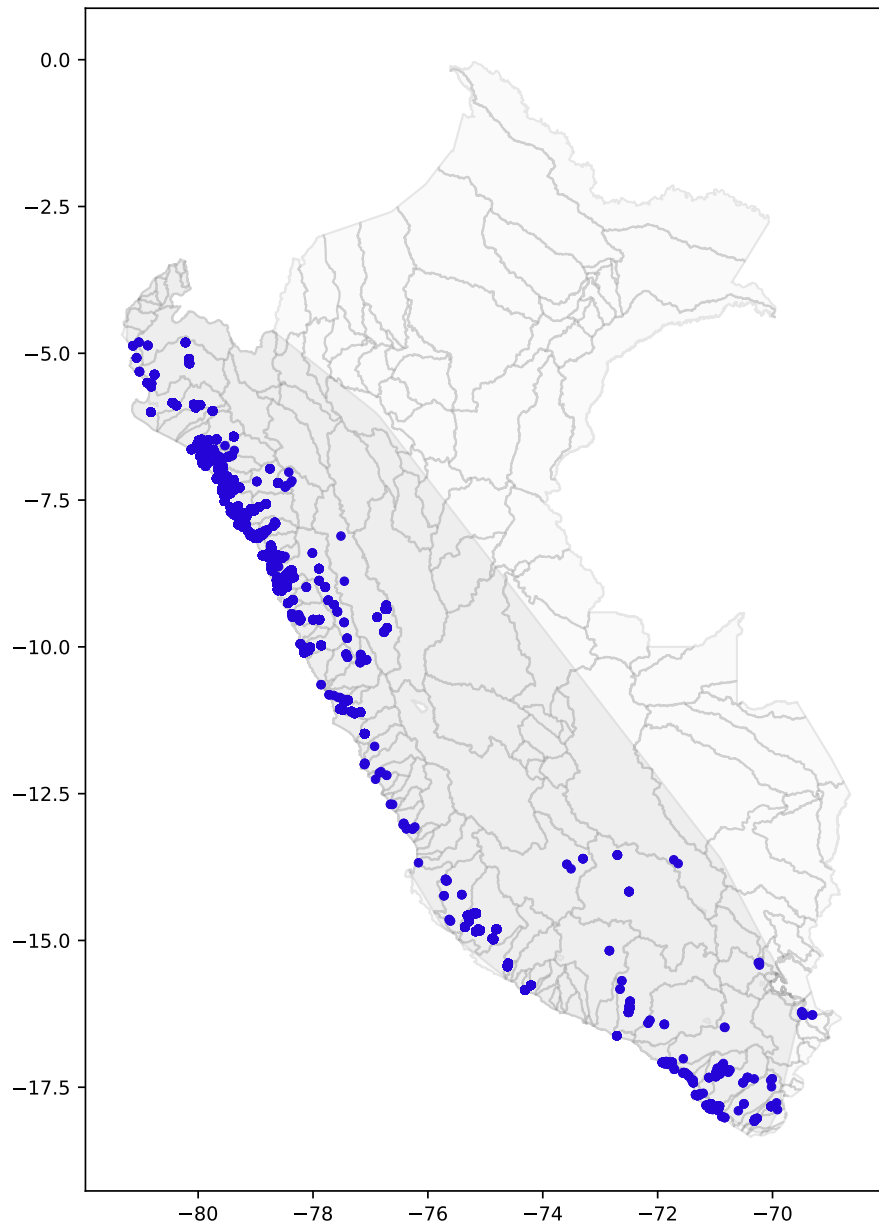
Notes. Examples of ceramic sculptures representing different themes. Own elaboration with images from the [Larco Museum](#) (Lima, Perú).

FIGURE A.3: Examples of Painted Representations



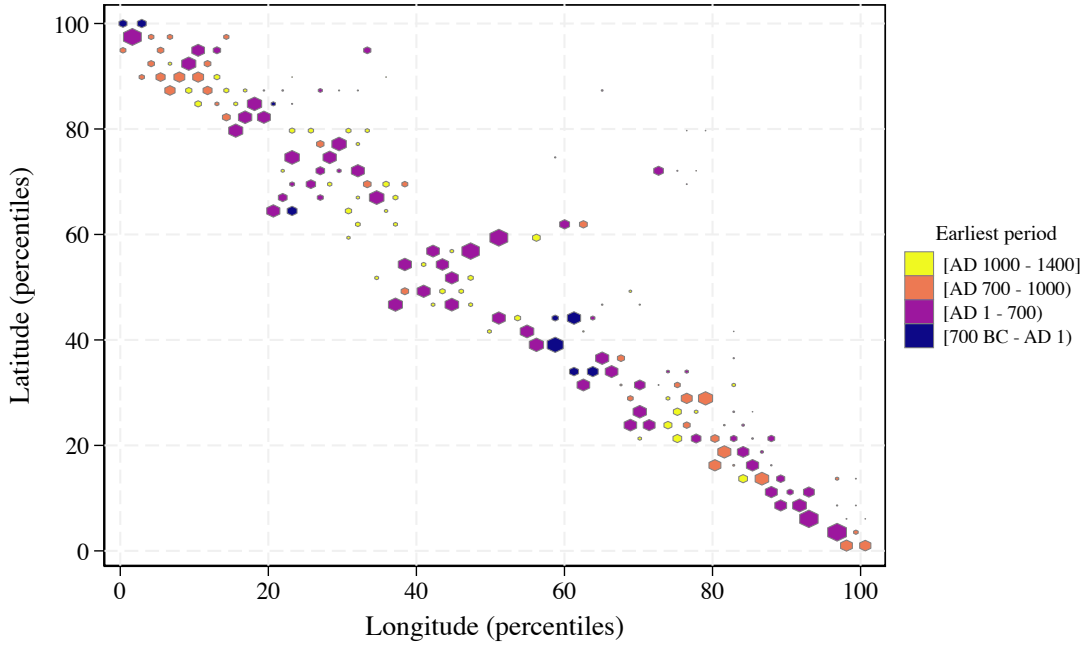
Notes. Examples of ceramic objects with different painted motifs. Own elaboration with images from the [Larco Museum](#) (Lima, Perú).

FIGURE A.4: Spatial Distribution of Archaeological Sites — Hydrographic Basins



Notes. Spatial distribution of archaeological sites. Each point represents a site where ceramic objects were recovered, mapped using the World Geodetic System projection (WGS 1984). The gray area represents the approximate territorial extent of the Inca between AD 1400 and 1525. Hydrographic basins in the background.

FIGURE A.5: Density of Ceramic Objects across Space



Notes. Density of ceramic objects across bins of latitude-longitude percentiles. Bin size represents the density of objects. The color legend indicates the period of the earliest object within each bin: Early Horizon (700 BC–AD 1), Early Intermediate Period (AD 1–700), Middle Horizon (AD 700–1000), or Late Intermediate Period (AD 1000–1400).

FIGURE A.6: Examples of Ceramic Objects by Group



(A) *Cupisnique* (Early Horizon, 700 BC–AD 1)



(B) *Salinar* (Early Horizon, 700 BC–AD 1)



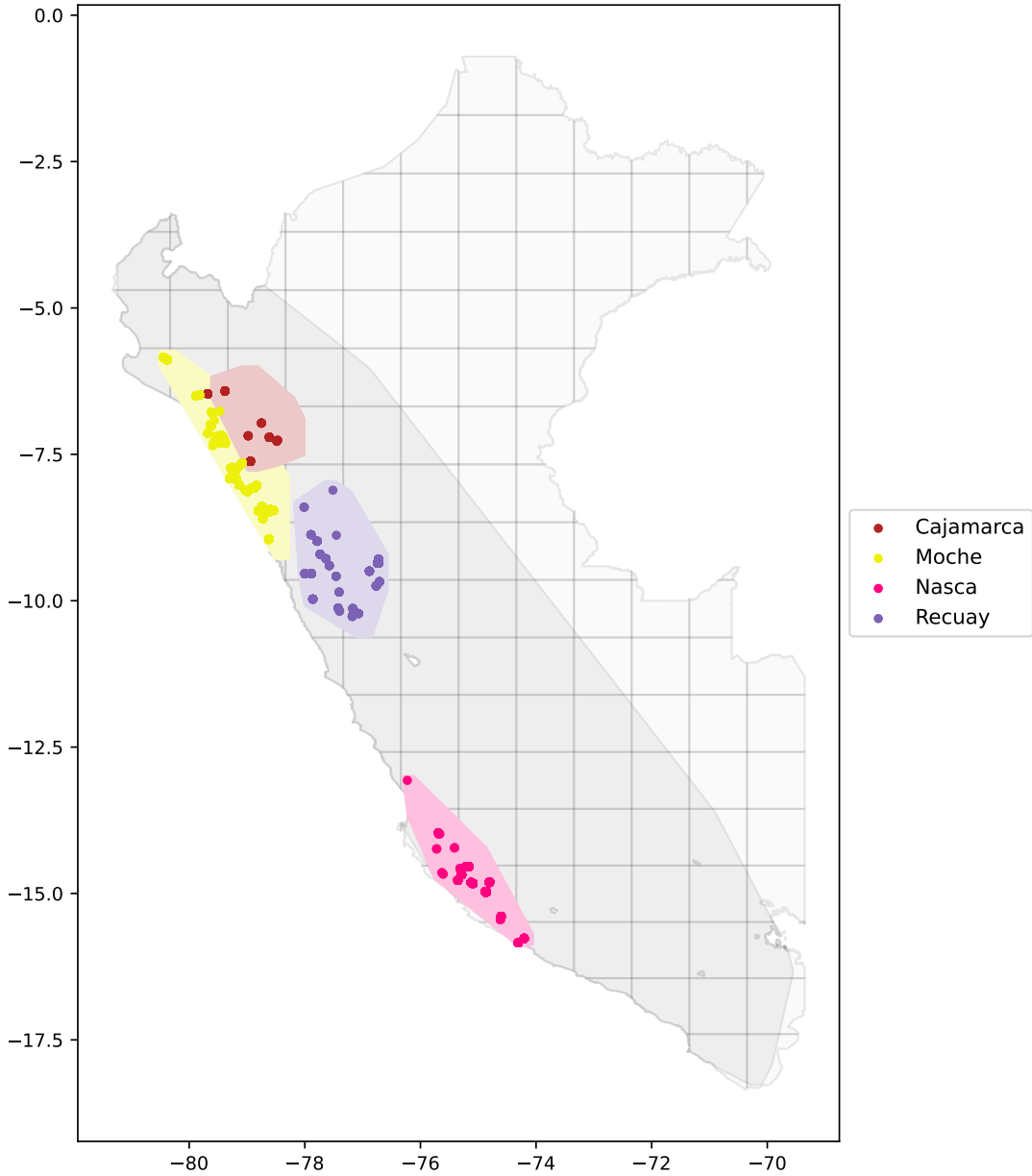
(C) *Sican-Lambayeque* (Middle Horizon, AD 700–1000)



(D) *Chimu* (Late Intermediate Period, AD 1000–1400)

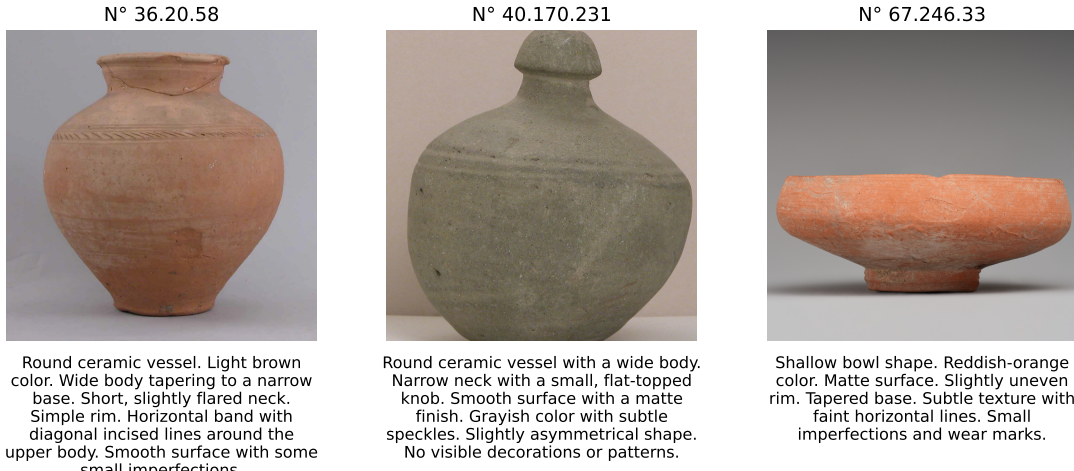
Notes. Examples of ceramic objects from the north and central-north coasts by archaeological group. Own elaboration with images from the [Larco Museum](#) (Lima, Perú).

FIGURE A.7: Spatial Distribution of Archaeological Sites — Early Intermediate Period



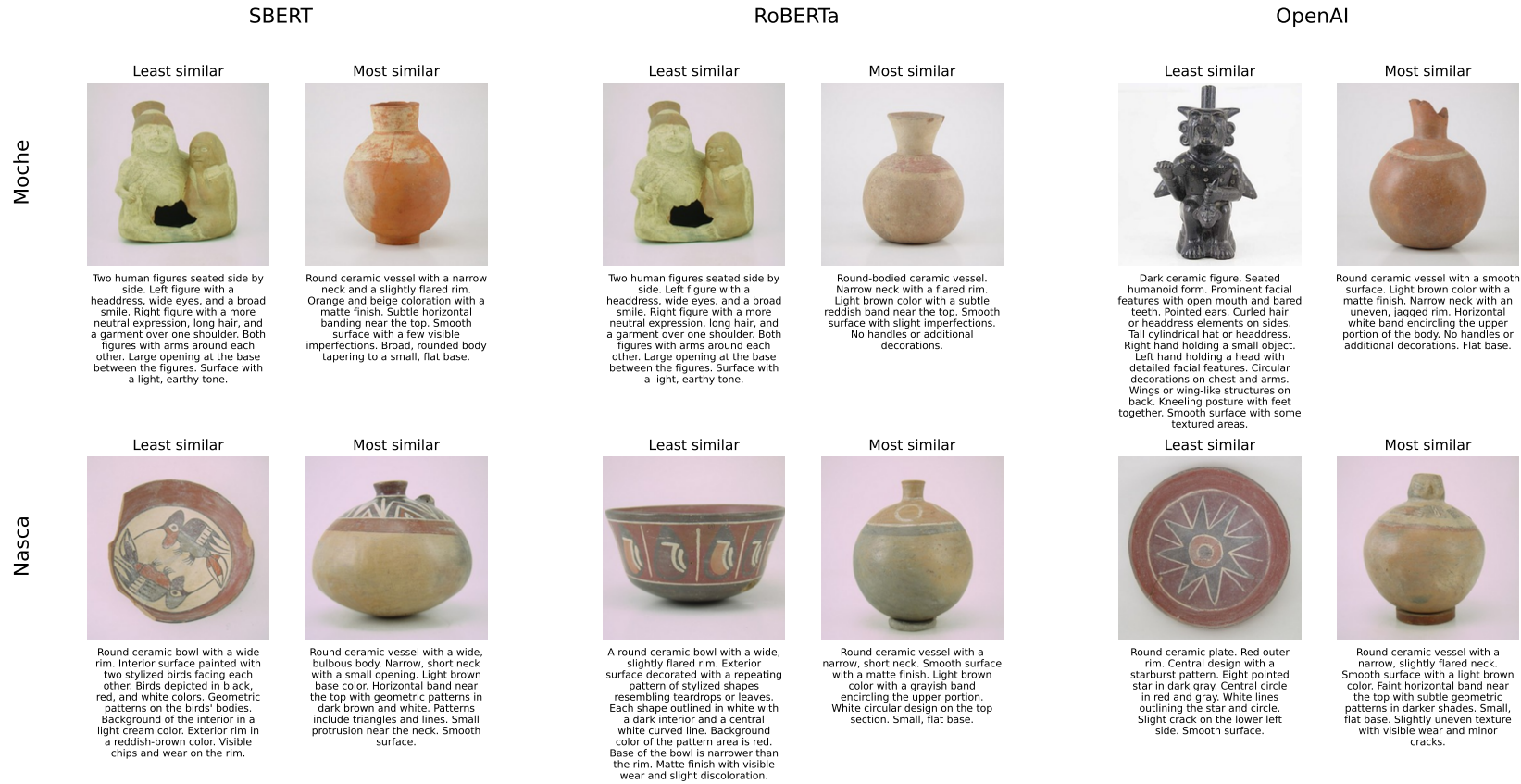
Notes. Spatial distribution of archaeological sites from the Early Intermediate Period (AD 1–700). Each point represents a site where ceramic objects were recovered, mapped using the World Geodetic System projection (WGS 1984). Colored areas represent the approximate homelands of the groups, according to the list of archaeological sites compiled from [Isbell and Silverman \(2002, 2008\)](#). The gray area represents the approximate territorial extent of the Inca between AD 1400 and 1525. Grid cells of approximately 1 degree by 1 degree at the equator in the background.

FIGURE A.8: Benchmark Ceramic Objects



Notes. Set of benchmark ceramic objects. Own elaboration with images from the open-access online collection of the [Metropolitan Museum of Art](#). English-language descriptions generated with GPT-4o (OpenAI et al. 2023).

FIGURE A.9: Examples of the Least and Most Similar Objects (Text Embeddings)



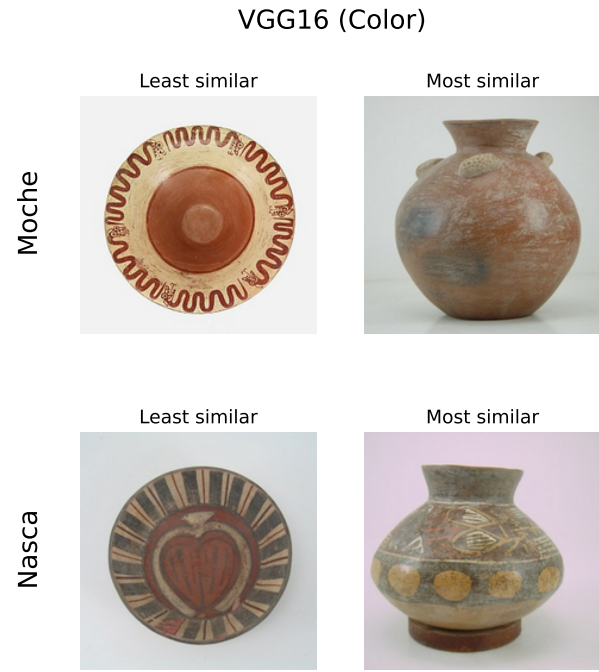
Notes. The figure presents examples of the least and most similar objects from Moche (top panel) and Nasca (bottom panel), based on their text-embedding similarity to the first object in the benchmark set (object N.36.20.58; see Figure A.8). The results are presented, separately, for Sentence-BERT (Reimers and Gurevych 2019), RoBERTa (Liu et al. 2019), and OpenAI's embedding model (`text-embedding-3-large` model). Own elaboration with images from the [Larco Museum](#) (Lima, Perú). English-language descriptions generated with GPT-4o (OpenAI et al. 2023).

FIGURE A.10: Examples of the Least and Most Similar Objects
(Spanish Text Embeddings)



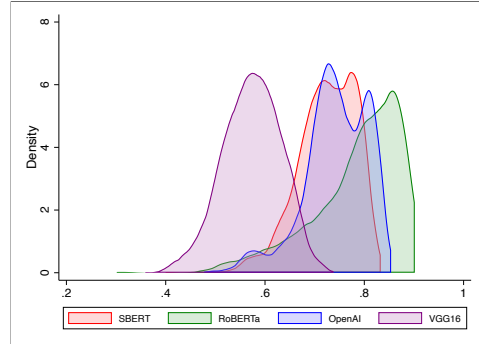
Notes. The figure presents examples of the least and most similar objects from Moche (top panel) and Nasca (bottom panel), based on their text-embedding similarity to the first object in the benchmark set (object N.36.20.58; see Figure A.8). Embeddings are generated using the Fandiño et al. (2022)'s RoBERTa model, which is pre-trained in Spanish. Own elaboration with images and Spanish-language descriptions from the [Larco Museum](#) (Lima, Perú).

FIGURE A.11: Examples of the Least and Most Similar Objects
(Image Embeddings)

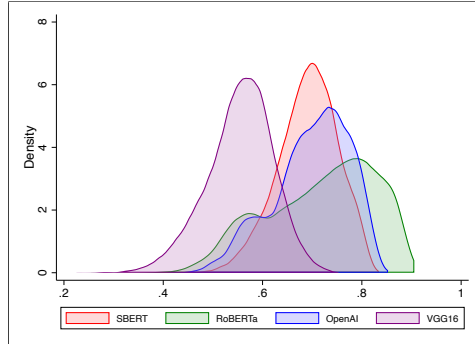


Notes. The figure presents examples of the least and most similar objects from Moche (top panel) and Nasca (bottom panel), based on their image-embedding similarity to the first object in the benchmark set (object N.36.20.58; see [Figure A.8](#)), generated with the VGG16 model ([Simonyan and Zisserman 2015](#)). Own elaboration with images from the [Larco Museum](#) (Lima, Perú).

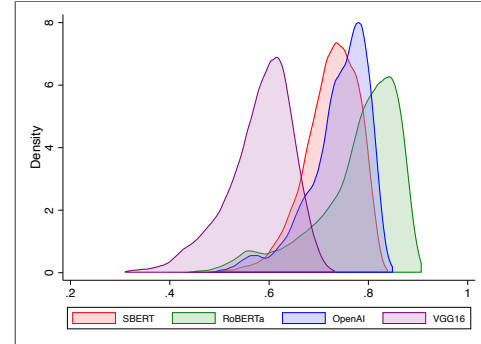
FIGURE A.12: Stylistic Distinctiveness — Densities of Embedding-Based Outcomes



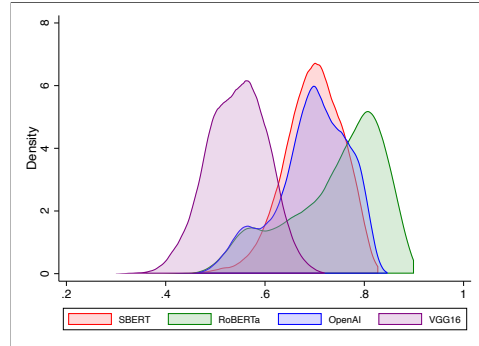
Period 1: Early Horizon



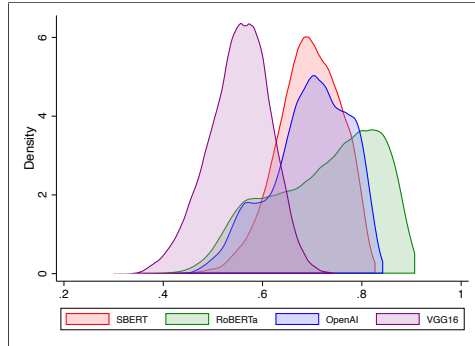
Period 2: Early Intermediate Period



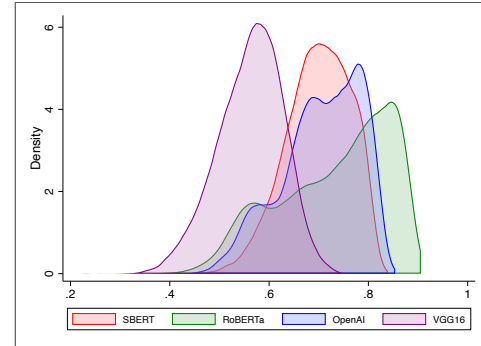
Period 3: Middle Horizon



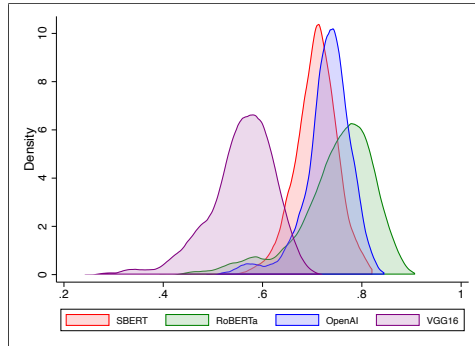
Period 4: Late Intermediate Period



Region: North Coast



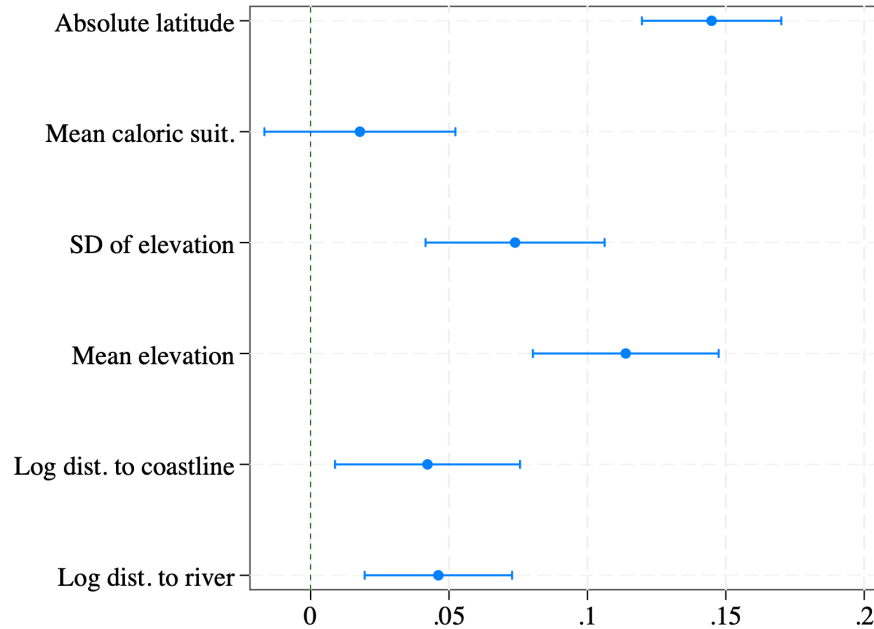
Region: Central-North Coast



Region: Central-South Coast

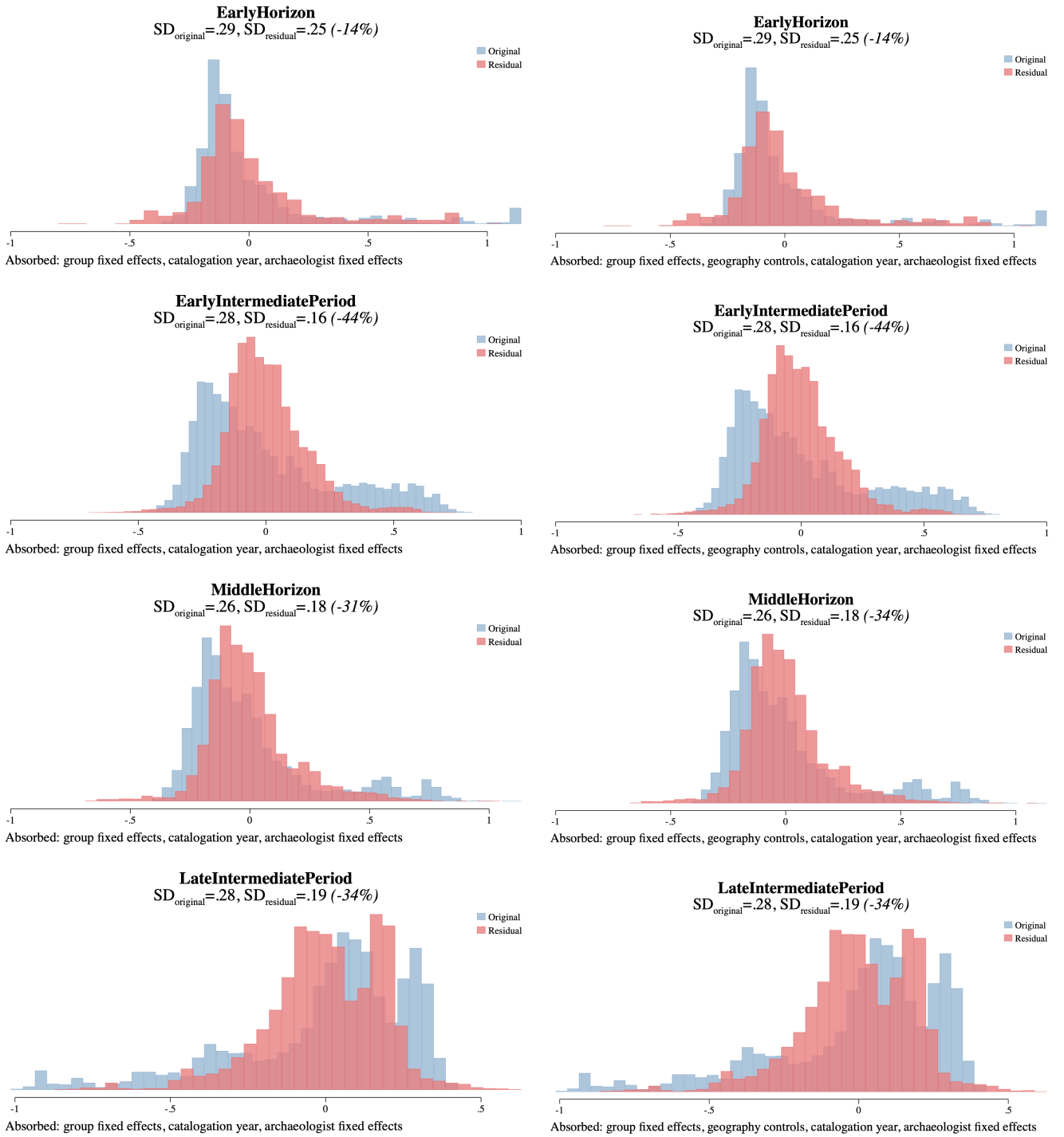
Notes. The figure displays the densities of the four outcomes of stylistic distinctiveness, based on (1) SBERT text embeddings, (2) RoBERTa text embeddings, (3) OpenAI text embeddings, and (4) VGG16 image embeddings, separately for each period and region.

FIGURE A.13: Stylistic Distinctiveness and Geographic Environment



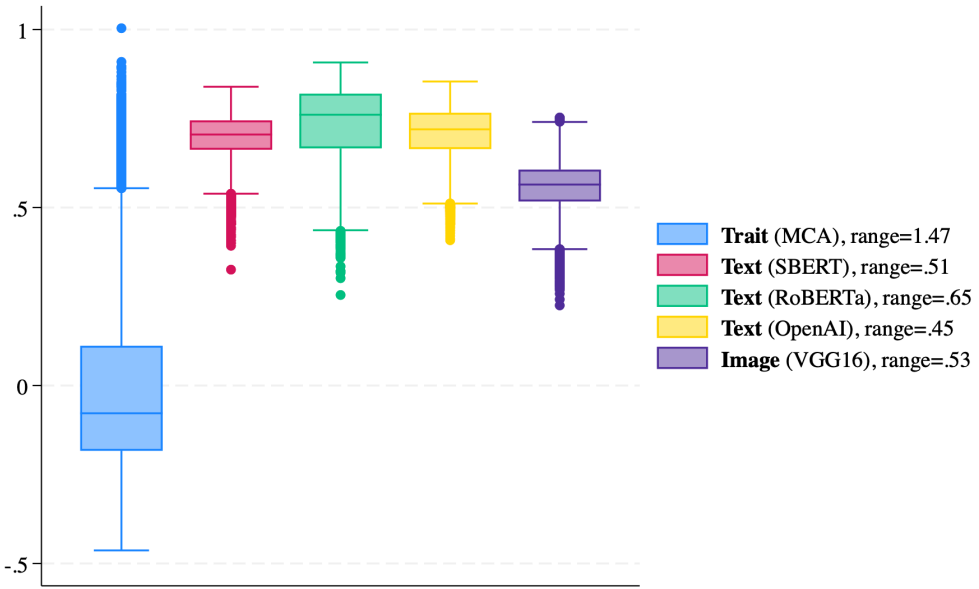
Notes. Standardized Average Effect Size (AES; Kling et al. 2004; Clingingsmith et al. 2009) and 95-percent confidence intervals for each geographic variable, separately. The standardized AES refers to the five outcomes of stylistic distinctiveness, based on (1) the first MCA dimension, (2) SBERT text embeddings, (3) RoBERTa text embeddings, (4) OpenAI text embeddings, and (5) VGG16 image embeddings. All regressions are estimated by OLS at the object level (with all objects, N=30,212) and include the year the object was electronically catalogued and archaeologist fixed effects. Standard errors are clustered at the site level.

FIGURE A.14: Stylistic Distinctiveness after Group FE and Geography Controls



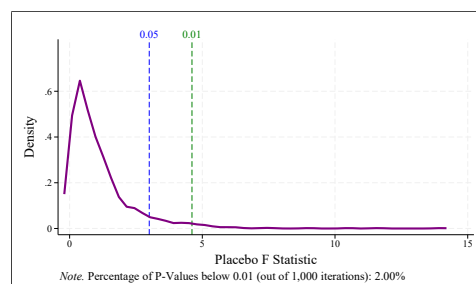
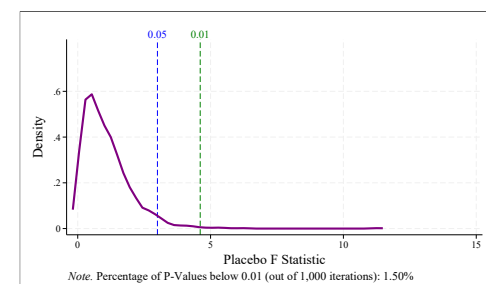
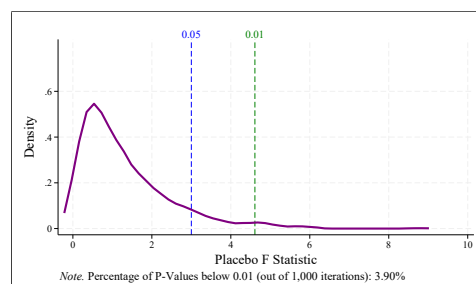
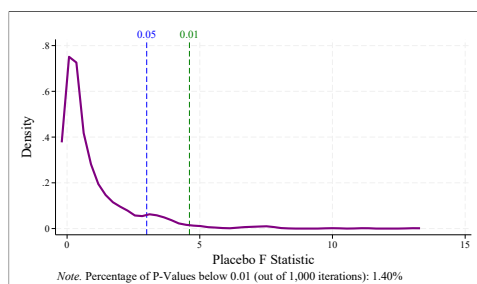
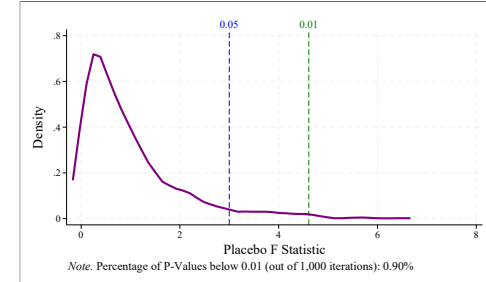
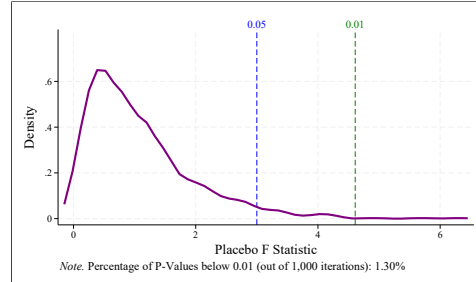
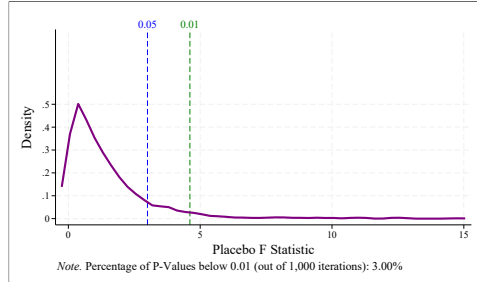
Notes. The left graphs show the distribution of stylistic distinctiveness based on the first MCA dimension (i.e., the score of the first dimension derived from applying MCA to the full repertoire of ceramic traits) after group fixed effects, cataloging year, and archaeologist fixed effects. The right graphs show the distribution after group fixed effects, cataloging year, archaeologist fixed effects, and geography controls (i.e., the site's absolute latitude, mean elevation, standard deviation of elevation, mean caloric suitability prior to AD 1500, log distance to the nearest river, and log distance to the coastline).

FIGURE A.15: Stylistic Distinctiveness — Boxplots



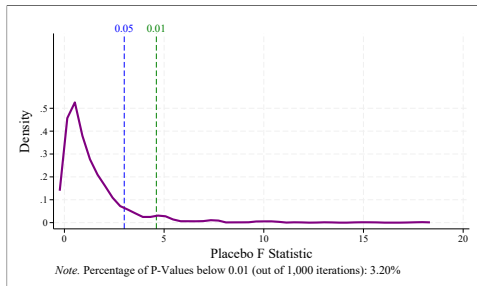
Notes. Boxplots of the five outcomes of stylistic distinctiveness, based on (1) the first MCA dimension, (2) SBERT text embeddings, (3) RoBERTa text embeddings, (4) OpenAI text embeddings, and (5) VGG16 image embeddings, considering all objects (N=30,212).

FIGURE A.16: Fictitious Group Identities — Distribution of F-Statistic (MCA)

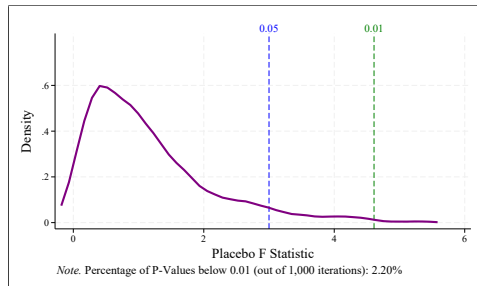


Notes. We randomly assign the group identity of each ceramic object while preserving original group sizes. We repeat the random assignment of fictitious group identities 1,000 times, separately for each period and region. The figures show the distribution of the F-statistic from the placebo exercise, using the measure of stylistic distinctiveness based on the first MCA dimension as the outcome variable. The note below each graph indicates the percentage of times in which the fixed effects for the fictitious group identities are jointly significant at the 1 percent level. The green and blue lines represent the thresholds at the 1 percent and 5 percent levels, respectively. All regressions are estimated by OLS at the object level and include fictitious-group fixed effects, the year the object was electronically catalogued, archaeologist fixed effects, and a vector of site-level geographic controls (absolute latitude, mean elevation, standard deviation of elevation, mean caloric suitability prior to AD 1500, log distance to the nearest river, and log distance to the coastline). Standard errors are clustered at the site level.

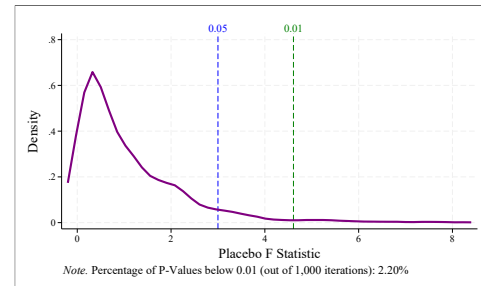
FIGURE A.17: Fictitious Group Identities — Distribution of F-Statistic (SBERT)



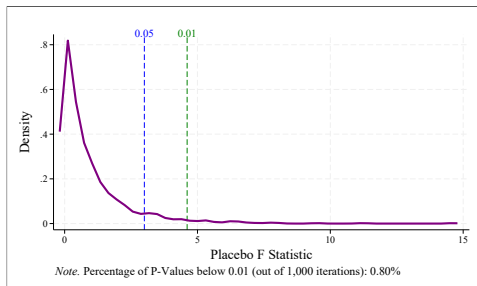
Period 1: Early Horizon



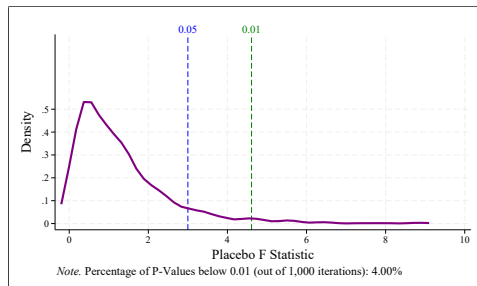
Period 2: Early Intermediate Period



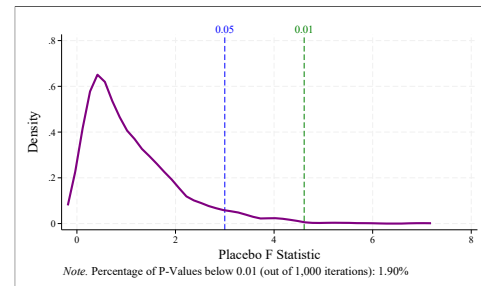
Period 3: Middle Horizon



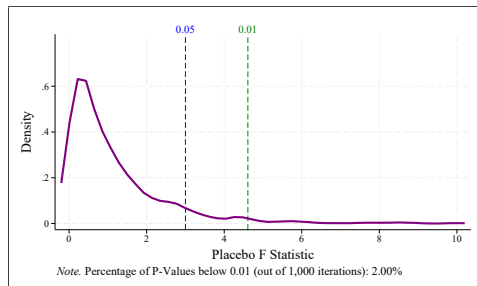
Period 4: Late Intermediate Period



Region: North Coast



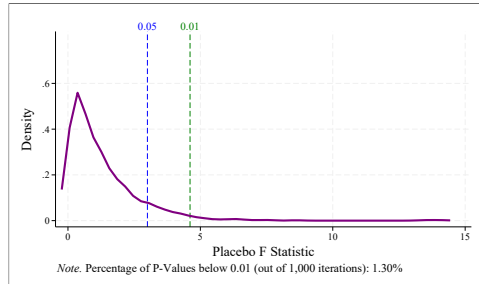
Region: Central-North Coast



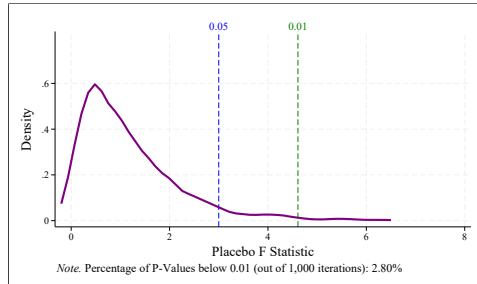
Region: Central-South Coast

Notes. We randomly assign the group identity of each ceramic object while preserving original group sizes. We repeat the random assignment of fictitious group identities 1,000 times, separately for each period and region. The figures show the distribution of the F-statistic from the placebo exercise, using the measure of stylistic distinctiveness based on SBERT text embeddings as the outcome variable. The note below each graph indicates the percentage of times in which the fixed effects for the fictitious group identities are jointly significant at the 1 percent level. The green and blue lines represent the thresholds at the 1 percent and 5 percent levels, respectively. All regressions are estimated by OLS at the object level and include fictitious-group fixed effects, the year the object was electronically catalogued, archaeologist fixed effects, and a vector of site-level geographic controls (absolute latitude, mean elevation, standard deviation of elevation, mean caloric suitability prior to AD 1500, log distance to the nearest river, and log distance to the coastline). Standard errors are clustered at the site level.

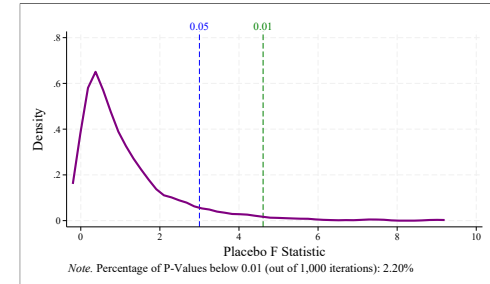
FIGURE A.18: Fictitious Group Identities — Distribution of F-Statistic (RoBERTa)



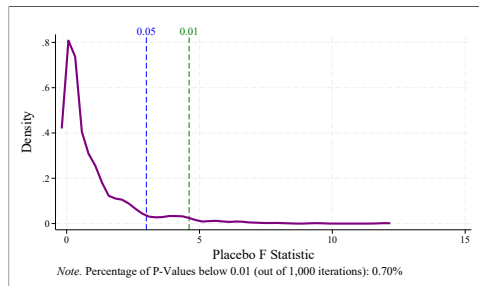
Period 1: Early Horizon



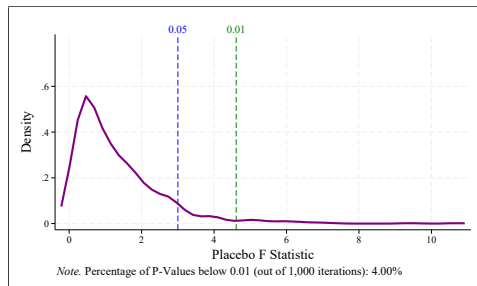
Period 2: Early Intermediate Period



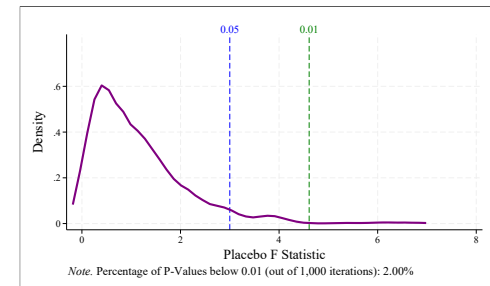
Period 3: Middle Horizon



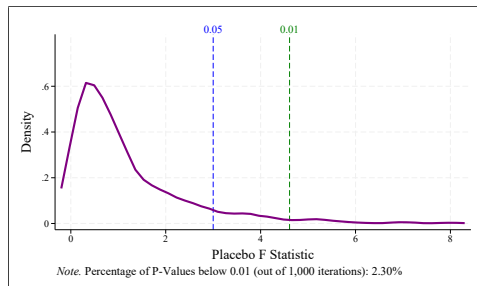
Period 4: Late Intermediate Period



Region: North Coast



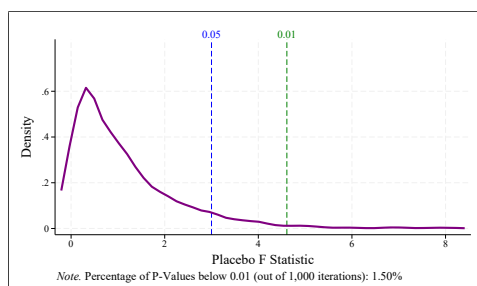
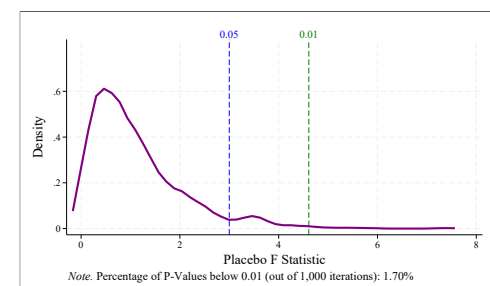
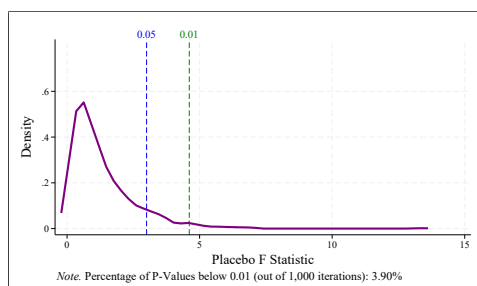
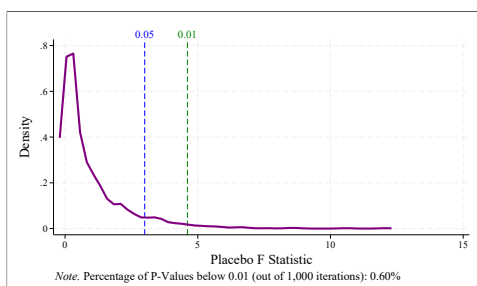
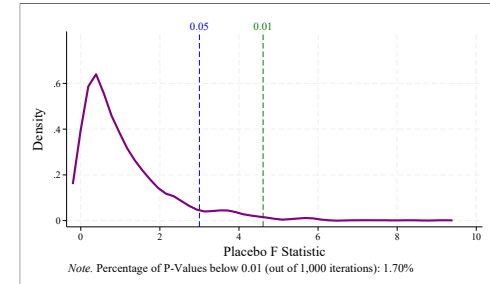
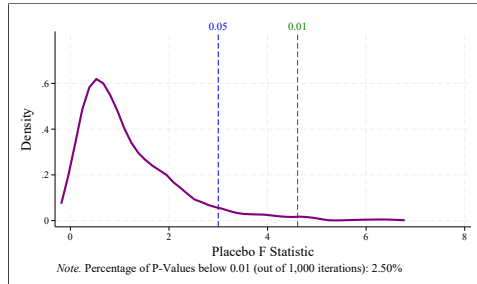
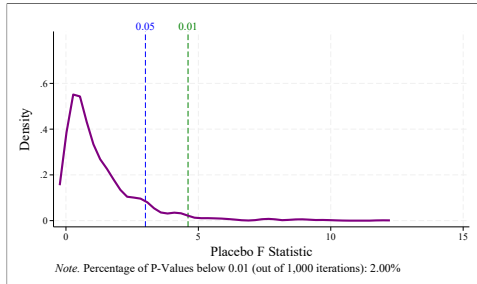
Region: Central-North Coast



Region: Central-South Coast

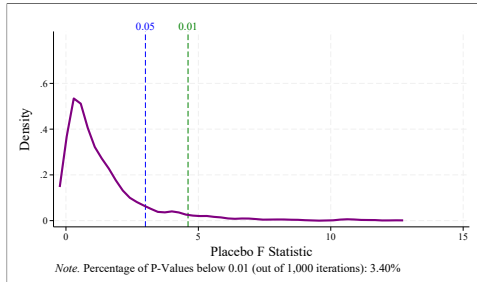
Notes. We randomly assign the group identity of each ceramic object while preserving original group sizes. We repeat the random assignment of fictitious group identities 1,000 times, separately for each period and region. The figures show the distribution of the F-statistic from the placebo exercise, using the measure of stylistic distinctiveness based on RoBERTa text embeddings as the outcome variable. The note below each graph indicates the percentage of times in which the fixed effects for the fictitious group identities are jointly significant at the 1 percent level. The green and blue lines represent the thresholds at the 1 percent and 5 percent levels, respectively. All regressions are estimated by OLS at the object level and include fictitious-group fixed effects, the year the object was electronically catalogued, archaeologist fixed effects, and a vector of site-level geographic controls (absolute latitude, mean elevation, standard deviation of elevation, mean caloric suitability prior to AD 1500, log distance to the nearest river, and log distance to the coastline). Standard errors are clustered at the site level.

FIGURE A.19: Fictitious Group Identities — Distribution of F-Statistic (OpenAI)

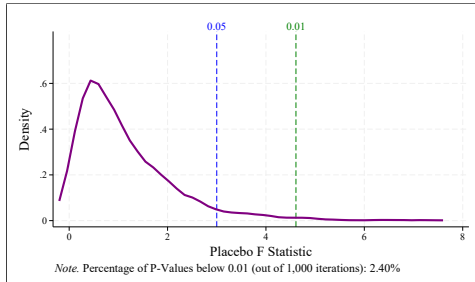


Notes. We randomly assign the group identity of each ceramic object while preserving original group sizes. We repeat the random assignment of fictitious group identities 1,000 times, separately for each period and region. The figures show the distribution of the F-statistic from the placebo exercise, using the measure of stylistic distinctiveness based on OpenAI text embeddings as the outcome variable. The note below each graph indicates the percentage of times in which the fixed effects for the fictitious group identities are jointly significant at the 1 percent level. The green and blue lines represent the thresholds at the 1 percent and 5 percent levels, respectively. All regressions are estimated by OLS at the object level and include fictitious-group fixed effects, the year the object was electronically catalogued, archaeologist fixed effects, and a vector of site-level geographic controls (absolute latitude, mean elevation, standard deviation of elevation, mean caloric suitability prior to AD 1500, log distance to the nearest river, and log distance to the coastline). Standard errors are clustered at the site level.

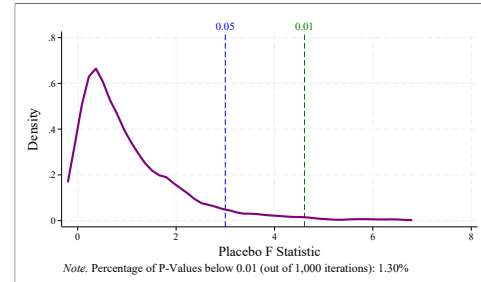
FIGURE A.20: Fictitious Group Identities — Distribution of F-Statistic (VGG16)



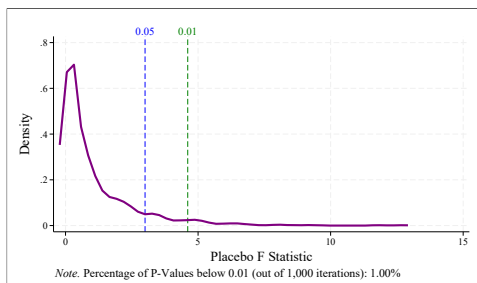
Period 1: Early Horizon



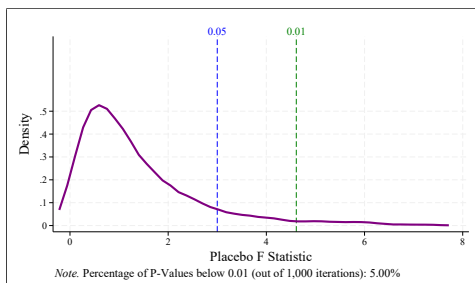
Period 2: Early Intermediate Period



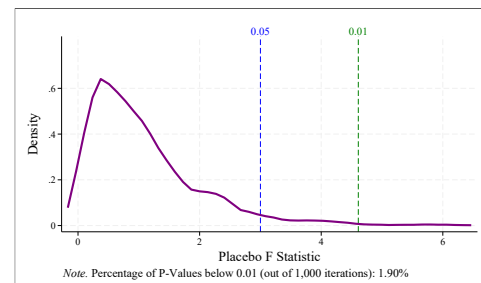
Period 3: Middle Horizon



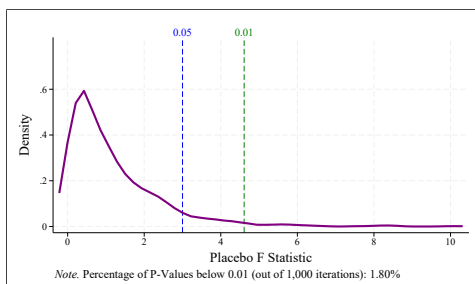
Period 4: Late Intermediate Period



Region: North Coast



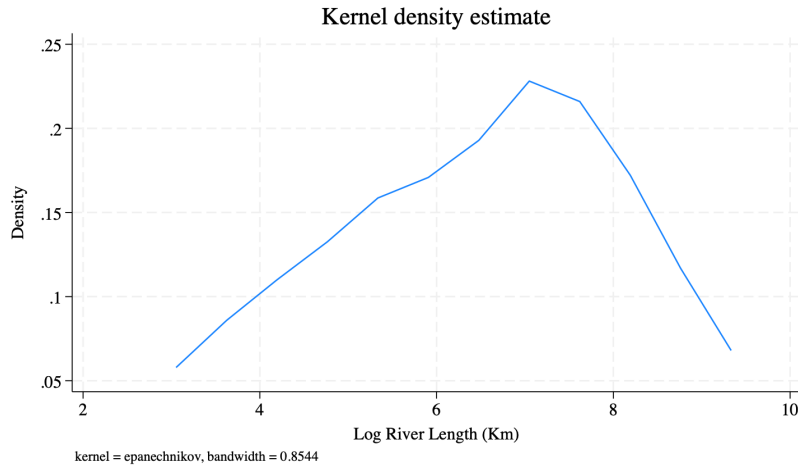
Region: Central-North Coast



Region: Central-South Coast

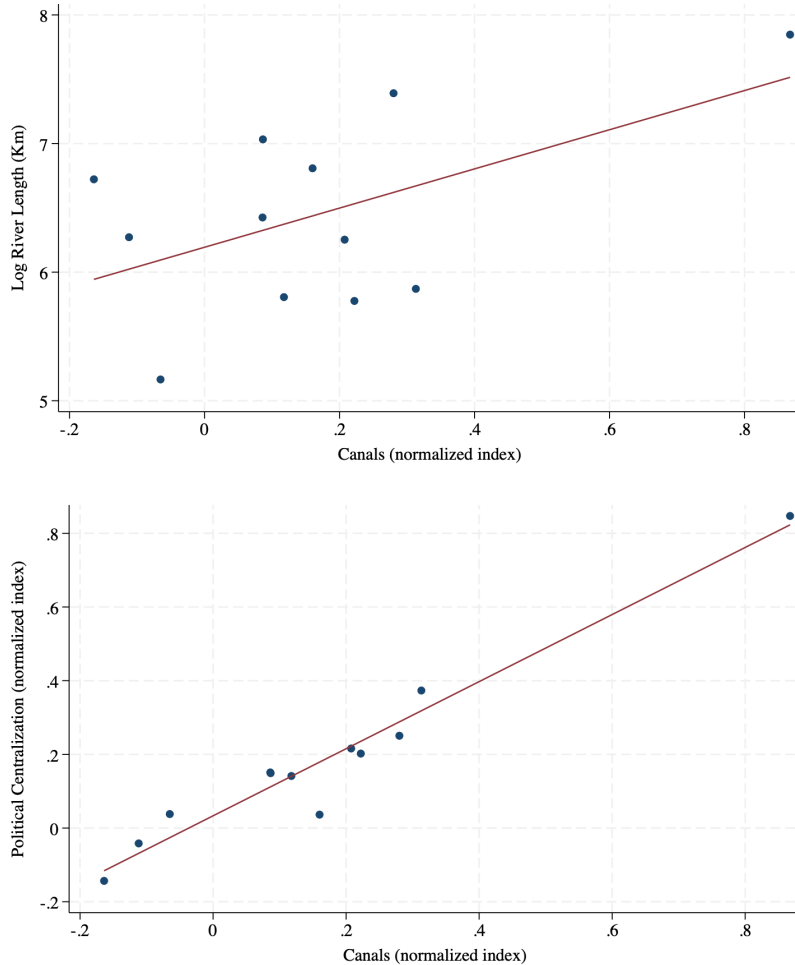
Notes. We randomly assign the group identity of each ceramic object while preserving original group sizes. We repeat the random assignment of fictitious group identities 1,000 times, separately for each period and region. The figures show the distribution of the F-statistic from the placebo exercise, using the measure of stylistic distinctiveness based on VGG16 image embeddings as the outcome variable. The note below each graph indicates the percentage of times in which the fixed effects for the fictitious group identities are jointly significant at the 1 percent level. The green and blue lines represent the thresholds at the 1 percent and 5 percent levels, respectively. All regressions are estimated by OLS at the object level and include fictitious-group fixed effects, the year the object was electronically catalogued, archaeologist fixed effects, and a vector of site-level geographic controls (absolute latitude, mean elevation, standard deviation of elevation, mean caloric suitability prior to AD 1500, log distance to the nearest river, and log distance to the coastline). Standard errors are clustered at the site level.

FIGURE A.21: Density of Log Perennial River Length at the Group Level



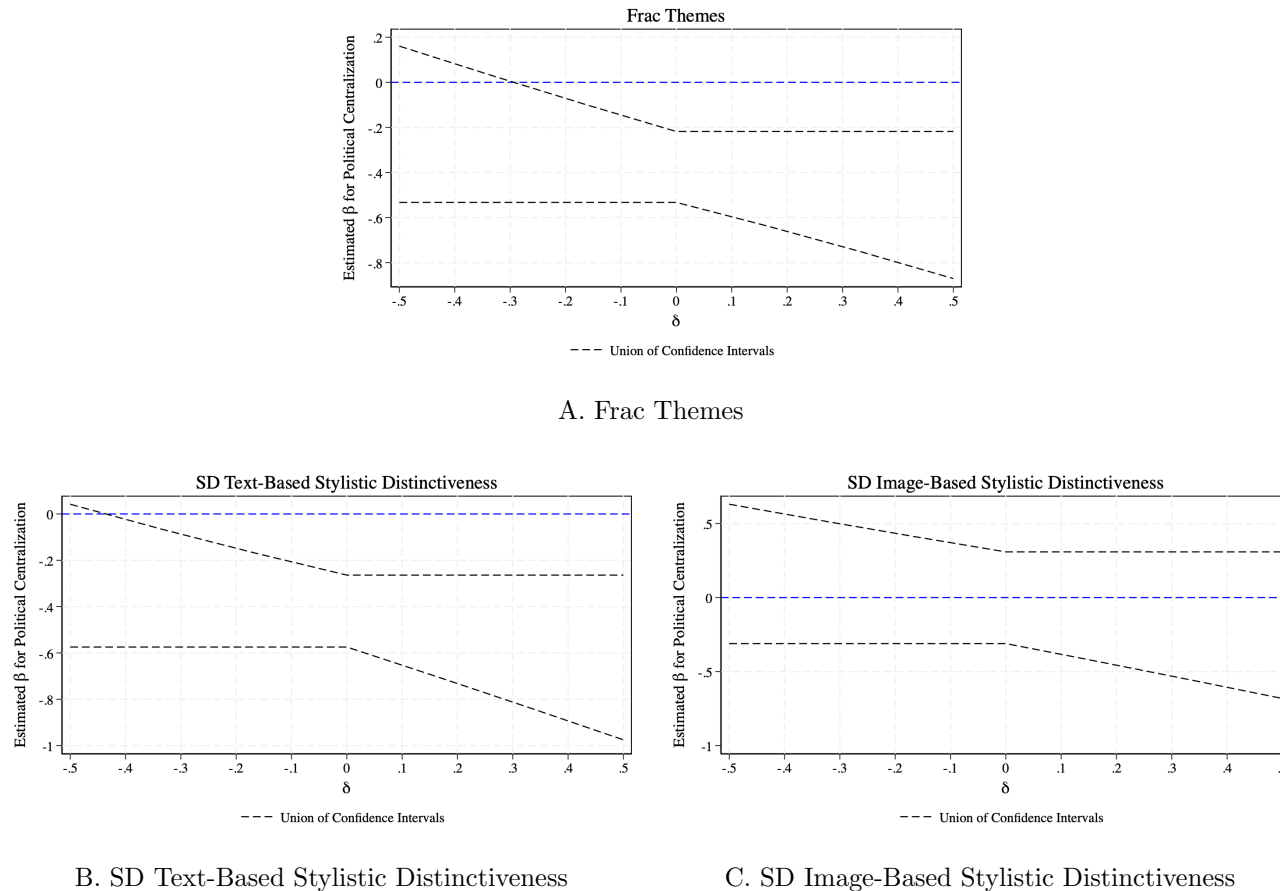
Notes. Kernel density of log perennial river length at the group level. Perennial river length is computed within each group's historical homeland (i.e., the set of 10×10 km grid cells occupied by the group in the corresponding period) using the river basemap from the Seamless Digital Chart of the World (SDCW).

FIGURE A.22: Canal Infrastructure, Log Perennial River Length, and Political Centralization



Notes. The top graph shows the relationship between log perennial river length and the canal index, while the bottom graph shows the relationship between political centralization and the canal index (bincscatters at the group level after controlling for the group's log mean temperature, temperature stability (isothermality), and a dummy variable equal to one if the number of mentions found for the group is above the median).

FIGURE A.23: Union of Confidence Intervals — Conley et al. (2012)'s Plausibly Exogenous Framework



Notes. Union of confidence intervals (UCI, 95 percent level) from Conley et al. (2012)'s plausibly exogenous framework for the coefficient on political centralization. The groups' level of political centralization is instrumented with the log of total perennial river length. The outcome variable is a site-level proxy for cultural dispersion. Panel A uses an index of thematic fractionalization, based on the share of objects classified by theme, to proxy for cultural dispersion. In Panel B and Panel C, we use the standard deviation of stylistic distinctiveness across objects within a site, based on SBERT text embeddings (Panel B) and VGG16 image embeddings (Panel C). All regressions include baseline controls, as well as the log of the group's area and the log of the group's number of sites. The set of baseline controls include the share of open-form objects, the share of close-form objects, the log number of objects, a dummy variable equal to one if the number of mentions found for the group is above the median, the group's log mean temperature and temperature stability (isothermality), and a vector of site-level geographic controls (absolute latitude, mean elevation, standard deviation of elevation, mean caloric suitability prior to AD 1500, log distance to the nearest river, and log distance to the coastline). Standard errors are clustered at the Group \times Region level.

TABLE A.1: Ceramic Traits

Trait ID	Trait
1	form modeling - open shapes - type - plate
2	form modeling - open shapes - type - bowl
3	form modeling - open shapes - type - <i>vaso kero</i>
4	form modeling - open shapes - type - cup
5	form modeling - open shapes - type - <i>escudilla</i>
6	form modeling - open shapes - base - yes - tripod
7	form modeling - open shapes - base - yes - pedestal
8	form modeling - open shapes - base - no
9	form modeling - closed shapes - type - jars, <i>cántaro</i>
10	form modeling - closed shapes - type - <i>olla</i>
11	form modeling - closed shapes - type - bottle
12	form modeling - closed shapes - type - <i>canchero</i>
13	form modeling - closed shapes - handle - type - <i>puentecito</i>
14	form modeling - closed shapes - handle - type - <i>estribo</i>
15	form modeling - closed shapes - handle - type - <i>lateral</i>
16	form modeling - closed shapes - handle - type - <i>canasta</i>
17	form modeling - closed shapes - handle - no
18	form modeling - closed shapes - body - double-chambered spout
19	form modeling - closed shapes - body - double spout with bridge
20	form modeling - closed shapes - body - <i>gollete</i>
21	form modeling - closed shapes - base - yes - type - tripod
22	form modeling - closed shapes - base - yes - type - pedestal
23	form modeling - closed shapes - base - no
24	molding - solid shapes - yes - sculpture - animal - birds

Continues on next page...

TABLE A.1: (continued)

Trait ID	Trait
25	molding - solid shapes - yes - sculpture - animal - sea animals
26	molding - solid shapes - yes - sculpture - animal - snakes
27	molding - solid shapes - yes - sculpture - animal - felines
28	molding - solid shapes - yes - sculpture - animal - camelids
29	molding - solid shapes - yes - sculpture - animal - monkeys
30	molding - solid shapes - yes - sculpture - animal - dogs
31	molding - solid shapes - yes - sculpture - animal - other
32	molding - solid shapes - yes - sculpture - other - flowers
33	molding - solid shapes - yes - sculpture - other - fruits
34	molding - solid shapes - yes - sculpture - other - crops
35	molding - solid shapes - yes - sculpture - other - seashells
36	molding - solid shapes - yes - sculpture - other - portrait
37	molding - solid shapes - yes - sculpture - other - figurine
38	molding - solid shapes - yes - sculpture - other - supernatural
39	molding - solid shapes - yes - sculpture - other - ceremonial
40	molding - solid shapes - yes - sculpture - other - musical
41	molding - solid shapes - yes - sculpture - other - sexual
42	molding - solid shapes - yes - sculpture - other - fertility, birthing
43	molding - solid shapes - yes - sculpture - other - war
44	molding - solid shapes - yes - sculpture - other - agriculture
45	molding - solid shapes - yes - sculpture - other - fishing
46	molding - solid shapes - yes - sculpture - other - hunting
47	molding - solid shapes - yes - sculpture - other - death
48	molding - solid shapes - yes - sculpture - other - other

Continues on next page...

TABLE A.1: (continued)

Trait ID	Trait
49	molding - solid shapes - yes
50	surface incising - yes
51	surface polishing - yes
52	surface relief - yes
53	painting (design) - yes - outline - no
54	painting (design) - yes - theme - geometric - vertical
55	painting (design) - yes - theme - geometric - horizontal
56	painting (design) - yes - theme - geometric - other
57	painting (design) - yes - theme - animal - birds
58	painting (design) - yes - theme - animal - sea animals
59	painting (design) - yes - theme - animal - snakes
60	painting (design) - yes - theme - animal - felines
61	painting (design) - yes - theme - animal - camelids
62	painting (design) - yes - theme - animal - dogs
63	painting (design) - yes - theme - animal - monkeys
64	painting (design) - yes - theme - animal - other
65	painting (design) - yes - theme - other - flowers
66	painting (design) - yes - theme - other - fruits
67	painting (design) - yes - theme - other - crops
68	painting (design) - yes - theme - other - seashells
69	painting (design) - yes - theme - other - supernatural
70	painting (design) - yes - theme - other - ceremonial
71	painting (design) - yes - theme - other - musical
72	painting (design) - yes - theme - other - sexual

Continues on next page...

TABLE A.1: (continued)

Trait ID	Trait
73	painting (design) - yes - theme - other - fertility, birthing
74	painting (design) - yes - theme - other - war
75	painting (design) - yes - theme - other - agriculture
76	painting (design) - yes - theme - other - fishing
77	painting (design) - yes - theme - other - hunting
78	painting (design) - yes - theme - other - death
79	painting (design) - yes - theme - other - other
80	painting (design) - yes - pigment - red
81	painting (design) - yes - pigment - orange
82	painting (design) - yes - pigment - brown
83	painting (design) - yes - pigment - yellow
84	painting (design) - yes - pigment - white
85	painting (design) - yes - pigment - cream
86	painting (design) - yes - pigment - gray
87	painting (design) - yes - pigment - black
88	painting (design) - yes - pigment - beige
89	painting (design) - yes - pigment - purple
90	painting (design) - yes - pigment - pink
91	painting (design) - yes - polychrome - yes
92	painting (design) - yes - number of pigments
93	painting (design) - yes - pigment combination (group)
94	height - quartile 1
95	height - quartile 2
96	height - quartile 3

Continues on next page...

TABLE A.1: (continued)

Trait ID	Trait
97	height - quartile 4
98	length - quartile 1
99	length - quartile 2
100	length - quartile 3
101	length - quartile 4
102	width - quartile 1
103	width - quartile 2
104	width - quartile 3
105	width - quartile 4
106	weight - quartile 1
107	weight - quartile 2
108	weight - quartile 3
109	weight - quartile 4

TABLE A.2: Full-Sample Regressions —
Stylistic Distinctiveness and Joint Significance of Group Fixed Effects

Period	Panel A: Cluster(Site)		Panel B: Conley 100km		Panel C: Conley 50km		Δ Adj. R^2
	(1) F-stat	(2) P-value	(3) χ^2 -stat	(4) P-value	(5) χ^2 -stat	(6) P-value	
MCA	840.0	< 0.001	13869.7	< 0.001	13869.7	< 0.001	14.0
SBERT	99.2	< 0.001	2214.3	< 0.001	2214.3	< 0.001	3.2
RoBERTa	98.4	< 0.001	1348.5	< 0.001	1348.5	< 0.001	2.8
OpenAI	134.7	< 0.001	3265.0	< 0.001	3265.0	< 0.001	5.6
VGG16	146.3	< 0.001	1616.1	< 0.001	1616.1	< 0.001	5.7
Catalog Year	Yes	Yes	Yes	Yes	Yes	Yes	Yes
Archaeologist FE	Yes	Yes	Yes	Yes	Yes	Yes	Yes
Geographic Controls	Yes	Yes	Yes	Yes	Yes	Yes	Yes
Region FE	Yes	Yes	Yes	Yes	Yes	Yes	Yes
N. Objects	30212	30212	30212	30212	30212	30212	30212

Notes. The table reports test results for the joint significance of group fixed effects. In each regression, the outcome variable is a measure of stylistic distinctiveness based on the first MCA dimension, SBERT text embeddings, RoBERTa text embeddings, OpenAI text embeddings, or VGG16 image embeddings (indicated in the first column). All regressions are estimated by OLS at the object level, including all objects in the sample, and include group fixed effects, the year the object was electronically catalogued, archaeologist fixed effects, the vector of site-level geographic controls (absolute latitude, mean elevation, standard deviation of elevation, mean caloric suitability prior to AD 1500, log distance to the nearest river, and log distance to the coastline) and region fixed effects. Standard errors are clustered at the site level in Panel A (Cluster Site), and adjusted for spatial correlation with distance cutoffs of approximately 100km and 50km at the equator (Conley 1999) in Panels B and C, respectively. The change in adjusted R^2 , relative to the specification without group fixed effects (Δ Adj. R^2), is reported in percentage terms.

TABLE A.3: Fictitious Group Identities —
Stylistic Distinctiveness and Joint Significance of Group Fixed Effects

		MCA (1)	SBERT (2)	RoBERTa (3)	OpenAI (4)	VGG16 (5)
Period	N. Groups	N. Objects	% P-val < 0.01			
Early Horizon	3	1299	3.00	3.20	1.30	2.00
Early Intermediate Period	4	17464	1.30	2.20	2.80	2.50
Middle Horizon	3	6192	0.90	2.20	2.20	1.70
Late Intermediate Period	2	5257	1.40	0.80	0.70	0.60
Region	N. Groups	N. Objects	% P-val < 0.01			
North Coast	4	5036	3.90	4.00	4.00	3.90
Central-North Coast	4	17706	1.50	1.90	2.00	1.70
Central-South Coast	3	4101	2.00	2.00	2.30	1.50
Catalog Year			Yes	Yes	Yes	Yes
Archaeologist FE			Yes	Yes	Yes	Yes
Geographic Controls			Yes	Yes	Yes	Yes

Notes. We randomly assign the group identity of each ceramic object while preserving original group sizes. We repeat the random assignment of fictitious group identities 1,000 times, separately for each period (top panel) and region (bottom panel). The table shows the percentage of times in which the fixed effects for the fictitious group identities are jointly significant at the 1 percent level. The outcome variable is a measure of stylistic distinctiveness based on the first MCA dimension (Column 1), SBERT text embeddings (Column 2), RoBERTa text embeddings (Column 3), OpenAI text embeddings (Column 4), or VGG16 image embeddings (Column 5). All regressions are estimated by OLS at the object level and include fictitious-group fixed effects, the year the object was electronically catalogued, archaeologist fixed effects, and a vector of site-level geographic controls (absolute latitude, mean elevation, standard deviation of elevation, mean caloric suitability prior to AD 1500, log distance to the nearest river, and log distance to the coastline). Standard errors are clustered at the site level.

TABLE A.4: Stylistic Distinctiveness (Trait-Based)
and Joint Significance of Group Fixed Effects — Conley SE (50km)

Period	N. Groups	N. Objects	Panel A		Panel B	
			(1)	(2)	(3)	(4)
Early Horizon	3	1299	107.6	< 0.001	40.1	< 0.001
Early Intermediate Period	4	17464	4368.4	< 0.001	2793.9	< 0.001
Middle Horizon	3	6192	5154.3	< 0.001	111.9	< 0.001
Late Intermediate Period	2	5257	253.1	< 0.001	143.8	< 0.001
Region	N. Groups	N. Objects	χ^2 -stat	P-value	χ^2 -stat	P-value
North Coast	4	5036	3231.4	< 0.001	2562.5	< 0.001
Central-North Coast	4	17706	1916.4	< 0.001	1545.1	< 0.001
Central-South Coast	3	4101	2687.8	< 0.001	549.1	< 0.001
Catalog Year			Yes	Yes	Yes	Yes
Archaeologist FE			Yes	Yes	Yes	Yes
Geographic Controls			No	No	Yes	Yes

Notes. The table reports χ^2 -test results for the joint significance of group fixed effects. The top panel presents one regression per period, while the bottom panel presents one regression per region. All regressions are estimated by OLS at the object level, with the measure of stylistic distinctiveness based on the first MCA dimension as outcome variable (i.e., the score of the first dimension derived from applying MCA to the full repertoire of ceramic traits). All regressions include group fixed effects. In Panel A, regressions also include the year the object was electronically cataloged and archaeologist fixed effects. In Panel B, the vector of site-level geographic controls includes the site's absolute latitude, mean elevation, standard deviation of elevation, mean caloric suitability prior to AD 1500, log distance to the nearest river, and log distance to the coastline. Standard errors are adjusted for spatial correlation with a distance cutoff of approximately 50km at the equator (Conley 1999).

TABLE A.5: Stylistic Distinctiveness (Trait-Based)
and Joint Significance of Group Fixed Effects — Conley SE (100km)

Period	N. Groups	N. Objects	Panel A		Panel B	
			(1)	(2)	(3)	(4)
Early Horizon	3	1299	116.3	< 0.001	41.2	< 0.001
Early Intermediate Period	4	17464	6270.3	< 0.001	3141.7	< 0.001
Middle Horizon	3	6192	8069.4	< 0.001	137.3	< 0.001
Late Intermediate Period	2	5257	200.8	< 0.001	274.3	< 0.001
Region	N. Groups	N. Objects	χ^2 -stat	P-value	χ^2 -stat	P-value
North Coast	4	5036	2384.6	< 0.001	60.2	< 0.001
Central-North Coast	4	17706	5861	< 0.001	3722.9	< 0.001
Central-South Coast	3	4101	3622.5	< 0.001	514.6	< 0.001
Catalog Year			Yes	Yes	Yes	Yes
Archaeologist FE			Yes	Yes	Yes	Yes
Geographic Controls			No	No	Yes	Yes

Notes. The table reports χ^2 -test results for the joint significance of group fixed effects. The top panel presents one regression per period, while the bottom panel presents one regression per region. All regressions are estimated by OLS at the object level, with the measure of stylistic distinctiveness based on the first MCA dimension as outcome variable (i.e., the score of the first dimension derived from applying MCA to the full repertoire of ceramic traits). All regressions include group fixed effects. In Panel A, regressions also include the year the object was electronically cataloged and archaeologist fixed effects. In Panel B, the vector of site-level geographic controls includes the site's absolute latitude, mean elevation, standard deviation of elevation, mean caloric suitability prior to AD 1500, log distance to the nearest river, and log distance to the coastline. Standard errors are adjusted for spatial correlation with a distance cutoff of approximately 100km at the equator (Conley 1999).

TABLE A.6: Stylistic Distinctiveness (Text- and Image-Based) and Joint Significance of Group Fixed Effects — Conley SE (50km)

Panel A: Text-Based (SBERT)				Panel B: Text-Based (RoBERTa)	
	(1)	(2)		(3)	(4)
Period	N. Groups	N. Objects	χ^2 -stat	P-val	χ^2 -stat
Early Horizon	3	1299	144.4	< 0.001	97.7
Early Intermediate Period	4	17464	34.1	< 0.001	143.7
Middle Horizon	3	6192	118.8	< 0.001	229.0
Late Intermediate Period	2	5257	85.8	< 0.001	10.2
Region	N. Groups	N. Objects	χ^2 -stat	P-val	χ^2 -stat
North Coast	4	5036	2307.0	< 0.001	475.3
Central-North Coast	4	17706	834.3	< 0.001	287.7
Central-South Coast	3	4101	169.6	< 0.001	130.5
Panel C: Text-Based (OpenAI)				Panel D: Image-Based (VGG16)	
	(5)	(6)		(7)	(8)
Period	N. Groups	N. Objects	χ^2 -stat	P-val	χ^2 -stat
Early Horizon	3	1299	763.7	< 0.001	476.4
Early Intermediate Period	4	17464	42.6	< 0.001	18.1
Middle Horizon	3	6192	217.0	< 0.001	148.1
Late Intermediate Period	2	5257	14.4	0.001	10.6
Region	N. Groups	N. Objects	χ^2 -stat	P-val	χ^2 -stat
North Coast	4	5036	1182.5	< 0.001	1988.7
Central-North Coast	4	17706	1044.7	< 0.001	1093.1
Central-South Coast	3	4101	63.4	< 0.001	100.0
Catalog Year			Yes	Yes	Yes
Archaeologist FE			Yes	Yes	Yes
Geographic Controls			Yes	Yes	Yes

Notes. The table reports χ^2 -test results for the joint significance of group fixed effects. The outcome variable is a measure of average stylistic distinctiveness based on text embeddings (SBERT in Panel A, RoBERTa in Panel B, OpenAI's embedding model in Panel C) or image embeddings (VGG16, Panel D). In each panel, the top sub-panel presents one regression per period, while the bottom sub-panel presents one regression per region. All regressions are estimated by OLS at the object level and include group fixed effects, the year the object was electronically catalogued, archaeologist fixed effects, and a vector of site-level geographic controls (absolute latitude, mean elevation, standard deviation of elevation, mean caloric suitability prior to AD 1500, log distance to the nearest river, and log distance to the coastline). Standard errors are adjusted for spatial correlation with a distance cutoff of approximately 50km at the equator (Conley 1999).

TABLE A.7: Stylistic Distinctiveness (Text- and Image-Based) and Joint Significance of Group Fixed Effects — Conley SE (100km)

Panel A: Text-Based (SBERT)				Panel B: Text-Based (RoBERTa)	
	(1)	(2)		(3)	(4)
Period	N. Groups	N. Objects	χ^2 -stat	P-val	χ^2 -stat
Early Horizon	3	1299	258.5	< 0.001	146.3
Early Intermediate Period	4	17464	34.9	< 0.001	143.0
Middle Horizon	3	6192	121.1	< 0.001	243.9
Late Intermediate Period	2	5257	135.0	< 0.001	14.4
Region	N. Groups	N. Objects	χ^2 -stat	P-val	χ^2 -stat
North Coast	4	5036	6868.2	< 0.001	2272.4
Central-North Coast	4	17706	3336.5	< 0.001	1573.1
Central-South Coast	3	4101	527.2	< 0.001	453.9
Panel C: Text-Based (OpenAI)				Panel D: Image-Based (VGG16)	
	(5)	(6)		(7)	(8)
Period	N. Groups	N. Objects	χ^2 -stat	P-val	χ^2 -stat
Early Horizon	3	1299	1256.4	< 0.001	694.8
Early Intermediate Period	4	17464	34.4	< 0.001	22.2
Middle Horizon	3	6192	214.8	< 0.001	99.9
Late Intermediate Period	2	5257	16.7	< 0.001	13.4
Region	N. Groups	N. Objects	χ^2 -stat	P-val	χ^2 -stat
North Coast	4	5036	3827.0	< 0.001	256.9
Central-North Coast	4	17706	3639.9	< 0.001	6484.7
Central-South Coast	3	4101	62.6	< 0.001	1384.2
Catalog Year			Yes	Yes	Yes
Archaeologist FE			Yes	Yes	Yes
Geographic Controls			Yes	Yes	Yes

Notes. The table reports χ^2 -test results for the joint significance of group fixed effects. The outcome variable is a measure of average stylistic distinctiveness based on text embeddings (SBERT in Panel A, RoBERTa in Panel B, OpenAI's embedding model in Panel C) or image embeddings (VGG16, Panel D). In each panel, the top sub-panel presents one regression per period, while the bottom sub-panel presents one regression per region. All regressions are estimated by OLS at the object level and include group fixed effects, the year the object was electronically catalogued, archaeologist fixed effects, and a vector of site-level geographic controls (absolute latitude, mean elevation, standard deviation of elevation, mean caloric suitability prior to AD 1500, log distance to the nearest river, and log distance to the coastline). Standard errors are adjusted for spatial correlation with a distance cutoff of approximately 100km at the equator (Conley 1999).

TABLE A.8: Stylistic Distinctiveness (TF-IDF) and Joint Significance of Group Fixed Effects

	N. Groups	N. Objects	Panel A: Cluster(Site)		Panel B: Conley 100km		Panel C: Conley 50km	
			(1)	(2)	(3)	(4)	(5)	(6)
Period								
Early Horizon	3	1299	53.4	< 0.001	284.3	< 0.001	145.8	< 0.001
Early Intermediate Period	4	17464	35.4	< 0.001	71.8	< 0.001	81.2	< 0.001
Middle Horizon	3	6192	87.6	< 0.001	189.4	< 0.001	181.5	< 0.001
Late Intermediate Period	2	5257	5.6	.019	8.3	.004	5.3	.021
Region								
North Coast	4	5036	94.2	< 0.001	1661.5	< 0.001	1383.9	< 0.001
Central-North Coast	4	17706	139.9	< 0.001	4521.9	< 0.001	8113.8	< 0.001
Central-South Coast	3	4101	41.9	< 0.001	63.6	< 0.001	107.1	< 0.001
Catalog Year			Yes	Yes	Yes	Yes	Yes	Yes
Archaeologist FE			Yes	Yes	Yes	Yes	Yes	Yes
Geographic Controls			Yes	Yes	Yes	Yes	Yes	Yes

Notes. The table reports test results for the joint significance of group fixed effects. The top panel presents one regression per period, while the bottom panel presents one regression per region. All regressions are estimated by OLS at the object level, with the measure of stylistic distinctiveness based on frequency-based embeddings (TF-IDF) as outcome variable. All regressions include group fixed effects, the year the object was electronically catalogued, archaeologist fixed effects, and a vector of site-level geographic controls (absolute latitude, mean elevation, standard deviation of elevation, mean caloric suitability prior to AD 1500, log distance to the nearest river, and log distance to the coastline). In Panel A, standard errors are clustered at the site level; in panels B and C, standard errors are adjusted for spatial correlation with a distance cutoff of approximately 100km and 50km at the equator (Conley 1999), respectively.

TABLE A.9: Stylistic Distinctiveness (Spanish-RoBERTa) and Joint Significance of Group Fixed Effects

		Panel A: Cluster(Site)		Panel B: Conley 100km		Panel C: Conley 50km		
		(1)	(2)	(3)	(4)	(5)	(6)	
Period	N. Groups	N. Objects	F-stat	P-value	χ^2 -stat	P-value	χ^2 -stat	P-value
Early Horizon	3	1299	11.4	< 0.001	61.9	< 0.001	44.4	< 0.001
Early Intermediate Period	4	17464	16.7	< 0.001	45	< 0.001	33.7	< 0.001
Middle Horizon	3	6192	153.2	< 0.001	627	< 0.001	495.4	< 0.001
Late Intermediate Period	2	5257	2.7	.099	3	.082	1.8	.175
Region	N. Groups	N. Objects	F-stat	P-value	χ^2 -stat	P-value	χ^2 -stat	P-value
North Coast	4	5036	12.2	< 0.001	176.9	< 0.001	98.9	< 0.001
Central-North Coast	4	17706	83.5	< 0.001	645.5	< 0.001	468.6	< 0.001
Central-South Coast	3	4101	52.9	< 0.001	733.3	< 0.001	157.3	< 0.001
Catalog Year			Yes	Yes	Yes	Yes	Yes	Yes
Archaeologist FE			Yes	Yes	Yes	Yes	Yes	Yes
Geographic Controls			Yes	Yes	Yes	Yes	Yes	Yes

Notes. The table reports test results for the joint significance of group fixed effects. The top panel presents one regression per period, while the bottom panel presents one regression per region. All regressions are estimated by OLS at the object level. The outcome variable is the measure of stylistic distinctiveness based on Spanish text embeddings, generated using the RoBERTa model pre-trained in Spanish by Fandiño et al. (2022). All regressions include group fixed effects, the year the object was electronically cataloged, archaeologist fixed effects, and a vector of site-level geographic controls (absolute latitude, mean elevation, standard deviation of elevation, mean caloric suitability prior to AD 1500, log distance to the nearest river, and log distance to the coastline). In Panel A, standard errors are clustered at the site level; in panels B and C, standard errors are adjusted for spatial correlation with a distance cutoff of approximately 100km and 50km at the equator (Conley 1999), respectively.

TABLE A.10: Beyond Object Form — Alternative Models

			Panel A: MCA Residuals				Panel B: SBERT Residuals				Panel C: RoBERTa Residuals				Panel D: OpenAI Residuals			
			(1)	(2)	(3)		(4)	(5)	(6)		(7)	(8)	(9)		(10)	(11)	(12)	
Period	N. Groups	N. Objects	F-stat	P-value	Δ Adj. R2		F-stat	P-value	Δ Adj. R2		F-stat	P-value	Δ Adj. R2		F-stat	P-value	Δ Adj. R2	
Early Horizon	3	1299	20.7	< 0.001	1.3		59.2	< 0.001	6.2		42.3	< 0.001	2.8		183.6	< 0.001	11	
Early Intermediate Period	4	17464	3.8	.012	.1		5.9	.001	.1		14.5	< 0.001	.2		6.2	.001	.2	
Middle Horizon	3	6192	43.7	< 0.001	2.9		50.6	< 0.001	2.5		81.6	< 0.001	3		149	< 0.001	6.9	
Late Intermediate Period	2	5257	60.1	< 0.001	1.4		1.4	.241	0		2.1	.152	0		7.1	.008	.1	
Region	N. Groups	N. Objects	F-stat	P-value	Δ Adj. R2		F-stat	P-value	Δ Adj. R2		F-stat	P-value	Δ Adj. R2		F-stat	P-value	Δ Adj. R2	
North Coast	4	5036	908.7	< 0.001	26		116.6	< 0.001	2.6		23	< 0.001	1.3		102.9	< 0.001	4.2	
Central-North Coast	4	17706	381.2	< 0.001	12.8		166.8	< 0.001	2.8		93	< 0.001	1.8		288.6	< 0.001	5.7	
Central-South Coast	3	4101	59.6	< 0.001	2.6		14.9	< 0.001	1.1		41.2	< 0.001	2.1		14.7	< 0.001	1.1	
Catalog Year			Yes	Yes	Yes		Yes	Yes	Yes		Yes	Yes	Yes		Yes	Yes	Yes	
Archaeologist FE			Yes	Yes	Yes		Yes	Yes	Yes		Yes	Yes	Yes		Yes	Yes	Yes	
Type of Form FE			No	No	No		No	No	No		No	No	No		No	No	No	
Geographic Controls			Yes	Yes	Yes		Yes	Yes	Yes		Yes	Yes	Yes		Yes	Yes	Yes	

Notes. The table reports F-test results for the joint significance of group fixed effects. The top panel presents one regression per period; the bottom panel presents one regression per region. Each regression is estimated by OLS at the object level and includes group fixed effects, the year the object was electronically cataloged, archaeologist fixed effects, and geographic controls. The vector of site-level geographic controls includes the site's absolute latitude, mean elevation, standard deviation of elevation, mean caloric suitability prior to AD 1500, log distance to the nearest river, and log distance to the coastline. The outcome variables are the residuals from regressions of stylistic distinctiveness against form fixed effects. The measures of stylistic distinctiveness are based on the score of the first MCA dimension (Panel A) or text embeddings (SBERT in Panel B, RoBERTa in Panel C, OpenAI's embedding model in Panel D). Standard errors are clustered at the site level. The change in adjusted R^2 , relative to the specification without group fixed effects (Δ Adj. R^2), is expressed in percentage terms.

TABLE A.11: The Symbolic Content of Ceramics — Alternative Standard Errors

	Religious (1)	Fertility (2)	Death (3)	Agriculture (4)	Fishing (5)	War (6)
Panel A: Baseline Controls						
Stylistic Distinct. (group-retrieved)	0.089 (0.022)*** [0.017]*** [[0.020]]***	-0.005 (0.001)*** [0.001]*** [[0.001]]***	-0.005 (0.001)*** [0.001]*** [[0.002]]***	0.001 (0.001) [0.001]* [[0.001]]*	0.002 (0.001)** [0.001]** [[0.001]]**	0.015 (0.006)** [0.004]*** [[0.004]]***
Panel B: Type of Form FE						
Stylistic Distinct. (group-retrieved)	0.087 (0.022)*** [0.017]*** [[0.020]]***	-0.004 (0.001)*** [0.001]*** [[0.001]]***	-0.005 (0.001)*** [0.002]*** [[0.002]]***	0.001 (0.001) [0.001]* [[0.001]]	0.002 (0.001)** [0.001]** [[0.001]]**	0.015 (0.007)* [0.004]*** [[0.004]]***
Panel C: Period and Region FE						
Stylistic Distinct. (group-retrieved)	0.115 (0.050)** [0.030]*** [[0.029]]***	-0.005 (0.001)*** [0.001]*** [[0.001]]***	-0.002 (0.002) [0.002] [[0.002]]	0.004 (0.002)* [0.001]*** [[0.001]]***	0.002 (0.001)* [0.002] [[0.002]]	0.017 (0.011) [0.006]*** [[0.006]]***
Mean Dep. Var.	0.129	0.005	0.009	0.001	0.003	0.031
N	30212	30212	30212	30212	30212	30212

Notes. All regressions are estimated by OLS at the object level. Each column presents the results for a different outcome variable—a dummy variable indicating whether a trait is present in sculpted and/or painted form. The table reports the estimated coefficient on the measure of stylistic distinctiveness retrieved from the group fixed effects. This measure corresponds to the estimated group fixed effects from a regression of image-based stylistic distinctiveness (based on VGG16 image embeddings) on group fixed effects and baseline controls (geography, cataloging year, and archaeologist fixed effects). The measure is normalized between 0 and 1, with 1 corresponding to the group with the highest value. All regressions include baseline controls (the year the object was electronically cataloged, archaeologist fixed effects, and a vector of site-level geographic controls, including absolute latitude, mean elevation, standard deviation of elevation, mean caloric suitability prior to AD 1500, log distance to the nearest river, and log distance to the coastline). In Panel B, the regressions also include fixed effects for type of form (open forms, closed forms, and molded sculptures). In Panel C, the regressions additionally include period and region fixed effects. Standard errors in (\cdot) are clustered at the group level; in $[\cdot]$ and $[[\cdot]]$, standard errors are adjusted for spatial correlation with a distance cutoff of approximately 50km and 10km at the equator (Conley 1999), respectively. We weight observations by the inverse of the standard errors from the first-stage estimates of the group fixed effects. *** p<0.01, ** p<0.05, * p<0.1.

TABLE A.12: The Symbolic Content of Ceramics —
Coarsened Exact Matching (CEM, Alternative Standard Errors)

	Religious (1)	Fertility (2)	Death (3)	Agriculture (4)	Fishing (5)	War (6)
Panel A: Baseline Controls						
Stylistic Distinct. (group-retrieved)	0.103 (0.026)* [0.018]*** [[0.016]]***	-0.012 (0.005)** [0.003]*** [[0.003]]***	-0.007 (0.002)** [0.004]* [[0.004]]	0.000 (0.000) [0.000] [[0.000]]	0.007 (0.003)* [0.003]** [[0.003]]**	0.018 (0.008)* [0.005]*** [[0.006]]***
Panel B: Stratum FE						
Stylistic Distinct. (group-retrieved)	0.089 (0.006)*** [0.013]*** [[0.011]]***	-0.010 (0.005)* [0.003]*** [[0.003]]***	-0.008 (0.002)*** [0.007] [[0.008]]	0.000 (0.000)*** [0.000]** [[0.000]]**	0.002 (0.001) [0.002] [[0.002]]	0.017 (0.003)*** [0.003]*** [[0.003]]***
Panel C: Period and Region FE						
Stylistic Distinct. (group-retrieved)	0.122 (0.051)* [0.080] [[0.080]]	-0.008 (0.033) [0.032] [[0.029]]	-0.020 (0.006)** [0.022] [[0.020]]	-0.000 (0.001) [0.001] [[0.001]]	-0.009 (0.002)*** [0.005] [[0.004]]*	0.019 (0.011) [0.025] [[0.024]]
Mean Dep. Var.	0.150	0.005	0.010	0.001	0.005	0.034
N	5697	5697	5697	5697	5697	5697

Notes. All regressions are estimated by OLS at the object level for the matched sample. We use Coarsened Exact Matching (CEM, [Iacus et al. 2012](#)) to create this matched sample of objects, which are (i) statistically similar in terms of geography and cataloging year, and (ii) identical in terms of form type and archaeologist identity. Each column presents the results for a different outcome variable—a dummy variable indicating whether a trait is present in sculpted and/or painted form. The table reports the estimated coefficient on the measure of stylistic distinctiveness retrieved from the group fixed effects. This measure corresponds to the estimated group fixed effects from a regression of image-based stylistic distinctiveness (based on VGG16 image embeddings) on group fixed effects and baseline controls (geography, cataloging year, and archaeologist fixed effects). The measure is normalized between 0 and 1, with 1 corresponding to the group with the highest value. All regressions include baseline controls (the year the object was electronically cataloged and a vector of site-level geographic controls, including absolute latitude, mean elevation, standard deviation of elevation, mean caloric suitability prior to AD 1500, log distance to the nearest river, and log distance to the coastline). In Panel B, the regressions also include stratum fixed effects. In Panel C, the regressions additionally include period and region fixed effects. Standard errors in (·) are clustered at the group level; in [·] and [[·]], standard errors are adjusted for spatial correlation with a distance cutoff of approximately 50km and 10km at the equator ([Conley 1999](#)), respectively. We weight observations by the inverse of the standard errors from the first-stage estimates of the group fixed effects. *** p<0.01, ** p<0.05, * p<0.1.

TABLE A.13: The Symbolic Content of Ceramics — Religious and Animal Traits

	Religious: Ancestor-Related (1)	Religious: Creation-Related (2)	Animals: Snake (3)	Animals: Feline (4)	Animals: Birds (5)	Animals: Other (6)
Panel A: Baseline Controls						
Stylistic Distinct. (group-retrieved)	-0.004 (0.005)	0.091*** (0.022)	0.088*** (0.015)	0.049*** (0.017)	0.028 (0.027)	-0.274** (0.103)
Panel B: Type of Form FE						
Stylistic Distinct. (group-retrieved)	-0.004 (0.004)	0.089*** (0.020)	0.087*** (0.014)	0.048** (0.019)	0.024 (0.021)	-0.280*** (0.096)
Panel C: Period and Region FE						
Stylistic Distinct. (group-retrieved)	-0.008 (0.009)	0.122** (0.047)	0.068** (0.027)	0.032 (0.032)	0.028 (0.040)	0.039 (0.041)
Mean Dep. Var.	0.032	0.099	0.053	0.092	0.133	0.118
N	30212	30212	30212	30212	30212	30212

Notes. All regressions are estimated by OLS at the object level. Each column presents the results for a different outcome variable—a dummy variable indicating whether a trait is present in sculpted and/or painted form. The table reports the estimated coefficient on the measure of stylistic distinctiveness retrieved from the group fixed effects. This measure corresponds to the estimated group fixed effects from a regression of image-based stylistic distinctiveness (based on VGG16 image embeddings) on group fixed effects and baseline controls (geography, cataloging year, and archaeologist fixed effects). The measure is normalized between 0 and 1, with 1 corresponding to the group with the highest value. All regressions include baseline controls (the year the object was electronically cataloged, archaeologist fixed effects, and a vector of site-level geographic controls, including absolute latitude, mean elevation, standard deviation of elevation, mean caloric suitability prior to AD 1500, log distance to the nearest river, and log distance to the coastline). In Panel B, the regressions also include fixed effects for type of form (open forms, closed forms, and molded sculptures). In Panel C, the regressions additionally include period and region fixed effects. Standard errors clustered at the Group \times Region level (25 clusters) in parentheses. We weight observations by the inverse of the standard errors from the first-stage estimates of the group fixed effects. *** p<0.01, ** p<0.05, * p<0.1.

TABLE A.14: The Symbolic Content of Ceramics —
Religious and Animal Traits (Alternative Standard Errors)

	Religious: Ancestor-Related (1)	Religious: Creation-Related (2)	Animals: Snake (3)	Animals: Feline (4)	Animals: Birds (5)	Animals: Other (6)
Panel A: Baseline Controls						
Stylistic Distinct. (group-retrieved)	-0.004 (0.006) [0.005] [[0.006]]	0.091 (0.022)*** [0.017]*** [[0.020]]***	0.088 (0.012)*** [0.009]*** [[0.010]]***	0.049 (0.017)* [0.009]*** [[0.009]]***	0.028 (0.027) [0.014]** [[0.012]]**	-0.274 (0.132)* [0.033]*** [[0.037]]***
Panel B: Type of Form FE						
Stylistic Distinct. (group-retrieved)	-0.004 (0.005) [0.005] [[0.006]]	0.089 (0.022)*** [0.017]*** [[0.019]]***	0.087 (0.011)*** [0.009]*** [[0.009]]***	0.048 (0.020)** [0.010]*** [[0.009]]***	0.024 (0.020) [0.013]* [[0.011]]**	-0.280 (0.124)** [0.032]*** [[0.035]]***
Panel C: Period and Region FE						
Stylistic Distinct. (group-retrieved)	-0.008 (0.011) [0.008] [[0.008]]	0.122 (0.046)** [0.028]*** [[0.028]]***	0.068 (0.023)** [0.016]*** [[0.015]]***	0.032 (0.033) [0.020] [[0.018]]*	0.028 (0.043) [0.022] [[0.024]]	0.039 (0.046) [0.026] [[0.026]]
Mean Dep. Var.	0.032	0.099	0.053	0.092	0.133	0.118
N	30212	30212	30212	30212	30212	30212

Notes. All regressions are estimated by OLS at the object level. Each column presents the results for a different outcome variable—a dummy variable indicating whether a trait is present in sculpted and/or painted form. The table reports the estimated coefficient on the measure of stylistic distinctiveness retrieved from the group fixed effects. This measure corresponds to the estimated group fixed effects from a regression of image-based stylistic distinctiveness (based on VGG16 image embeddings) on group fixed effects and baseline controls (geography, cataloging year, and archaeologist fixed effects). The measure is normalized between 0 and 1, with 1 corresponding to the group with the highest value. All regressions include baseline controls (the year the object was electronically cataloged, archaeologist fixed effects, and a vector of site-level geographic controls, including absolute latitude, mean elevation, standard deviation of elevation, mean caloric suitability prior to AD 1500, log distance to the nearest river, and log distance to the coastline). In Panel B, the regressions also include fixed effects for type of form (open forms, closed forms, and molded sculptures). In Panel C, the regressions additionally include period and region fixed effects. Standard errors in (·) are clustered at the group level; in [·] and [[·]], standard errors are adjusted for spatial correlation with a distance cutoff of approximately 50km and 10km at the equator (Conley 1999), respectively. We weight observations by the inverse of the standard errors from the first-stage estimates of the group fixed effects. *** p<0.01, ** p<0.05, * p<0.1.

TABLE A.15: Cultural Dispersion and Political Centralization —
Alternative Standard Errors (OLS Results)

	Alternative Standard Errors			Wild Cluster Bootstrap		
	Frac Themes	Text-Based (SBERT)	Image-Based (VGG16)	Frac Themes	Text-Based (SBERT)	Image-Based (VGG16)
	(1)	(2)	(3)	(4)	(5)	(6)
Panel A: Baseline Controls						
Political Centr.	-0.410 (0.066)*** [0.050]*** [[0.060]]***	-0.306 (0.067)*** [0.060]*** [[0.056]]***	-0.090 (0.072) [0.053]* [[0.043]]**	-0.410** (0.099) [0.083]* [[0.043]]**	-0.306** (0.083) [0.065]	-0.090 (0.065)
Adj R^2	0.797	0.414	0.387	0.797	0.414	0.387
Panel B: Group-Level Controls						
Political Centr.	-0.480 (0.083)*** [0.053]*** [[0.063]]***	-0.269 (0.109)** [0.067]*** [[0.068]]***	0.038 (0.076) [0.052] [[0.053]]	-0.480*** (0.095) [0.084] [[0.053]]	-0.269 (0.109) [0.070]	0.038 (0.070)
Adj R^2	0.843	0.428	0.412	0.843	0.428	0.412
Panel C: Period and Region FE						
Political Centr.	-0.546 (0.124)*** [0.082]*** [[0.100]]***	-0.339 (0.091)*** [0.078]*** [[0.077]]***	-0.029 (0.131) [0.106] [[0.102]]	-0.546*** (0.123) [0.084] [[0.077]]	-0.339*** (0.084) [0.058] [[0.077]]	-0.029 (0.128)
Adj R^2	0.868	0.482	0.458	0.868	0.482	0.458
N	422	422	422	422	422	422

Notes. All regressions are estimated by OLS at the site level. The dependent variables are the index of thematic fractionalization (columns 1 and 4), the standard deviation of stylistic distinctiveness based on SBERT text embeddings (columns 2 and 5), and the standard deviation of stylistic distinctiveness based on VGG16 image embeddings (columns 3 and 6), across all objects from a site. The table reports the estimated coefficient on the group-level index of political centralization. In Panel A, the set of baseline controls includes the share of open-form objects, the share of close-form objects, the log number of objects, a dummy variable equal to one if the number of mentions found for the group is above the median, and a vector of site-level geographic controls (absolute latitude, mean elevation, standard deviation of elevation, mean caloric suitability prior to AD 1500, log distance to the nearest river, and log distance to the coastline). In Panel B, the regressions additionally include the log of the group's area and the log of the group's number of sites. In Panel C, the regressions additionally include period and region fixed effects. For columns (1)-(3): Standard errors in (-) are clustered at the group level; in [·] and [[·]], standard errors are adjusted for spatial correlation with a distance cutoff of approximately 50km and 10km at the equator (Conley 1999), respectively. For columns (4)-(6): Standard errors from wild cluster bootstrap (WCB) inference in parentheses, with 5000 bootstrap repetitions. All variables are standardized to have zero mean and standard deviation equal to one. *** p<0.01, ** p<0.05, * p<0.1.

TABLE A.16: Geographic Coverage of Irrigation Potential Data

Region	Crop	% Sites	% Cells
North Coast	Groundnut	0.16	0.07
	Maize	0.11	0.05
	Beans	0.11	0.06
	Sweet Potato	0.05	0.05
	White Potato	0.01	0.01
Central-North Coast	Groundnut	0.45	0.17
	Maize	0.12	0.04
	Beans	0.25	0.07
	Sweet Potato	0.22	0.06
	White Potato	0.12	0.04
Central-South Coast	Groundnut	0.63	0.31
	Maize	0.35	0.13
	Beans	0.57	0.19
	Sweet Potato	0.48	0.16
	White Potato	0.32	0.11

Notes. We use raster data from the FAO-GAEZ v4 project (grid cells of approximately 10×10 km at the equator). The first column (% Sites) reports the share of sites with at least one grid cell containing non-missing information on irrigation potential by crop. Combining grid cells from all sites, the second column (% Cells) reports the share of cells with non-missing data across all sites. Irrigation potential is defined as the ratio of maximum attainable yield under irrigation *versus* rainfed conditions. We use data on potential attainable yields (1961-1990 average) under low level inputs and no CO_2 fertilization, to approximate pre-colonial conditions.

TABLE A.17: Cultural Dispersion and Log Perennial River Length

	Frac Themes			Text-Based (SBERT)			Image-Based (VGG16)		
	(1)	(2)	(3)	(4)	(5)	(6)	(7)	(8)	(9)
Log River Length	-0.563*** (0.168)	-0.540*** (0.191)	-0.546*** (0.160)	-0.629*** (0.105)	-0.597*** (0.125)	-0.638*** (0.120)	-0.002 (0.247)	-0.041 (0.280)	-0.029 (0.236)
Mean Caloric Suitability		-0.054 (0.123)			-0.074 (0.052)		0.092 (0.193)		
Mean Caloric Suitability (maize)			-0.189 (0.277)			0.112 (0.161)		0.304 (0.254)	
Adj. R^2	0.835	0.836	0.836	0.482	0.482	0.481	0.442	0.442	0.443
N	422	422	422	422	422	422	422	422	422
Baseline Controls	Yes	Yes	Yes	Yes	Yes	Yes	Yes	Yes	Yes
Group-Level Controls	Yes	Yes	Yes	Yes	Yes	Yes	Yes	Yes	Yes

Notes. All regressions are estimated by OLS at the site level. The dependent variables are the index of thematic fractionalization (columns 1-3), the standard deviation of stylistic distinctiveness based on SBERT text embeddings (columns 4-6), and the standard deviation of stylistic distinctiveness based on VGG16 image embeddings (columns 7-9), across all objects from a site. The table reports the estimated coefficient on the log of total perennial river length, measured at the group level within the group's pre-colonial homeland. The set of baseline controls includes the share of open-form objects, the share of close-form objects, the log number of objects, a dummy variable equal to one if the number of mentions found for the group is above the median, the group's log mean temperature and temperature stability (isothermality), and a vector of site-level geographic controls (absolute latitude, mean elevation, standard deviation of elevation, mean caloric suitability prior to AD 1500, log distance to the nearest river, and log distance to the coastline). The set of group-level controls refers to the log of the group's area and the log of the group's number of sites. Standard errors clustered at the Group \times Region level (22 clusters) in parentheses. All variables are standardized to have zero mean and standard deviation equal to one.

TABLE A.18: Politically Complex *versus* Placebo Random Areas —
No Logarithmic Transformation (2SLS Results)

	Homeland: Political Sites Only			Homeland: 20% Random			Homeland: 60% Random		
	Frac Themes	SD Text	SD Image	Frac Themes	SD Text	SD Image	Frac Themes	SD Text	SD Image
	(1)	(2)	(3)	(4)	(5)	(6)	(7)	(8)	(9)
Political Centr.	-0.428*** (0.046)	-0.242*** (0.068)	0.071 (0.069)	-0.591** (0.282)	0.397 (1.054)	1.223 (1.921)	-0.930 (2.091)	1.610 (7.764)	3.446 (14.327)
N	422	422	422	422	422	422	422	422	422
F-Stat (excluded instrument)	486.91	486.91	486.91	0.35	0.35	0.35	0.05	0.05	0.05
Baseline Controls	Yes	Yes	Yes	Yes	Yes	Yes	Yes	Yes	Yes
Group-Level Controls	Yes	Yes	Yes	Yes	Yes	Yes	Yes	Yes	Yes

Notes. 2SLS results at the site level. In columns (1), (4), and (7) the dependent variable is the index of thematic fractionalization, based on the share of objects classified by theme. In the remaining columns, the dependent variables correspond to the standard deviation of stylistic distinctiveness, based on SBERT text embeddings (columns 2, 5, and 8) or VGG16 image embeddings (columns 3, 6, and 9), across all objects from a site. The table reports the estimated coefficient on the group-level index of political centralization, instrumented with the total length of perennial rivers. Columns (1)–(3) use river length within politically complex areas of the group’s pre-colonial homeland. Columns (4)–(6) use a 20 percent random portion of the homeland without evidence of political complexity, and columns (7)–(9) use a 60 percent random portion. The set of baseline controls includes the share of open-form objects, the share of close-form objects, the log number of objects, a dummy variable equal to one if the number of mentions found for the group is above the median, the group’s log mean temperature and temperature stability (isothermality), and a vector of site-level geographic controls (absolute latitude, mean elevation, standard deviation of elevation, mean caloric suitability prior to AD 1500, log distance to the nearest river, and log distance to the coastline). The set of group-level controls refers to the log of the group’s area and the log of the group’s number of sites. Standard errors clustered at the Group×Region level (22 clusters) in parentheses. All variables are standardized to have zero mean and standard deviation equal to one. F-Stat (excluded instrument) reports the F-statistic on the excluded instrument from the first stage regression. *** p<0.01, ** p<0.05, * p<0.1.

TABLE A.19: Cultural Dispersion and Political Centralization —
Alternative Standard Errors (2SLS Results)

	Frac Themes			Text-Based (SBERT)			Image-Based (VGG16)		
	(1)	(2)	(3)	(4)	(5)	(6)	(7)	(8)	(9)
Political Centr.	-0.157 (0.130) [0.085]* [[0.089]]*	-0.375 (0.086)*** [0.067]*** [[0.072]]***	-0.579 (0.058)*** [0.057]*** [[0.056]]***	-0.388 (0.096)*** [0.099]*** [[0.095]]***	-0.419 (0.075)*** [0.076]*** [[0.076]]***	-0.463 (0.090)*** [0.089]*** [[0.090]]***	-0.295 (0.176)* [0.104]*** [[0.109]]***	-0.001 (0.168) [0.110] [[0.128]]	0.135 (0.158) [0.126] [[0.122]]
N	422	422	422	422	422	422	422	422	422
F-Stat (excluded instrument)	22.28	51.44	94.33	22.28	51.44	94.33	22.28	51.44	94.33
F-Stat (AR)	1.13	11.23	438.49	22.44	65.51	43.12	2.98	0.00	0.84
P-value (AR)	0.311	0.006	0.000	0.001	0.000	0.000	0.112	0.995	0.378
Baseline Controls	Yes	Yes	Yes	Yes	Yes	Yes	Yes	Yes	Yes
Group-Level Controls	No	Yes	Yes	No	Yes	Yes	No	Yes	Yes
Period and Region FE	No	No	Yes	No	No	Yes	No	No	Yes

Notes. 2SLS results at the site level. In column (1)-(3), the dependent variable is the index of thematic fractionalization, based on the share of objects classified by theme. In columns (4)-(6) and (7)-(9), the dependent variables correspond to the standard deviation of stylistic distinctiveness, based on SBERT text embeddings (column 2) or VGG16 image embeddings (column 3), across all objects from a site. The table reports the estimated coefficient on the group-level index of political centralization, instrumented with the log of the total length of perennial rivers within each group's historical homeland. The set of baseline controls includes the share of open-form objects, the share of close-form objects, the log number of objects, a dummy variable equal to one if the number of mentions found for the group is above the median, the group's log mean temperature and temperature stability (isothermality), and a vector of site-level geographic controls (absolute latitude, mean elevation, standard deviation of elevation, mean caloric suitability prior to AD 1500, log distance to the nearest river, and log distance to the coastline). Columns (2), (5), and (8) additionally include the log of the group's area and the log of the group's number of sites. In columns (3), (6), and (9), the regressions additionally include period and region fixed effects. Standard errors in (-) are clustered at the group level; in [-] and [[-]], standard errors are adjusted for spatial correlation with a distance cutoff of approximately 50km and 10km at the equator (Conley 1999), respectively. All variables are standardized to have zero mean and standard deviation equal to one. F-Stat (excluded instrument) reports the F-statistic on the excluded instrument from the first stage regression with standard errors clustered at the group level. Accordingly, F-Stat (AR) and p-value (AR) refer to the Anderson-Rubin Wald test with standard errors clustered at the group level. *** p<0.01, ** p<0.05, * p<0.1.

TABLE A.20: Cultural Dispersion and Political Centralization —
2SLS Results (Log River Density)

	Frac Themes			Text-Based (SBERT)			Image-Based (VGG16)		
	(1)	(2)	(3)	(4)	(5)	(6)	(7)	(8)	(9)
Political Centr.	-0.695*** (0.258)	-0.543*** (0.143)	-0.569*** (0.095)	-0.618*** (0.200)	-0.564*** (0.149)	-0.469*** (0.101)	0.188 (0.263)	0.034 (0.200)	0.125 (0.180)
N	422	422	422	422	422	422	422	422	422
F-Stat (excluded instrument)	7.44	22.02	154.04	7.44	22.02	154.04	7.44	22.02	154.04
F-Stat (AR)	17.46	15.07	55.25	29.34	50.64	27.38	0.53	0.03	0.52
P-value (AR)	0.000	0.001	0.000	0.000	0.000	0.000	0.474	0.874	0.478
Baseline Controls	Yes	Yes	Yes	Yes	Yes	Yes	Yes	Yes	Yes
Group-Level Controls	No	Yes	Yes	No	Yes	Yes	No	Yes	Yes
Period and Region FE	No	No	Yes	No	No	Yes	No	No	Yes

Notes. 2SLS results at the site level. In column (1)-(3), the dependent variable is the index of thematic fractionalization, based on the share of objects classified by theme. In columns (4)-(6) and (7)-(9), the dependent variables correspond to the standard deviation of stylistic distinctiveness, based on SBERT text embeddings (column 2) or VGG16 image embeddings (column 3), across all objects from a site. The table reports the estimated coefficient on the group-level index of political centralization, instrumented with the log of river density, defined as total length of perennial rivers divided by the group's historical area. The set of baseline controls includes the share of open-form objects, the share of close-form objects, the log number of objects, a dummy variable equal to one if the number of mentions found for the group is above the median, the group's log mean temperature and temperature stability (isothermality), and a vector of site-level geographic controls (absolute latitude, mean elevation, standard deviation of elevation, mean caloric suitability prior to AD 1500, log distance to the nearest river, and log distance to the coastline). Columns (2), (5), and (8) additionally include the log of the group's number of sites. In columns (3), (6), and (9), the regressions additionally include period and region fixed effects. Standard errors clustered at the Group×Region level (22 clusters) in parentheses. All variables are standardized to have zero mean and standard deviation equal to one. F-Stat (excluded instrument) reports the F-statistic on the excluded instrument from the first stage regression. F-Stat (AR) and p-value (AR) refer to the Anderson-Rubin Wald test. *** p<0.01, ** p<0.05, * p<0.1.